RESEARCH TRIANGLE INSTITUTE

Contract Number HO346015

GAS DETECTION INSTRUMENTATION USING METAL OXIDE SENSOR TECHNOLOGY

P. A. Lawless, J. W. Harrison
A. D. Brooks, and P. K. Ajmera

United States
Department of the Interior
Bureau of Mines

USBM Contract Report (HO346015)

Date January 1976

Research Triangle Institute

RESEARCH TRIANGLE PARK, NORTH CAROLINA 27709

DISCLAIMER NOTICE

The views and conclusions contained in this document are those of the authors and should not be interpreted as necessarily representing the official policies or recommendations of the Interior Department's Bureau of Mines or the U. S. Government.

FOREWORD

This report was prepared by the Research Triangle Institute, Energy and Environmental Research Division, Research Triangle Park, North Carolina under USBM Contract Number H0346015. The contract was initiated under the Coal Mine Health and Safety Program. It was administered under the technical direction of PMSRC, with Dr. George Schnakenberg acting as the Technical Project Officer. Mrs. Pearl A. Shapert was the contract administrator for the Bureau of Mines.

This report is a summary of the work recently completed as part of this contract during the period May 29, 1974 to October 15, 1975. This report was submitted by the authors on March 1, 1976.

TABLE OF CONTENTS

LIST OF FIGURES

LIST OF TABLES

1.0 INTRODUCTION

The objective of the research performed for the Bureau of Mines on this contract was to develop a portable instrument for the detection of carbon monoxide (CO) in a mine environment. The desired characteristics were sensitivity and specificity for CO with a stable calibration. The sensor of the instrument was to be of metal oxide composition, requiring low power for compatibility with the types of batteries presently used in personal equipment in mines. The solid state design was also desired for ruggedness and small size. A key design feature of the instrument was to be provided by adherence to the intrinsic safety design requirements for electrical equipments operated in potentially exposive mine atmosphere.

The Research Triangle Institute has prior experience in developing a solid state oxygen sensor using a thin film of zinc-oxide (Ref. 1) and experience in fabricating thin film devices. Solid state sensors utilized by other workers (Refs. 2, 3, 4, 5, 6) have included metal and semiconductor films and crystals of materials like carbon and aluminum oxide for the measurement of water vapor in the air and have relied upon measuring resistance and capacitance changes in the sensor in response to adsorbed vapors or gases. Since the effect of carbon monoxide in changing the resistance of various materials such as molybdenum, platinum, and zinc oxide had been reported (Refs. 7, 8, 9, 10), the requirements appeared to be realisable, although it was recognized even at the inception of the work that specificity to carbon monoxide might require the incorporation of more than one sensor.

In a prior study evaluating commercially available carbon monoxide meters for the National Institute of Occupational Safety and Health (Ref. 11), RTI had found several problems.

Three of six instruments evaluated measured CO concentration by the electrical resistance change of metal-oxide sensors of undisclosed natures. A fourth unit measured electrically the amount of heat produced by the oxidation of CO with a Hopcalite catalyst, a mixture of Ag_2O, CO_3O_4, and MnO_2. The remaining two instruments used non-electrical sensing techniques.

In general, the metal-oxide sensors exhibited inadequacies in maintaining their calibrations, in sensitivity to temperature changes, and in response to interfering species.

Based on the experiments with the commercial instruments, the problems faced by the research team were: 1) obtaining adequate sensitivity for the detection of CO, 2) obtaining calibration stability for the sensor, 3) minimizing effects of humidity and temperature on the response of the sensor, and 4) minimizing or compensating for the response of the sensor to interferants present in mines: CO_2, NO, NO_2 and CH_4.

The weight and power limitations inherent in the design of a portable or personal monitor would bias the choice of sensors against those requiring the use of dessicants or operation at extreme elevated temperatures.

In the next three sections, the theoretical and experimental work describing the interaction of gases with solids (semiconductors) and the ways in which particular molecules can affect the conductivity of the solid are reviewed. This review forms the context for the sensor research performed by RTI, presented in Section 5, and the interpretation of the results presented in Section 6. Recommendations derived from this work are presented in the final section of this report.

2.0 ELECTRONIC INTERACTIONS OF GASES AND SOLIDS

The surfaces of all solids exposed to the atmosphere become coated with a layer of adsorbed molecules, especially oxygen and water vapor.

When a gas molecule approaches a solid surface, it can be adsorbed on that surface by one of two kinds of electronic interaction: the Van der Waals interaction or the exchange interaction. The Van der Waals interaction is electrostatic in nature and can be described in classical terms as the interaction of mutually-induced electric dipoles in the molecule and the surface. The exchange interaction is a binding process in which one or more electrons is transferred (or shared) between two atoms.

In the terminology of Vol'kenshtein (Ref. 12), the Van der Waals force is responsible for "physical" adsorption while the exchange interaction gives rise to "chemical" adsorption. The electron exchange usually amounts to a sharing of the electron (covalent bonding) but there may be ionic character to the bond as well.

The binding energy for physical adsorption is on the order of 10^{-2}-10^{-1} electron volts, while for chemisorption it is on the order of 1 e.v. Thus, physically sorbed molecules are rather easily desorbed by heat, but chemisorbed molecules are not, since the average thermal energy at room temperature is approximately 2.5×10^{-2} e.v. Because of the weakness of the interaction in physical adsorption, the gas molecule can exert very little influence on the electrical conductivity of the solid. It is of little further interest for this reason.

2.1 Chemisorption of Gases on Solids

A detailed discussion of the features of chemisorption and the effect of chemisorbed molecules on the electronic properties of a semiconductor is given in Appendix 1. The major points of the discussion in Appendix 1 are summarized below.

1) Chemisorption is the adsorption process involving exchange of electrons between the gas molecule and the surface. In weak chemisorption the bound molecule remains electrically neutral; in strong chemisorption, the bound molecule has an electric charge.

2) Strong chemisorption accounts for only a few percent of the sorbed molecules, yet it is the process by which the charge carriers in the solid are influenced.

3) Strongly chemisorbed molecules can either increase or decrease the number of free carriers near the surface, depending on the type of gas and the semiconductor. On intrinsic semiconductors, donor- and acceptor-type gases increase the number of charge carriers. On n-type doped semiconductors, donor-type gases increase the number of carriers and acceptor gases decrease the number. The opposite effects hold for p-type doped semiconductors.

4) Donor-type gases are sorbed in large numbers and have greater influence on the number of charge carriers, on p-type semiconductors; acceptor-type gases are sorbed in large numbers and influence the number of free carriers more, on n-type semiconductors.

2.2 Influence of Surface States on Conductivity

The effect of strongly chemisorbed molecules on the resistance of a thin slab of semiconductor is discussed and modeled in Appendix 2. The results of the analysis indicate that the surface to volume ratio of the material must be very large if the absorbed gas molecules are to have a measurable effect on conductivity. Reproducible thin films of metal oxides may be obtained by sputtering or by evaporation and oxidation. As will be discussed below in Section 5, a significant amount of the experimental phase of this effort was spent in the investigation of such thin films of various metal oxides.

Another method of obtaining a high surface to volume ratio is by the use of finely divided material. A compact sensor of such material may be obtained by pressing or sintering, but the reproducibility of structures made in this manner is poor. Gray (Ref. 25) has modeled the electrical properties of such structures, showing that the impedance presented depends upon the frequency of measurement in a manner determined by the mix of boundary layer and bulk properties. Appendix 3 briefly discusses the features of this analysis.

3.0 THERMAL AND CHEMICAL EFFECTS

In the previous discussion little consideration has been given to the actual semiconductor used. The particular semiconductors deemed most promising for the detection of carbon monoxide were the metal oxides. As mentioned in the introduction, several commercial units already use metal oxide sensors. A review of the literature turned up reports by several workers of resistance changes in response to CO, and revealed that many oxides have been investigated for use as oxidation catalysts for CO, indicating a preferential adsorption for CO.

Catalysis proceeds with the weak form of chemisorption in which the binding energies of the molecules to the surface are relatively small. This implies that catalytic efficiency and changes in electrical conductivity are not directly related; but, on the other hand, weak chemisorption is a precursor state to strong chemisorption, indicating that the catalytically active substance may well be useful as a detector material.

Some of the specific properties of metal oxides that contribute to their use as sensors are considered below. Although many of the points refer as well to other semiconductors, emphasis is on the metal oxides.

3.1 Stoichiometry

When the composition of metal oxides is examined, stoichiometry is the exception rather than the rule [Ref. 15]. Variation of the oxygen partial pressure in the atmosphere in contact with the oxide produces a continuously changing quantity of oxygen in the substance. The non-stoichiometry can be manifested as oxygen deficiency or as metal deficiency.

The deficient species may leave vacancies in the crystal structure, or there may be excess atoms of the other species placed interstitially between atoms of the crystal.

These excesses or deficiencies are the source of the semiconductive properties of the oxide. In the regular crystal, the oxygen atoms have a valence charge of -2; the metal atoms, depending on the compound, have a positive valence charge of a magnitude that makes the crystal electrically neutral; for zinc, it would be +2. An oxygen vacancy created in the crystal would have also 2 negative charges associated with the vacancy. This charge is the same as for the regular oxygen atoms, and so with respect to the crystal the vacancy is neutral. If one or both charges are moved away from the vacancy, it becomes positively charged with respect to the crystal. Thus the vacancy becomes an acceptor state, or "hole," in the semiconductor sense as well as in the physical sense.

Metal ion vacancies may similarly be either neutral or effectively negatively charged. On the other hand, interstitial atoms represent excess ions which are injected into the lattice; therefore, a metal ion interstitial is positively charged, and an oxygen interstitial is negative. Because the crystal is electrically neutral, the number of all effective negative charges equals the number of effective positive charges.

In oxygen-deficient oxides of the form MO, with oxygen vacancies predominant, there is a dependence of concentration of defects on the partial pressure of oxygen. If neutral vacancies are formed, the concentration varies as $pO_2^{-1/2}$, where pO_2 is the partial pressure of oxygen. If charged (in the relative sense) oxygen vacancies are formed, there must be a corresponding concentration of electrons to maintain charge neutrality. The concentration of singly charged vacancies then

depends on $pO_2^{-1/4}$, and the concentration of doubly charged vacancies varies as $pO_2^{-1/6}$. These dependences on pO_2 assume that the particular charged vacancy is much more numerous than the other types. The concentration of these defects may show a pressure dependence that varies from $pO_2^{-1/2}$ to $pO_2^{-1/6}$.

If the oxygen deficiency is a result of metal interstitial ions, the same equilibrium conditions apply. Thus, neutral metal interstitials exhibit a $pO_2^{-1/2}$ dependence; singly charged interstitials, a $pO_2^{-1/4}$ dependence; and doubly charged interstitials, a $pO_2^{-1/6}$ dependence. Thus we cannot distinguish between oxygen vacancies and metal interstitials by pressure dependence for compounds of the form MO.

In compounds of the form MO_2, it is possible to separate the effects of the two types of ions in the situation where one type of defect dominates the other. Assuming that only the doubly charged ion species are the predominant ones, when oxygen vacancies are most dominant, the oxygen vacancy concentration varies as $pO_2^{-1/6}$ as before, while the metal ion vacancy varies as $pO_2^{-2/3}$, much more rapidly. If the metal ions dominate the oxygen vacancies, then the metal ion concentration varies as $pO_2^{-1/3}$, while the oxygen vacancy concentration varies as $pO_2^{+1/6}$, actually reversing the direction of its dependence.

In metal deficient oxides of the form MO, neutral defects exhibit a pressure dependence of $pO_2^{1/2}$. Similarly, singly and doubly charged metal vacancies, and the corresponding hole concentrations, vary as $pO_2^{1/4}$ and $pO_2^{1/6}$, respectively. In this type of oxide, the vacancy concentration increases with pressure.

If the compound is close to stoichiometry, then intrinsic ionization of electron and hole pairs has a strong influence on the

concentration of charged vacancies. However, the intrinsic ionization is independent of oxygen partial pressure, so that the pressure dependencies are unchanged.

All of these concentration dependencies are derived from the law of mass action as it applies to the equilibrium of ions which react with one another. As with all mass action phenomena, the equilibrium relation between charged and uncharged defects is a strong function of temperature.

As applied to a practical carbon monoxide detector at atmospheric pressure, the oxygen partial pressure dependencies should have little effect on the equilibrium concentration of vacancies. Barometric pressure changes amount to only a few percent, and the concentration variations are $\underline{n}$ times smaller, where $\underline{n}$ is the exponent of the pressure dependence.

In the laboratory, on the other hand, it is common practice to expose the substance to either air, pure oxygen, or some inert gas such as nitrogen. In such a situation, the partial pressure of oxygen can be varied drastically and the effects on electrical conductivity observed. This provides an important tool for identifying the types of carriers involved in the transport of current.

The temperature dependence of the defect concentrations is another matter. In addition to the equilibrium concentration dependence upon temperature there is a marked effect on the mobility of the defects in the crystal. These imperfections in the crystal can move from one location to another, constituting a diffusion of defects through the crystal. Vacancies can move relatively easily, with a nearest neighbor atom moving from its normal position into the vacancy. Interstitial atoms can move into the next interstitial spot, but the move requires considerable

distortion of the crystal lattice and so is more difficult (less probable). Another mode is called the interstitialcy mechanism (Ref. 15); it involves an interstitial atom moving into a normal location and crowding the normal atom into a vacant interstitial spot.

These diffusion mechanisms provide for the movement of electric charge through the crystal and for the exchange of oxygen atoms in the crystal with those in the air at the surface of the crystal. Because of the finite time required for such transport, there may be a gradual change in the defect population, resulting in a gradual shift of electrical characteristics. Control of this drift, for stable operation of a sensor, requires control of the oxide temperature.

3.2 Competitive Adsorption

The preceding discussion considered only the effect of a single gas adsorbed on the surface of a semiconductor, influencing its conductivity. In a gas mixture, adsorption is competitive, and all the gases in the atmosphere surrounding the semiconductor will be adsorbed on it to some extent.

For strongly chemisorbed gases, the competition takes place not simply because of surface coverage, but because of the influence of the sorbed gases on the chemical potential at the surface. For weak chemisorption, in which the chemical potential is unaffected, competition occurs because of occupancy of adsorption sites.

It should be noted that competition is not necessarily detrimental to the adsorption of a given gas. For example, oxygen strongly chemisorbed on a semiconductor behaves as an acceptor gas, thereby localizing free electrons at the surface and lowering the chemical potential. This makes it easier for a donor gas, such as carbon monoxide, to become ionized and

strongly chemisorbed. Another way of looking at this result is to consider that the negative charges at the surface act to attract more positive holes from the bulk than would normally be the present. The donor gas therefore has a greater hole population to interact with.

Since the effect of interest is the electrical conductivity, competitive adsorption can influence the conductivity in two ways: by covering sites with neutral or weakly sorbed molecules, and by directly influencing the conductivity by strong chemisorption. The weak chemisorption can be expected to reduce the sensitivity of the semiconductor to the presence of the desired gas, while the strong chemisorption can give false indications of the presence of the desired gas.

The strongly chemisorbed molecules also occupy sites in competition with the desired gas, but since the number of chemisorbed molecules is only a few percent of the total of the given species, and since the effect on conductivity of the strongly sorbed molecules is much greater than a simple blocking of the site would produce, the effect of the strongly sorbed molecules by site occupation is negligible.

In a simple model, the area covered by an adsorbed gas can be related to the partial pressure of the gas. Originally developed by Langmuir (Ref. 16), it assumes that condensation and evaporation from a surface are independent processes and that condensation is proportional to the pressure, P, of the gas. Then, if the gas molecule is assumed to occupy only one adsorption site, adsorbate interaction is neglected, and all adsorption sites are assumed equivalent,

$$\theta = \frac{bP}{1 + bP} \tag{1}$$

where θ is the fractional coverage of the surface and $\underline{b}$ is a quantity

that depends on temperature generally and is a function of the condensation and evaporation coefficients. When $\underline{b}$ is small (or P), so that $bP << 1$, then the coverage is proportional to the pressure. When $bP >> 1$, then the coverage is essentially unity, i.e., a monomolecular layer.

This model is so simple that it is remarkable how well it describes the sorption characteristics of many gases over wide ranges of temperature and pressure. If it is assumed applicable to a metal oxide carbon monoxide detector, the model indicates (without any specific knowledge of $\underline{b}$) that in the trace amounts for which measurement is desired, the coverage will be proportional to the gas partial pressure. Also, according to the Langmuir model, atmospheric oxygen will provide a large coverage because of its abundance and tendency to be bound to surfaces.

Mathematical treatments which include nearest-neighbor adsorbate interaction have been formulated [Ref. 27], but will not be discussed here. If there is adsorption of non-interacting molecules, each occupying a single adsorption site, extension of the Langmuir model gives the fractional coverage for each component as

$$\theta_i = \frac{b_i P_i}{1 + \Sigma_j b_j P_j} \qquad (2)$$

where P_i is the partial pressure of the i^{th} species and b_i is a ratio of factors which control the adsorption and desorption rates of the i^{th} species.

When a gaseous species must occupy two adjacent adsorption sites, the Langmuir model for non-interacting molecules has the form

$$\theta = \frac{\sqrt{bP}}{1 + \sqrt{bP}} \quad . \qquad (3)$$

The model could be extended to the case of mixed one-site and two-site non-interacting molecules, but the conformity of the model to a real situation would be difficult to ascertain due to the large number of variables involved. For example, in these models the b parameters have been assumed constant, for a given temperature. In reality, these will depend upon the degree of coverage because the adsorbate molecules will interact to some degree. In addition, as will be discussed below, the adsorbate-adsorbent electronic interactions will influence these rates. Furthermore, there will be a diversity of non-equivalent adsorption sites on the surface. This will also be discussed below. Therefore, the simple models can be used only as an indicator of what might be occurring, not as a definitive measure.

Even though strongly sorbed molecules would not seem to obey the Langmuir model, because the rate of evaporation is very small for a charged molecule, it must be remembered that there is an equilibrium between the populations of strongly sorbed and weakly sorbed molecules. Because of this equilibrium, specified by the chemical potential, a change in the population of the weakly chemisorbed molecules in accordance with the Langmuir model will be reflected in a change in the strongly chemisorbed population.

The Vol'kenshtein theory predicts that strongly chemisorbed gases will exert a direct, strong influence on the electrical conductivity of the semiconductor. If the desired gas to be detected is a donor on the particular semiconductor used, then a competitor gas that is also a donor will show up electrically as the desired gas. Not only that, but

it will also displace the chemical potential downward and make the ionization of the desired gas more difficult.

If the competitor gas is an acceptor, then it will raise the chemical potential and make the ionization of the donor gas much easier. Its effect on the electrical conductivity is in the opposite direction to the desired response (except in the rare case of the intrinsic semiconductor).

The relative displacements of the chemical potential for one added molecule of either gas depends on which energy level lies closer to the chemical potential of the semiconductor. The chemical potential tends to move so that the added energy level is half occupied, which means it moves downward from donor levels and upward from acceptor levels. (Refer to Figure A4 of Appendix 1).

Because of this property, a semiconductor can be made less sensitive to a competitor gas over the desired gas. By suitable doping of the semiconductor or suitable choice of stoichiometry of an oxide, the chemical potential may be situated so the desired gas effects the greater change in the level of the potential, thereby changing the concentration of charge carriers more than the competitor.

If the energy levels of the two gases are close to each other, within the thermal energy range, then the amount of enhancement of sensitivity of one over the other will be small. The only recourse in such a situation would be to pick another semiconductor compound in which the energy levels of the two gases are more widely separated.

When two or more competitor gases give responses similar to the desired gas, very little can be done to separate them by translation

of the chemical potential. The practical instrument must utilize sensors sensitive to each of the competitive gases and by combinations of the outputs of the sensors, the desired response can be deduced.

Finally, since temperature plays an important part in the occupancy of the energy levels, the operating temperature can be chosen to favor a response to the desired gas and decrease the response to an interfering gas.

3.3 Physical Surfaces

As pointed out above, the assumption that all sorption sites are equal, while convenient mathematically, is a very poor approximation for many real surfaces. On physical surfaces there are macroscopic and microscopic defects. Macroscopic defects are those large in comparison with a unit cell of the crystal. On the scale of a macroscopic defect, all the sorption sites can be considered equal, though they may be different away from the defect. Those defects which are of the same size as the unit cell are called microscopic. On this scale, an adsorbed molecule can be considered a defect.

Macroscopic defects can have an influence on the sorption capacity of a surface--for instance, when the crystal is anisotropic and the defect exposes a more (or less active) crystal facet to the gas. Temperature and stress can affect the size and rate of growth of these defects, and be reflected in changing sorption properties. Oxide semiconductors rely on the surface morphology for the exchange of oxygen with the atmosphere, since the binding energy of the oxygen atoms is less at defect locations [Ref. 15]. Other than this notable exception, macroscopic defects are

relatively little affected by the presence of sorbed gases and so have little direct influence on the properties of adsorption.

Micro-defects, whether adsorbed molecules, surface interstitials, or vacancies, behave very differently. They cause a distortion of the lattice in their neighborhood, and because of that distortion, can be influenced by or influence atoms some distance away.

The micro-defects are capable of moving, because the crystal lattice is essentially identical with a periodic variation of potential. In order for a defect to move from one equilibrium site to another, it must attain an excitation energy sufficient to cross the potential barrier between equilibrium sites. The mobility of defects is therefore strongly temperature dependent.

Because of the movement and the distortion of the lattice around the defects, micro-defects can interact with each other, either attracting or repelling each other. This is not because of any electrical charges involved, but because of the differences in lattice distortion and the energy associated with them.

The movement of micro-defects, particularly adsorbed oxygen atoms, is important in renewing the surface of metal oxides after CO is catalytically oxidized to CO_2. Without such a mechanism, the surface sites would have to be replenished through direct collisions with atmospheric oxygen molecules.

Micro-defects can attract free charges and add electrostatic forces to their interactions with one another. In this way, they come to play an important role in the sorption of gases. Charged micro-defects can also add to the electrical conductivity of the surface, although because of their site-hopping characteristics, they would respond only to direct currents or very low frequency alternating currents.

The free charges associated with defects can give a highly variable character to the surface. One region, with an electron bound to it loosely, would be a donor region, while another region, with an associated hole, could be an acceptor region. The areas in between could be neutral and most suited for weak chemisorption. Once the sites are occupied by adsorbed molecules, the local chemical potential is shifted in such a way as to minimize the differences in energy between the charged sites.

This type of inhomogeneous distribution of adsorption tends to average out over the surface, but the number of adsorption sites may be strongly reduced as compared with a defect free surface.

Defects associated with adsorbed oxygen can serve as sorption centers for carbon monoxide in a direct way. We have mentioned in the section on competitive adsorption that, by influencing the free charge distribution, oxygen could enhance the adsorption of CO. In this direct process, the oxygen-associated defect possesses an acceptor energy level that is more easily ionized than a conduction band hole, to which the donor type CO can be adsorbed.

Finally, the thermal and chemical history of the surface can have an important influence on the characterization of the surface. Adsorption of, or reaction with, certain gases may leave the surface in a highly irregular state, enhancing the number of adsorption sites significantly. For example, hydrogen can reduce copper oxide to the metal, and in so doing, leave the surface layer very roughened, with groups of one or more atoms projected well above the surface. Similarly, steam can be used to produce activated charcoal at elevated temperatures; the reaction produces microscopic pores in the charcoal and increases its surface area enormously.

Oppositely, moderate heating of a material can anneal out surface defects as they diffuse to grain boundaries or annihilate one another. Alternatively, oxygen atoms can recombine with the metal supra-surface atoms more tightly than with the ordinary surface atoms and effectively remove them from possible reactions.

All of these effects illustrate the influence of prior exposure on the sorption characteristics of the surface, and represent undesirable impediments to a gas sensor. This dependence on prior history will usually require rather complicated efforts to standardize the sensor, such as heating to a high temperature, purging with a gas, or renormalizing the calibration. It is desirable, if possible, to avoid this.

The theoretical considerations of this section and of Section 2 form the basis for the interpretation of experimental results presented later. To some extent, they influenced the choice of sensor materials (i.e. metal oxides), but more important, they describe the factors that would have to be measured and taken into account to build a successful CO sensor.

Because the search for a sensor was only partially successful, there was little opportunity or incentive to measure the effects described in these two sections, but they were used (in Section 6) to infer which mechanisms were active in the sensors tested.

4.0 PRIOR EXPERIMENTAL RESULTS

In this section, some of the prior experimental work that has been done with carbon monoxide and semiconductor surfaces will be reviewed. Not all of the investigators were directly concerned with electrical conductivity changes due to CO exposure. However, the works reviewed do reveal important aspects of the nature of CO interaction with metal oxide and other semiconductor surfaces.

Much of the prior work has been devoted to studies of the catalytic oxidation of CO to CO_2. It has been stated that catalysis relies on weak chemisorption, which is a precursor state to strong chemisorption. As a consequence, many of the materials which exhibit good catalytic properties will also show conductivity effects. Conversely, materials or treatments which are catalyst poisons will have an adverse effect on the change in conductivity. For these reasons, it is worthwhile to search the literature on catalysis as well as that dealing with electrical conductivity.

Pitzer and Frazer (Ref. 17) investigated manganese dioxide as an active oxidation catalyst. Their results indicated that an active room temperature catalyst could be prepared in a variety of sizes of particles and degrees of purity. Structural analysis of these catalysts indicated that the necessary conditions for oxidation demanded a metal-oxygen spacing of 1.75 Å to 1.85 Å, inclusive, and that the CO molecule be adsorbed with both atoms participating in the bond, i.e., "two-site" adsorption. The only oxides satisfying the interatomic spacing criterion are MnO_2, Co_3O_4, Co_2O_3, and Ni_2O_3. Cupric oxide, CuO, with a spacing of 1.87 Å, becomes active at 70°C.

This work is important for details of preparation of the catalyst and presenting some of the conditions important to room temperature catalysis. Some of these materials, given a suitable non-stoichiometric composition could become suitable gas sensors, when the strong and weak forms of chemisorption could be more competitive.

Terenin and Solonitzin (Ref. 18) studied photosorption and desorption of gases on zinc oxide. The technique allowed the type of surface ions to be determined. Ultraviolet light was used to produce excited states in the ZnO, and infrared light was used to produce thermal desorption. The pressure of the sorbed gas was used as the measure of gas on the surface.

Photodesorption of oxygen was observed only from zinc oxide with excess metal, and that was only for surfaces that had been exposed to oxygen for less than a few hours. The desorbable form of oxygen apparently converts to a more tightly bound form with time at a rather slow rate.

The same ultraviolet illumination leads to a permanent sorption of CO: the pressure drops during illumination and remains constant. Heating by infrared radiation causes a pressure rise which relaxes back to the original state when the radiation is removed.

These effects are attributed to the presence of electrons held at the surface on traps by various effects. The metal-rich semiconductor is an n-type, and the oxygen atoms, being acceptors, are normally bound strongly at the trap sites until a photon excites the complex enough to release them. The long term conversion to a more permanently sorbed form may be due to a change from molecular oxygen to atomic oxygen with consequent stronger bonds. The photosorption of CO is attributed to the oxidation of oxygen ions by the photons with subsequent chemisorption of

the donor-type CO on the oxygen sites. The CO is bound too strongly to be thermally desorbed at room temperature.

Garner, Gray, and Stone (Ref. 19) performed work on the oxidation of copper and the reactions of hydrogen and carbon monoxide with copper oxide. Their investigation included electrical conductivity measurements and are valuable for that reason.

They formed an activated oxide film by repeatedly oxidizing and reducing the copper at elevated temperatures, using oxygen and hydrogen gases. This led to a considerable roughening of the surface, visible to the eye. Then on the roughened copper a Cu_2O film was grown and subjected to reduction by carbon monoxide. The rate of reduction was similar to that obtained using hydrogen, but the process destroyed the activity of the surface. It was not possible to obtain two successive reductions with the carbon monoxide. The activity of the surface could be restored with an intervening hydrogen reduction.

An activated copper oxide sample was placed in a vacuum chamber where controlled amounts of carbon monoxide could be admitted. It was found that the amount adsorbed would cover less than 23% of the apparent (macroscopic) surface; the oxide is also capable of adsorbing oxygen in the activated form. Deactivation of the surface with carbon monoxide reduces or removes this capability.

If an activated oxide surface is exposed to carbon monoxide, then a three step process appears to take place. First, there is an initial rapid adsorption of carbon monoxide. Second, there is a slow reaction between CO and the oxygen adsorbed on the surface producing CO_2, which then evaporates. The last step is further adsorption of CO on the sites

left vacant by the CO_2. These and other results indicate that the surface is saturated with carbon monoxide before slower reactions are able to take place.

Measurements of resistance changes used thin films of copper deposited on Pyrex substrates. These were oxidized at 200°C until a constant resistance was obtained; at this temperature the oxide formed is cupric, CuO, although the presence of some carriers indicates a non-stoichiometric composition (Ref. 20).

Carbon monoxide produced changes in the resistance of CuO films. There was initially a rapid rise to a very high resistance, an equally rapid fall, and then a slight rise in resistance. However, the final resistance was greater than the initial resistance, and the surface was deactivated, as determined by the effect of oxygen on the surface.

Oxygen had the effect of producing an immediate constant decrease in resistance on an activated surface. On a deactivated surface, the decrease in resistance was much less.

When carbon monoxide was applied to a CuO-Cu_2O film that had not been activated with hydrogen, the resistance change, at 20°C, was rapid but small, on the order of 10%; it was reversible, though. The resistance returned to its base line value when all the CO was pumped away.

The interpretation of these resistance changes follows the theory described in Section 2. Oxygen adsorbed on the activated surface acts as an acceptor; it is assumed to be bound in a molecular form, since it can be thermally desorbed. The presence of the negative surface charge increases the hole concentration and therefore lowers the resistance. If the oxygen is desorbed, the hole concentration returns to its former value and the resistance resumes its original value.

The carbon monoxide initially adsorbs at a copper atom, and being a donor gas, quickly binds a hole to it, reducing the hole concentration and raising the resistance. This part of the adsorption is reversible. The carbon monoxide then reacts with mobile oxygen on the surface. The driving force which brings the CO and oxygen together is the electrostatic attraction of the bound hole and electron. The rate of reaction is determined by the activation energy for hopping from one site to another. When the two molecules react, they form a stable carbonate ion, which is negatively charged. This action releases the bound hole which is then free to carry current, and the resistance drops. The CO_2 molecule thus formed is thermally desorbed, leaving behind one oxygen atom. The surface has become deactivated in the process, and the binding energy of the oxygen probably changes, accounting for the slight increase of resistance and its value higher than the original value.

The reversibly bound CO is responsible for the resistance change of the film, while the carbonate ion has only a slight effect. These results also indicate the relation between catalytical activity and resistance change: the unactivated surface at room temperature also showed resistance change, but to a very much smaller degree.

5.0 EXPERIMENTAL WORK

Since the aim of the research program was directed to producing a prototype CO detecting instrument suitable for use in coal mine environments, the top priority initially was given to finding a suitable sensor for the task. This led to a number of simultaneous, parallel efforts. A subcontractor (NCSU) was given responsibility for making thin films of desired semiconductors by inert and reactive gas sputtering methods, and performing the initial screening of these films. The Research Triangle Institute performed detailed testing of those most promising films and also prepared other metal oxide forms for use as candidate sensors.

The oxides and materials tested can be classified in four broad categories according to their form: thin films, compressed powders, evaporated slurries, and miscellaneous. The thin films were the sputtered or evaporated films of the metal oxides envisioned in the original proposal. Compressed powders were samples of commercially available metal oxides, pressed into pellets with various binders and/or holders. The evaporated slurries were oxides prepared in a manner similar to that described by Bott, et al. (Ref. 21). The miscellaneous category includes techniques and devices which are not related to the other types of sensors; they represent some of the imaginative and/or naive suggestions of people involved with this project and their colleagues.

In general, the most sensitive sensors were those in the classes of compressed powders and evaporated slurries. The only devices sensitive to carbon monoxide at room temperature were the slurries. Most of the

thin films made were totally insensitive to CO; some showed slight sensitivity. The miscellaneous devices all failed to show sensitivity to CO. All of the sensors which did respond to CO were not sufficiently reproducible under test conditions to be used in a measuring instrument.

This lack of reproducibility frustrated a thorough investigation of each sensor, since no reliance could be put on measurements taken before and after significant exposures to CO, or temperature cycling. Some sensors even initially exhibited a good response to CO, but subsequently failed completely; it was not possible to determine the causes of the failures, other than by inference.

5.1 Experimental Arrangement

A test chamber which would provide means for heating the sample to well-defined temperatures, for altering the composition of the gas, and for relatively easy exchanging of samples was designed and built. This test chamber is shown in photographs in Figure 1. Sample heating was accomplished with a 100-watt cartridge heater placed in a brass block. The block temperature was measured with a Chromel-Alumel thermocouple inserted into a hole in the block near the upper surface where films were placed. Electrical contact to the prototype sensors was made through two beryllium copper springs providing pressure contacts to either the film directly or to metal electrodes evaporated on the films. The cover for the chamber was made of quartz with a Viton o-ring providing a gas tight seal at the base of the chamber. The volume of the whole chamber was about 120 cm^3, so that a gas flow rate of 100 cm^3/min gave a 1.2-minute time constant, assuming perfect mixing.

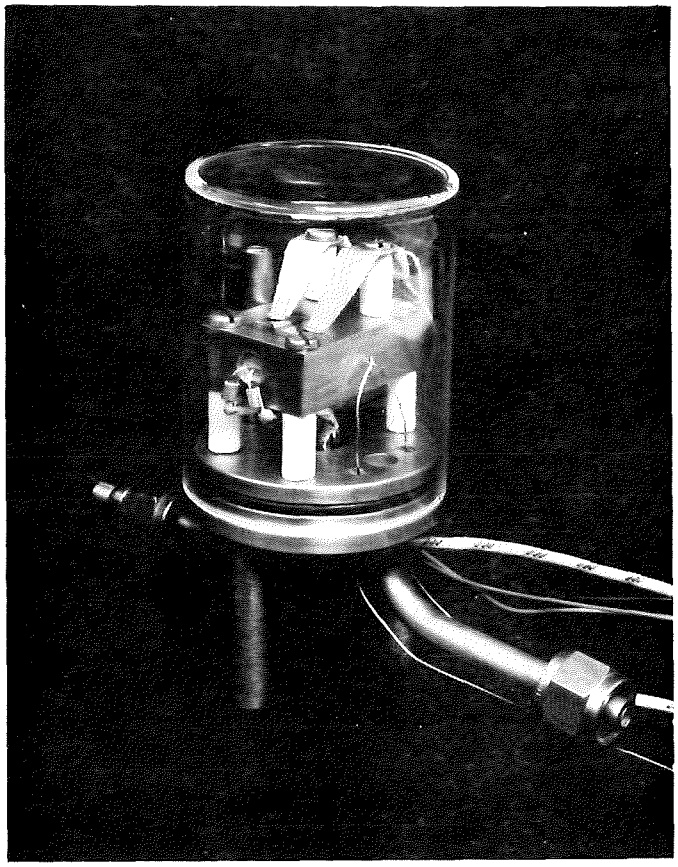

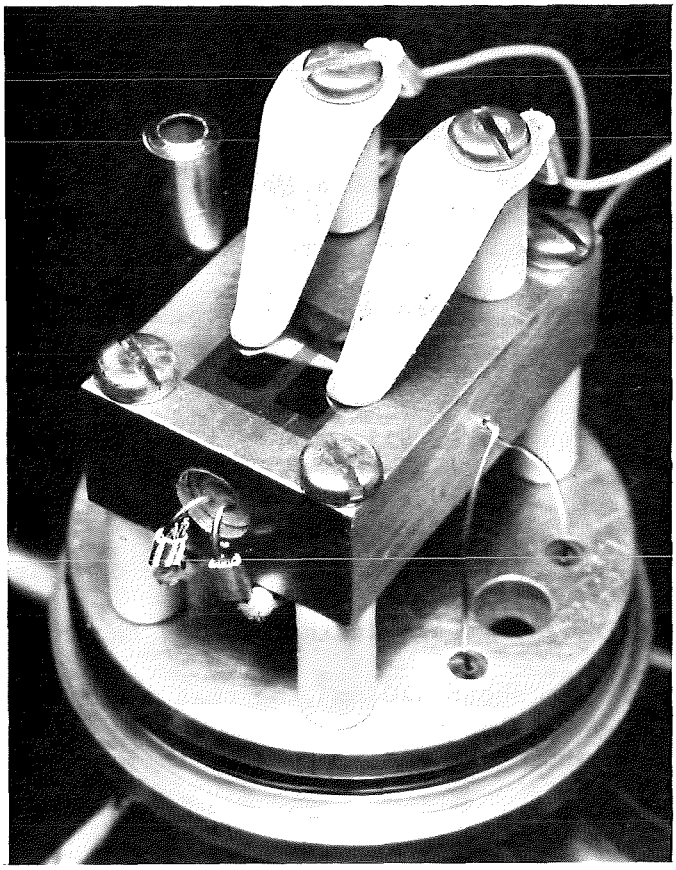

Figure 1. The Test Chamber.

The system controlling gas flow into the test chamber is illustrated in Figure 2. Rotameter flow meters measured the flows of each individual gas, and a single flow meter was used to measure the total flow. Usually, either air or a single CO-air mixture would be used to provide step changes in CO concentration. In testing for response to interfering gases, however, it was necessary (and desirable) to be able to mix several gases at one time. Carbon monoxide-air mixtures, supplied by Scott Research Laboratories, Inc.,* at concentrations of 10.3 ppm, 36.9 ppm, 81.0 ppm, 154.0 ppm and 248 ppm by volume, $\pm$2% tolerance, were used to obtain calibration of sensor response to CO.

In addition to the standard cylinder gases, it is also necessary to provide a source of water vapor, since the mine environment in which the instrument would have to operate is very humid. Standard techniques for humidifying air involve bubbling the air through a water bath maintained at a constant temperature. Since carbon monoxide and the interfering gases are all soluble in water to some extent, this method was not suitable. A diffusion source, illustrated in Figure 3, was used instead. Calibration to verify that the desired quantity of water vapor was being added to the gas stream was obtained by cold trapping moisture and weighing to determine the average mass flow rate at a given water bath temperature and the gas flow rate. The latter was maintained at 100 cm^3/min.

The mass flow rate of water vapor was converted to the environment partial pressure, which was then related to the saturation temperature of the water by dewpoint tables. The calibration curve for this vapor source is shown in Figure 4. From it, the humidity in the gas stream can be set to correspond to a particular saturation temperature by picking the appropriate flask temperature.

*Mention of commercial product names is for informational purposes only and does not imply endorsement by the Bureau of Mines.

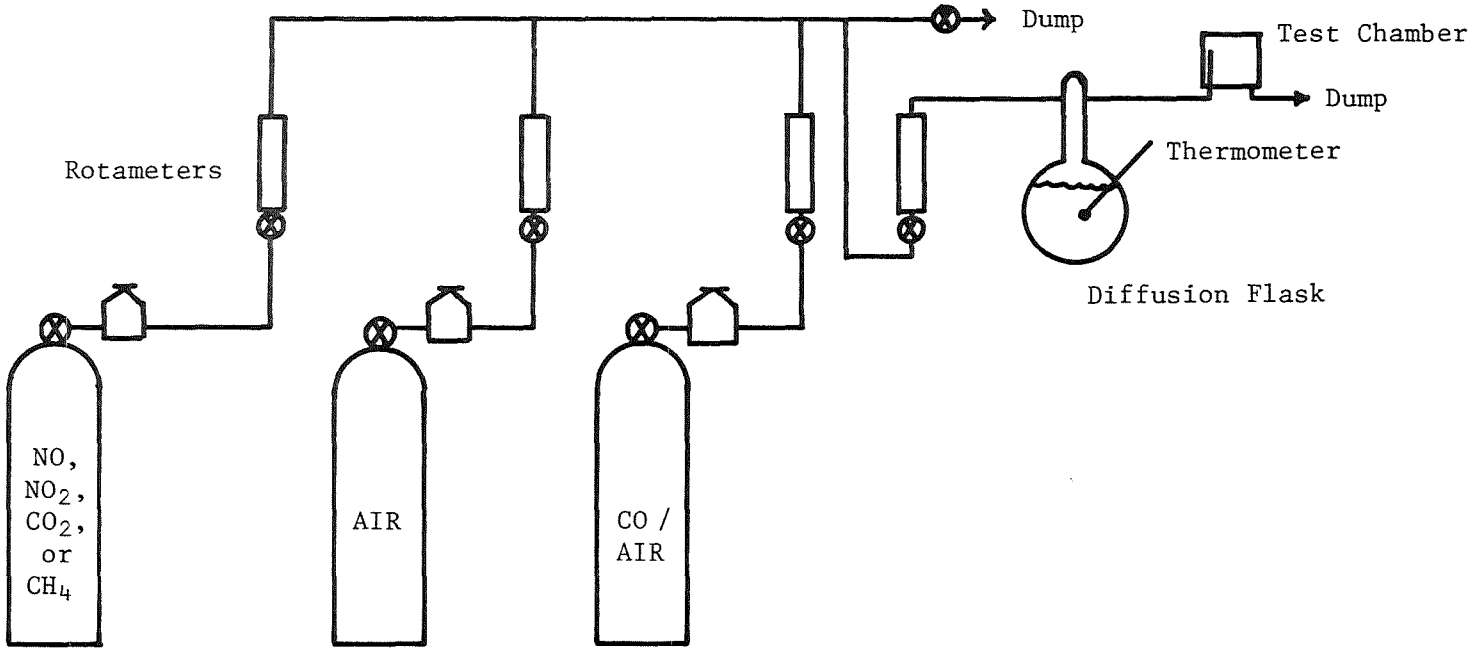

Figure 2. Gas Flow System.

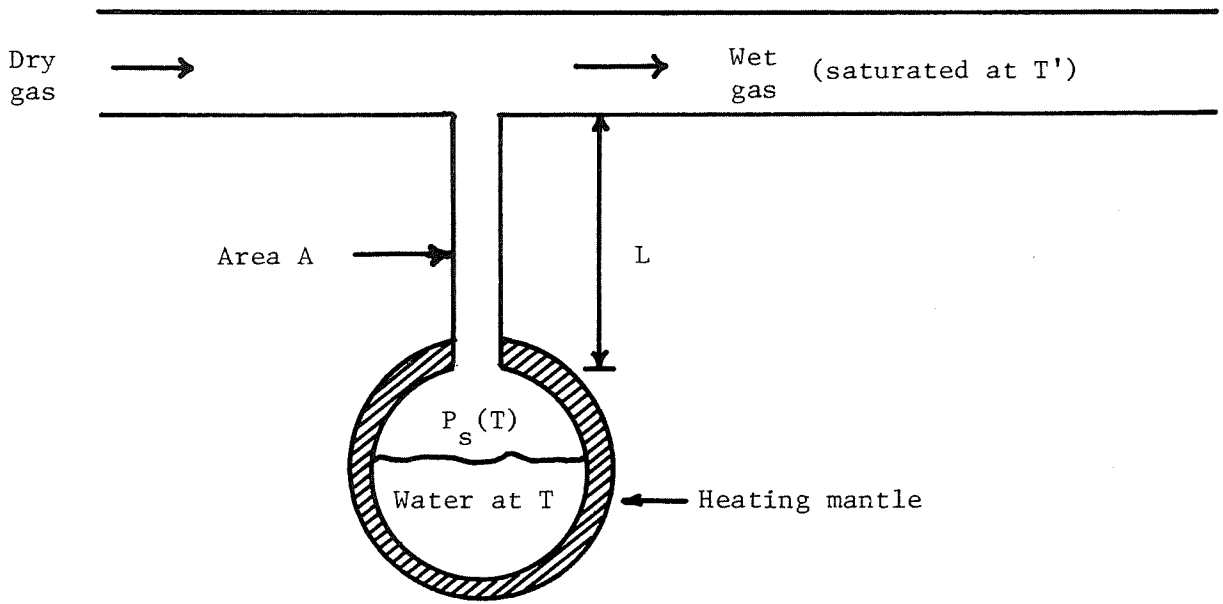

Figure 3. Diffusion Flask.

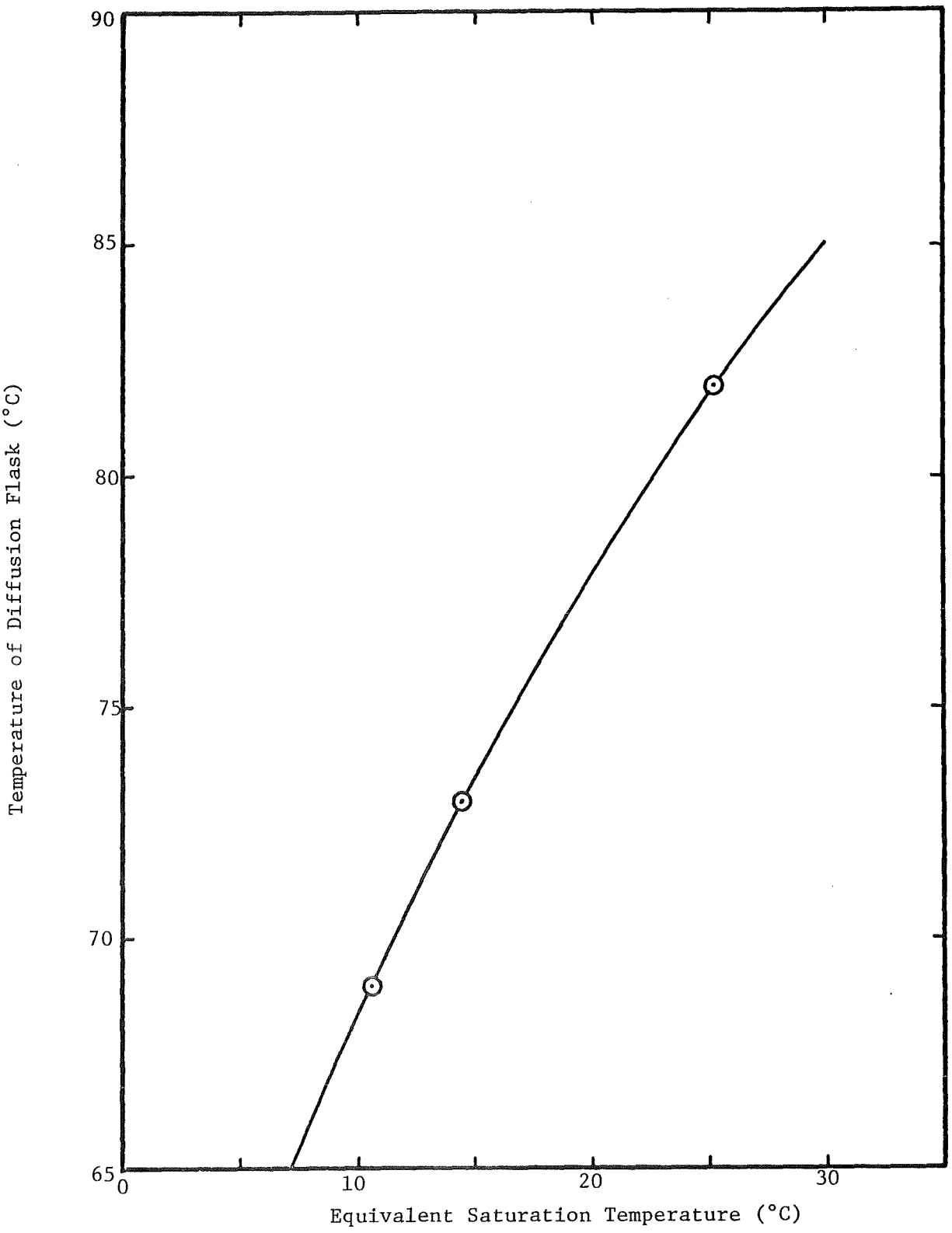

Figure 4. Diffusion Humidifier Calibration.

One unfortunate consequence of this humidifying scheme is its large dead volume. The flask is a 1-liter distilling flask, approximately half full of water. When operated at a temperature of 73°C, the vapor pressure is about 265 mm. This means that approximately 325 cm^3 of volume is available to the flowing gas stream. Interchange of gas in the flowing stream with gas in this volume can occur by diffusion. Therefore, concentration changes in the gas stream will be influenced by this dead volume for a long period of time.

The upper limit for the mass flux of carbon monoxide into the dead volume can be estimated as follows. In the steady state case, the mass flow by diffusion down the length of the tube is given by:

$$\dot{Q} = D \cdot \frac{A}{L} \cdot C_o \ , \qquad (4)$$

where $\dot{Q}$ is the mass flow rate, D is the diffusion constant for carbon monoxide, A is the cross-sectional area of the connecting tube, L the length of the connecting tube, and C_o the concentration within the flask. Assuming that C_o is 248 ppm carbon monoxide, which was the highest concentration used in the tests, then the diffusion from the flask into a gas stream of zero concentration would produce an effective concentration of 7 ppm.

This is a worst case concentration, because it would decrease as the concentration in the flask falls, being proportional to C_o. This source of carbon monoxide in the "zero-concentration" stream is generally negligible for the sensors we evaluated, but for a careful calibration of a sensor, it would certainly have to be taken into account. It would also be important for runs of a low concentration of CO immediately following a run of high concentration.

5.2 Thin Film Sensors

The response to CO of the thin film sensors evaluated in this research are summarized in Figure 5. Of all the sputtered films tested, only MnO_2 and copper oxide showed any response to carbon monoxide. This material responded slightly at temperatures of 250-300°C when freshly prepared. Subsequent measurements showed no response.

For the purpose of defining a resistance response to CO, we define the quantity Δ:

$$\Delta = \frac{R-R_o}{R_o} , \qquad (5)$$

where R is the resistance at a given CO concentration and R_o is the resistance at zero concentration. A negative Δ implies a decrease in resistance. The concentration at which Δ is measured will be specified because there is no indication that Δ is proportional to the concentration.

A more detailed description of the preparation and characteristics of each type of film will follow.

ZnO:

ZnO films were sputtered in argon at room temperature, 100°C, and 200°C. With ohmic aluminum contacts on top of the film, resistances were too high to measure ($\sim$100 MΩ) at temperatures less than 300°C, the highest temperature attainable. These films showed no sensitivity to CO, that is, no decrease of resistance to a measurable value.

ZnO films with contacts underneath the film showed somewhat lower resistance ($\sim$30M) and were very sensitive to water vapor. No response to CO was observed. Resistances on these films were unstable at T>150°C, with R slowly rising. All the films were 1800Å thick.

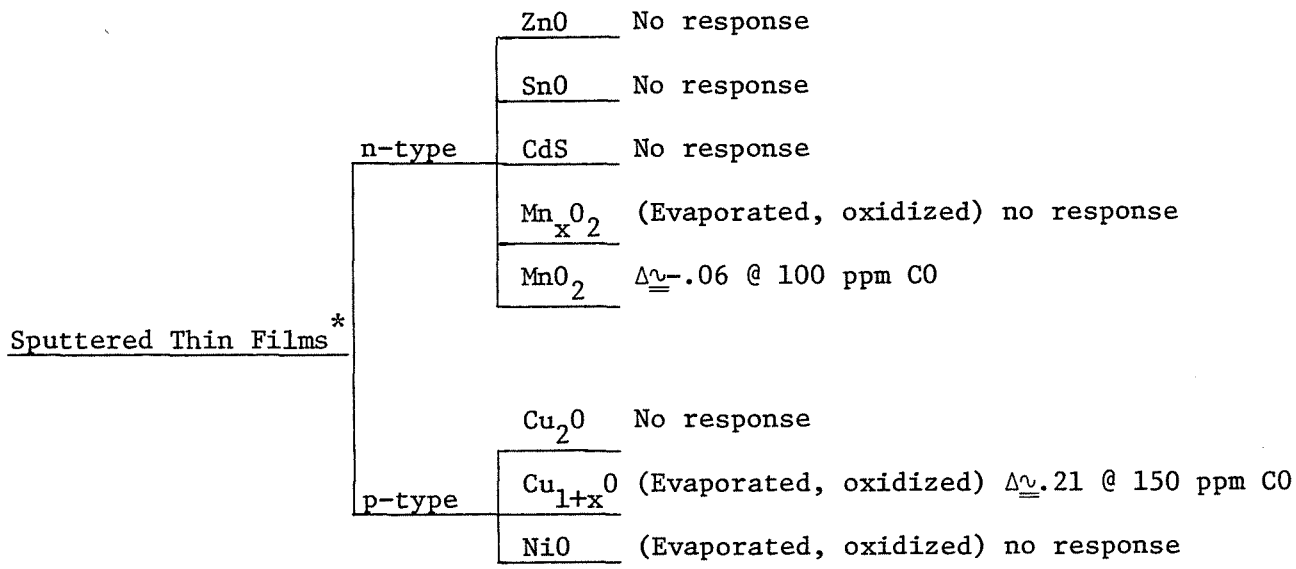

*(Evaporated if noted)

Figure 5. Response of Thin Films.

SnO:

1500-Å films were sputtered on glass slides and tested at 25°C-150°C. The impedance was ∿2-4.3 × $10^9\Omega$, and there was no response to 36.9 ppm CO/air (humidity generator, 65°C). There was an impedance drift unrelated to CO concentration.

CdS:

CdS films were sputtered on glass slides. Aluminum contacts evaporated on top of the films were found to be ohmic. Various combinations of substrate temperatures (27°C, 100°C, 200°C, and 300°C), film thickness (600 to 2400 Angstroms), and plasmas (100% Ar, 50% Ar-50% N_2) were tried. All cadmium sulphide films exhibited cracking and none had any measurable response to CO (100 ppm) mixed in air. Typically film resistance was 50 MΩ.

Mn_xO_2:

∿10,000-Å film of Mn were evaporated on glass slides and oxidized at 200°C in dry O_2 for 6 days. They were tested at temperatures of 25°C-200°C, exhibited impedances near 1 × 10^{10} ohms, and showed no response to 248 ppm CO/air. The actual oxidation state of the manganese was unknown.

MnO_2:

MnO_2 films were sputtered in argon and argon-oxygen mixtures in various thicknesses. The films that showed response to CO were those with oxygen sputtering concentrations greater than 50% and thicknesses of 1200 to 3000 Å. The film impedances were on the order of 2 × 10^6 ohms, and response to CO was $\Delta \simeq -.06$ at 100 ppm CO for T = 250-325°C. Films showing no response had impedances on the order of 2 × 10^8 ohms. The response to CO could not be reproduced in moving from NCSU to the Research Triangle Park. A more detailed description of the sputtered MnO_2 films is contained in Appendix 4.

$Cu_{1+x}O$:

2000-Å films of copper were evaporated on glass slides and oxidized in O_2 at 380°C for 16 hours; these conditions favor strongly the formation of CuO. The film impedance was about 1×10^5 ohms. Response to 154 ppm CO at 200°C was $\Delta \simeq .21$, the resistance increasing. The response time was very long, greater than one hour to equilibrate in CO or in returning to pure air.

NiO

2000-Å films of Ni were evaporated on glass slides and oxidized at 360°C in dry O_2 for 20 hours. At test temperatures of 25°C-200°C, the impedance was $\sim 5 \times 10^8$ ohms, but there was no response to 248 ppm CO.

The first sputtered films of ZnO and all of the CdS films had aluminum contacts evaporated over the ends of the films for contacts. The high resistances encountered led to a procedure of putting the aluminum contacts on the glass slides before the sputtering of the target material.

5.3 Miscellaneous Devices

One of the first devices tested as a carbon monoxide sensor was a thermistor. Thermistors are composed of sintered oxides of uranium, thorium and other metals and are produced with a resistance characteristic which is a strong fucntion of temperature. We were interested in its response to CO, however.

The thermistor used was a Yellow Springs Instruments #44018. The thermistor itself is a small epoxy-coated bead with wires attached. The bead was mounted at the end of a glass tube with wax, and the tube-thermistor

combination was lapped on a flat plate with 12μ alumina until the active element appeared. The thermistor was demounted and cleaned with acetone, and then tested. It showed no response to CO at 100°C and 154 ppm CO.

This result, upon reflection, is not surprising, since the manufacturing process produces a densely sintered oxide with a relatively low resistance ($\sim 10^4$ ohms). There is, therefore, very little surface area on which gases can be sorbed. Nonetheless, the availability of these sensors, their compact size, and their reproducibility were attractive enough to make the attempt worthwhile.

Another commercial device that was tested was a transistor, specifically a 2N441 and a 2N526. These devices are non-passivated, meaning that the actual p-n junctions are exposed inside the transistor can. It was felt that the depletion region inside a reverse biased p-n junction would be very sensitive to carriers induced by an adsorbed gas.

On both types of transistors, some effects were observed at reverse biases of 5-10 volts (collector to base) initially. More careful measurements showed no response to 154 ppm CO at room temperature. It is suspected that the effects observed were due more to atmospheric oxygen and water vapor than anything else. Operation at elevated temperatures was not attempted, and, in any case, these germanium units could not be used above 80°C without thermal degradation of their performance.

A third method attempted to measure the heat of reaction of $CO + 1/2\ O_2 \rightarrow CO_2$. The idea was to measure the resistance of a germanium substrate (intrinsic conductivity) on which a catalytic film of CuO or

MnO_2 was deposited. Substrate thicknesses of 42 microns and 240 microns were used, the thinner ones produced by etching thicker ones. Metal films of copper or manganese, evaporated onto those substrates, were oxidized at 200°C in pure O_2. There was no response of either type of device to CO at room temperature, using 248 ppm CO.

The failure of this technique could be either in the small amount of heat produced by the CO reacting, or by failure of the specific films to be good catalysts. We feel it likely that the second explanation has the major bearing in this case. Calculations indicated that there should be a reasonably large change in resistance, provided most of the carbon monoxide was oxidized on the surface of the sensor.

The commercial CO instrument described in Section 1 uses a similar technique, catalytic oxidation with detection of heat generated, with the exception that a very much larger amount of catalyst is used, in a finely divided state. With larger gas flow rates possible, the heat generated would be much larger, and temperature differences easier to detect and measure.

The final unusual device to be tested was a radio-frequency resonant circuit with an MnO_2 catalyst in the tank circuit (placed within the inductance coil). As carbon monoxide is absorbed on the surface of the powder, the conductivity of the powder would change and affect the circulating current in the tank circuit. The potential value of the technique is based on two premises: 1) that radio-frequency currents can only penetrate a conductor to a depth known as the skin depth and 2) that the circulating currents in a high Q resonant circuit can be very large, so that the magnetic flux is much larger than in an inductor by itself.

If the skin depth is of the same order as the Debye length of a conductor, then only that region near the surface which is affected by adsorbed gases would contribute to the change in conductivity and hence the circulating current.

Also, the Q of the circuit is defined as the power stored per cycle. This can be written in terms of the inductive energy stored and resistive power dissipated as:

$$Q = 2\pi fLI^2/I^2R = X_L/R \tag{6}$$

where L is the circuit inductance, and X_L is its reactance. Analysis of the response of the resonant circuit also gives for Q,

$$Q = f_o/\Delta f \ , \tag{7}$$

where f_o is the resonant frequency, and Δf is the difference between the upper and lower half-power frequencies of the circuit. Combining the two, we obtain

$$R = 2\pi L\Delta f \ . \tag{8}$$

The advantage here is that frequencies can be measured with great precision, even when the differences are small. For a Q of 100, at a frequency of 10^7 Hz, the precision of Δf would be a part in 10^5 typically, and any small change in R would be easily measured as a change in Δf.

Unfortunately, calculation of the skin depth for MnO_2 yields a value larger than the size of the sample, meaning that no advantage is gained from that consideration. Also, the effective series resistance

of the MnO_2 is so low that the circuit elements have far greater losses in the simply constructed circuit tried. Therefore, the change in R in Equation (8) was so small as to be undetectable. This was borne out in the observations.

A series resonant circuit was used with a small series resistor to monitor the current. The coil was 1/2-inch in diameter and the coil sample filling factor was 40%, assuming a sample packing of 70%. At about 9 MHz, manganese dioxide gave a Q of 28, cupric sulfide gave 33, and ammonium molybdate gave 34; but no response to 154 ppm CO could be detected at room temperature for any of these compounds.

Given a material with more carefully chosen conductivity and components optimized at a given frequency, the method might have some chance of success, especially at elevated temperatures.

5.4 Compressed Powders

Because there have been many references in the literature to the use of powdered materials for the detection of carbon monoxide, a series of experiments was undertaken to investigate their potential. The first materials chosen were titanium and manganese dioxides, primarily because of their availability and prior use as catalytic agents.

The first attempts to form sensors involved pressing the powders with various binders to form pellets, and then removing the binder. Parafin was was a good binder in holding the powders, but when it was was burned out in an oxygen atmosphere at 200°C, the pellets collapsed. Ordinary water was tried as a binder. With it, no TiO_2 pellets could be formed, and the MnO_2 pellets cracked apart after partial drying. The pressure used in forming these pellets was 25,000 psia, applied by a piston in a die.

Attempts to solidify the powders into pellets without a binder also failed. A chemist at the Institute suggested a polymer binder, polyisoprene sulfone; it could be vaporized at temperatures of 140-200°C. The pellets formed from 50:50 mixtures of the powder and binder were stable at room temperature, but collapsed when heated. They were tested for response to carbon monoxide before being heated, but there was no response. This concluded attempts to find a binder, and also all efforts at using TiO_2 as a sensing material.

The next attempt with MnO_2 powder involved pressing a small amount into the surface of a small Teflon (PTFE) disc. There was enough pressure to embed MnO_2 particles in the surface. The room temperature resistance of such a disc was about 200 ohm. The disc exhibited the first fast response to CO that was observed. (The CuO evaporated film, with its slow response, has been the first sensor to respond to CO.) A plot of this response to step changes in CO concentration is shown in Figure 6.

The time response is so fast at the first step change that it is probably determined by the time constant of the test chamber itself. The response to the switching of flowing CO to zero is not as rapid; this is due to a non-linear response to the concentration of carbon monoxide. The figure also indicates that the zero-concentration resistance is not the same before and after exposure to CO.

One of the major limitations of the Teflon-disc sensor is its variability. Repeated cycles of CO in air followed by pure air do not give the same Δ. Temperature cycles also affected the discs, causing them to become intermittent and eventually open-circuited. Much of this variability is due to the mechanical movement of the powder,

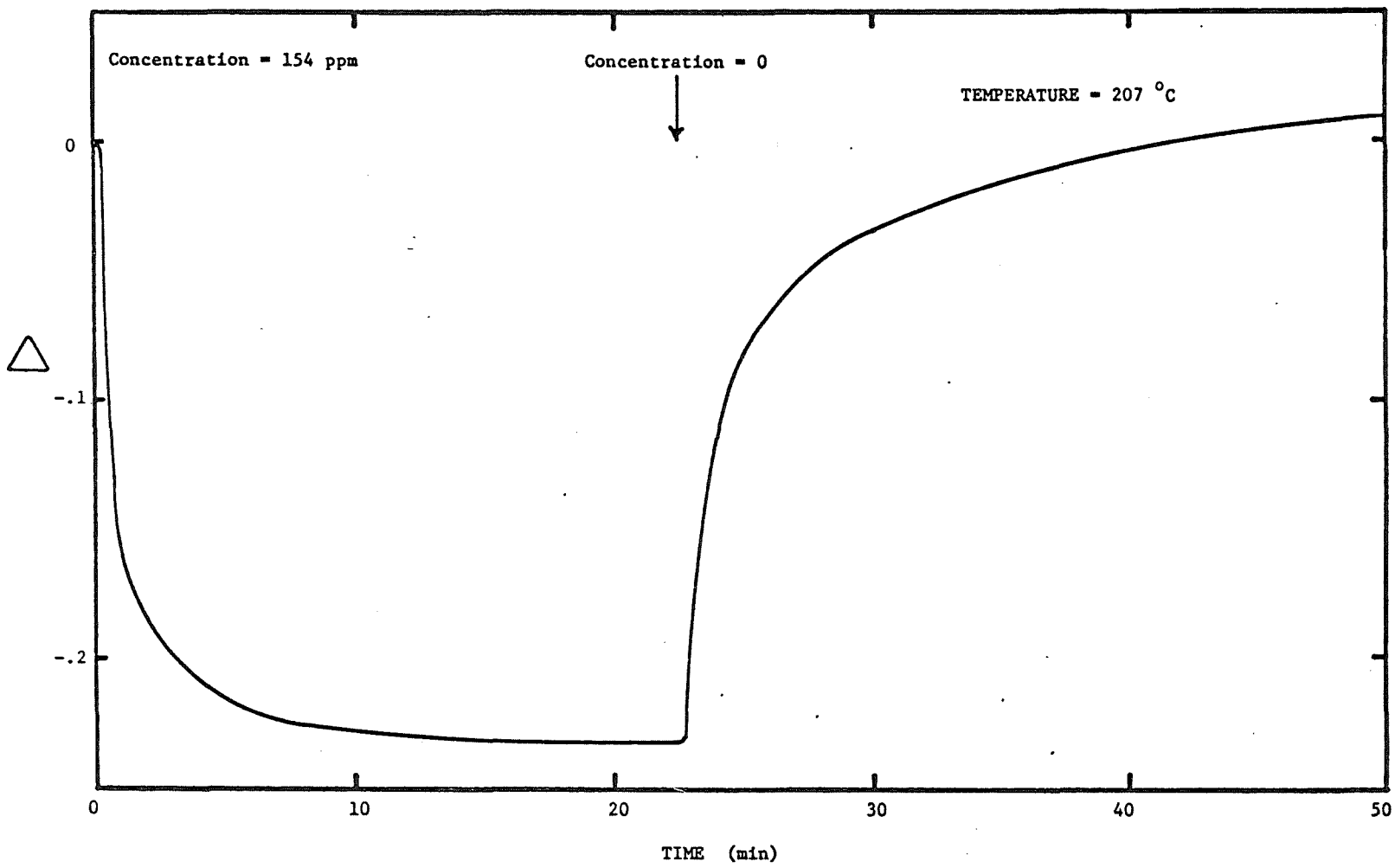

Figure 6. Response of MnO_2 Sensor to Step Changes of Carbon Monoxide.

either by thermal expansion of the Teflon, by mechanical vibration, or even by the chemical reactions on the surface of the material.

Since the MnO_2 powder showed no tendency to partially sinter under application of heat and pressure, even with electrical sintering (which causes strong local heating at the points of contact between grains), many different configurations and mounting techniques were tried in hopes of finding a reproducible sensor.

One approach was to sprinkle MnO_2 powders onto epoxy-coated glass substrates which were then allowed to cure. It was hoped that this would lead to a permanent arrangement of the fine crystals. Various epoxies were used, and in a few cases the powder was stirred into the curing epoxy.

These sensors exhibited moderate resistances at room temperature, but when heated, the resistance increased very rapidly, presumably due to the expansion of the epoxy. No response to CO was found.

Similar results were found using RTV-201, a self-vulcanizing rubber. The expansion coefficient for RTV rubber is even larger than for the epoxies used, and the resistance of the sensor quickly became infinite as the temperature was raised.

Some low expansion substrates (quartz, ceramic, and pyrex) were coated with some high temperature epoxies specifically designed for low thermal expansion. They were cured at 200°C. These sensors exhibited a resistance characteristic which decreased as the temperature was raised, indicating that it was primarily the semiconducting properties of the MnO_2 which were affecting the resistance. Nonetheless, these sensors showed no response to CO.

The ultimate configuration used was a Teflon disc with a shallow depression cut into its upper surface. Two small diameter gold wires were laid at the bottom of the cut-out for better contact to the pressed powder. This configuration allowed the powder to be pressed into a more cylindrical shape, and the elasticity of the Teflon walls of the cut-out provided a continuous force on the powder.

These sensors exhibited room temperature resistances from a few hundred ohms to a few thousand ohms. The resistance initially increased with temperature, reaching a peak at about 150°C and decreasing from there. The resistance at 200°C was usually less than the room temperature value. The peak in resistance is again due to the thermal expansion of the Teflon, since the contact between powder grains becomes worse as the force holding them together is reduced.

The overall characteristics are presented in the following figures. Figure 7 shows the concentration dependence of Δ for three different conditions of water vapor. Figure 8 (page 50) shows the temperature dependence of Δ at a fixed concentration, and Figure 9 (page52) shows the effects of interfering gases on Δ. The data shown are for different sensors in each figure and cannot therefore be compared with each other.

Figure 7 represents data taken on one of the early MnO_2-Teflon discs. All the points were taken at a sensor temperature of 207°C. The partial pressure of water vapor was determined from the flask calibration curve, Figure 4. Three standard CO mixtures were used: 36.9 ppm, 154 ppm, and 248 ppm; the total gas flow rate was held constant at 100 cm^3/min. The data shown are averages of several runs, with the error bars indicating the spread in measured values.

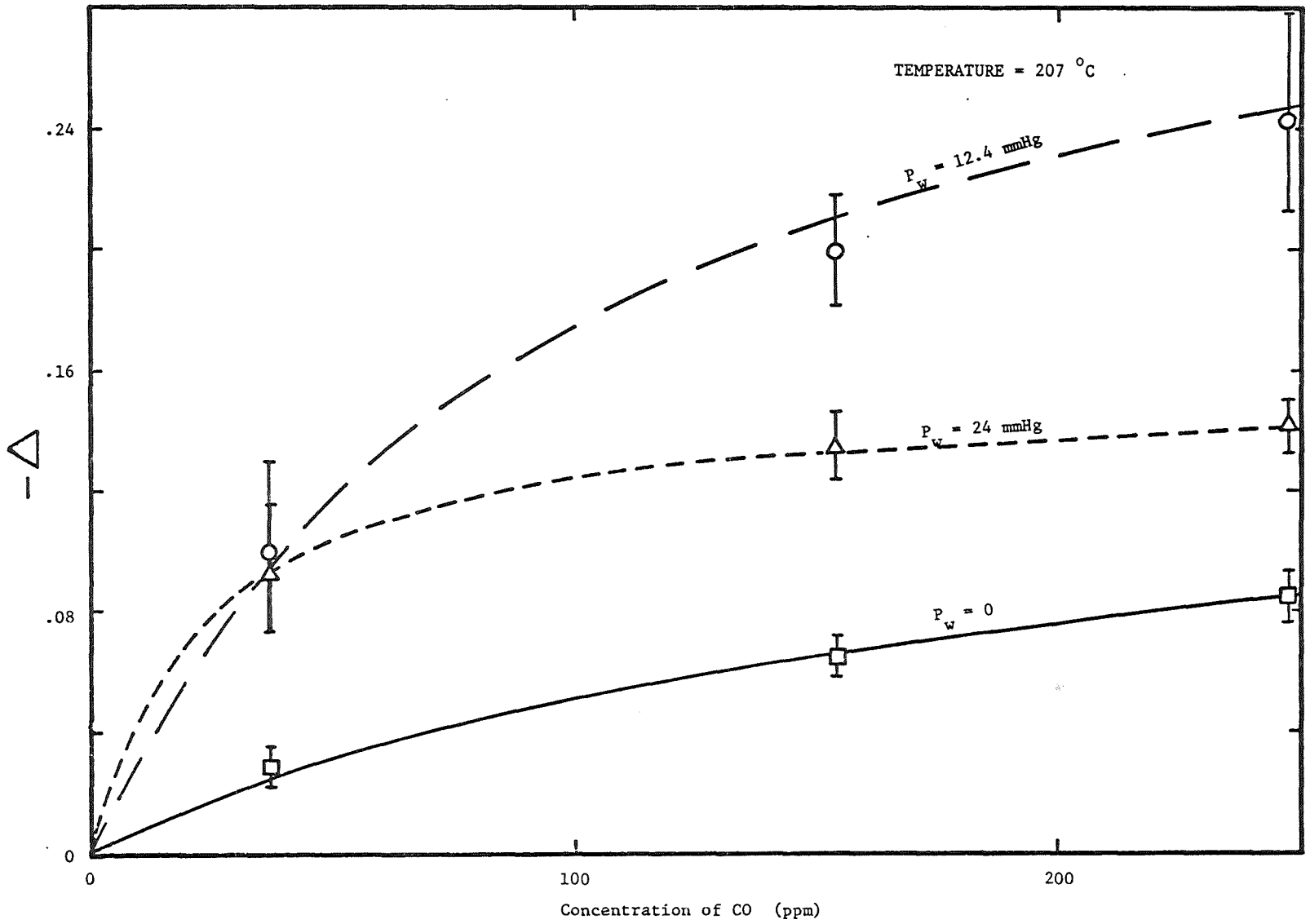

Figure 7. Response of MnO_2 Sensor to Carbon Monoxide with Water Vapor.

The curves drawn through each set of data points are expressions of Langmuir adsorption isotherms, Equation 1. The reasoning behind attempting such a fit is the following. Assuming the change in resistance, R_o-R, is proportional to the number of carriers added by the adsorbed gas, and if we also assume the gas molecules follow the Langmuir adsorption isotherm, then Δ should also. These assumptions are weak in the absence of confirming experimental evidence, but they should be at least approximately correct for small concentrations of gas. A more correct expression would involve the conductance intrinsic to the material, σ_i, and the conductance due to the adsorbed gas, σ_g.

Then, as long as the gas-induced conductance is proportional to the number of adsorbed molecules, as discussed in the models of Appendix 2, Δ can be shown to exhibit a Langmuirian dependence.

$$\Delta = A \cdot \frac{BP}{1+BP} , \qquad (9)$$

where P is the CO concentration in the air mixture.

The significance of the fit is not to be overemphasized, because there are only three data points to fit to two parameters; but the fits give an accurate representation of the data and illustrate two important points--namely, that the response of the sensor to CO is non-linear and that it tends to saturate at high concentrations.

From Figure 7, we see that the presence of water vapor tends to enhance the response of the sensor. As the water vapor pressure increases from zero to 12.4 mm, the response of the detector approximately triples for the concentrations measured. But as the water vapor pressure is further increased, the sensitivity decreases and the evidence of saturation begins to set in. The response to 36.9 ppm CO is nearly the

same for the two series with water vapor present, suggesting that at low concentrations of CO, the response is independent of water vapor pressure over certain broad ranges.

We speculate that adsorbed water molecules enhance the response of the sensor to CO by reducing the activation energy of chemisorption. Thus, for a fixed number of sites on the semiconductor, more of them will be occupied by strongly sorbed CO molecules when water molecules are present than when water molecules are not present. This may be the result of a hydrogen bond between the water molecule and the oxygen atom of the CO molecule, or it may be the result of formation of a radical involving atomic oxygen as well, such as a bicarbonate radical.

In any event, it appears that further increase in the pressure of water vapor results in competition for the available sites, with the result that Δ saturates at the higher concentrations of CO. A summary of the parameters of the fits is given in Table 1. The table also includes fitting parameters for the last MnO_2-Teflon sensor made, on which chemical interference tests were run, designated Unit 2.

Table 1

Fitting Parameters for $\Delta = A \frac{BP}{1+BP}$

	Water Vapor Pressure (mm)	A	B $(ppm)^{-1}$	A·B
Unit 1.	0.0	.156	.00495	7.72×10^{-4}
	12.4	.343	.0105	36.0×10^{-4}
	24.0	.156	.0405	63.2×10^{-4}
Unit 2.	0.0	.189	.00697	13.2×10^{-4}
	9.5	.281	.0226	63.5×10^{-4}
	12.4	.243	.0321	78.0×10^{-4}

The table illustrates some of the variability between units; for instance, Unit 2, under dry conditions exhibits almost twice the sensitivity (A·B) of Unit 1. The values of A are the saturation values for Δ, while the product A·B is the slope of the curve, or the sensitivity, at zero concentration.

There are two features of interest to be gleaned from the table. The saturation values of Δ for Unit 1 are the same for dry conditions and 24 mm water vapor pressure. Also, the saturation values for Units 1 and 2 with water vapor indicate that the response is enhanced most for the lowest pressure and declines with increasing pressure. These effects seem to be related and will be discussed in the next section.

The fact that the variation of Δ with concentration is not linear has implications for the observed rise and fall times of the sensor. Making the assumption that the actual concentration of CO in the test chamber is an exponentially changing function of time, and that Δ is given by Equation 9, we can derive expressions for the apparent time constant of the sensor. Assume the chamber time constant is τ, so that on increasing the concentration from zero to C_M, the concentration in the chamber obeys:

$$C(t) = C_M[1 - e^{-t/\tau}] \tag{10}$$

and upon decreasing the flow concentration to zero, the chamber concentration responds:

$$C(t) = C_M e^{-t/\tau}. \tag{11}$$

We define the effective time constant of the sensor on filling by the relation:

$$\Delta(\tau_1) = \Delta_M[1 - e^{-1}], \tag{12}$$

and the effective time constant on emptying the chamber by:

$$\Delta(\tau_2) = \Delta_M e^{-1}, \tag{13}$$

where Δ_M is the equilibrium value of Δ for a given CO concentration, C_M. That is, on filling, Δ will reach 63% of its final value in time τ_1 and, on emptying, will lose 63% of its initial value in time τ_2. These are standard definitions of time constants. We then derive the following relations for τ_1 and τ_2.

$$\tau_1 = -\tau \ln \left[\frac{e^{-1}(1 + B\ C_M)}{(1 + e^{-1}\ B\ C_M)}\right]. \tag{14}$$

$$\tau_2 = -\tau \ln \left[\frac{e^{-1}}{(1 + B\ C_M(1-e^{-1}))}\right]. \tag{15}$$

Both of the logarithm terms are negative, so that τ_1 and τ_2 are positive. For any concentration, C_M, τ_1 is always less than τ and τ_2 is always greater than τ.

The fact that τ_1 and τ_2 depend on the concentration of CO used indicates that the rise and fall responses are not truly exponential. This may not always be apparent on a recorder chart without careful point-plotting, and it is reasonable that the definitions of τ_1 and τ_2 given by Equations 12 and 13 will be used. Table 2 gives some representative values for τ_1 and τ_2, using the value of B for Unit 1-dry from Table 1.

Table 2

Values of τ_1 and τ_2

C_M(ppm)	τ_1	τ_2
36.9	.89τ	1.10τ
154	.67τ	1.38τ
248	.56τ	1.56τ

The table shows that the difference between the effective time constants becomes larger as the higher concentrations are used.

Figure 6 shows the time response of Unit 1-dry, and the values of τ_1 and τ_2 are .75 min and 2.25 min, respectively, for 154 ppm CO. These values indicate a test chamber time constant of $\sim$1.3 min, but predictions taken from Table 2 are not exact. This may be due to the fact that the mixing of gases in the chamber is not perfect, giving the chamber itself a nonexponential characteristic. Furthermore, τ_1 and τ_2 are determined primarily by the low concentration dependence of Δ through the term BC_M, so that the paucity of data may be responsible.

This calculated chamber time constant of 1.3 min is in good agreement with the time constant calculated from the flow rate and chamber volume, approximately 1.2 min.

In principle it is possible to eliminate τ between Equations 14 and 15 and so obtain BC_M from measured rise and fall times. The equation so derived is not analytic, though, and would have to be solved numerically. Still, this is a possible way to determine the concentration dependence from its response time characteristics.

The temperature dependence of Δ in Figure 8 shows the steep characteristic of an activation-energy-determined process. The peaking at high temperatures indicates an activation of all possible states, so that Δ no longer depends on temperature exponentially, and desorption of the molecules becomes the determining factor on Δ.

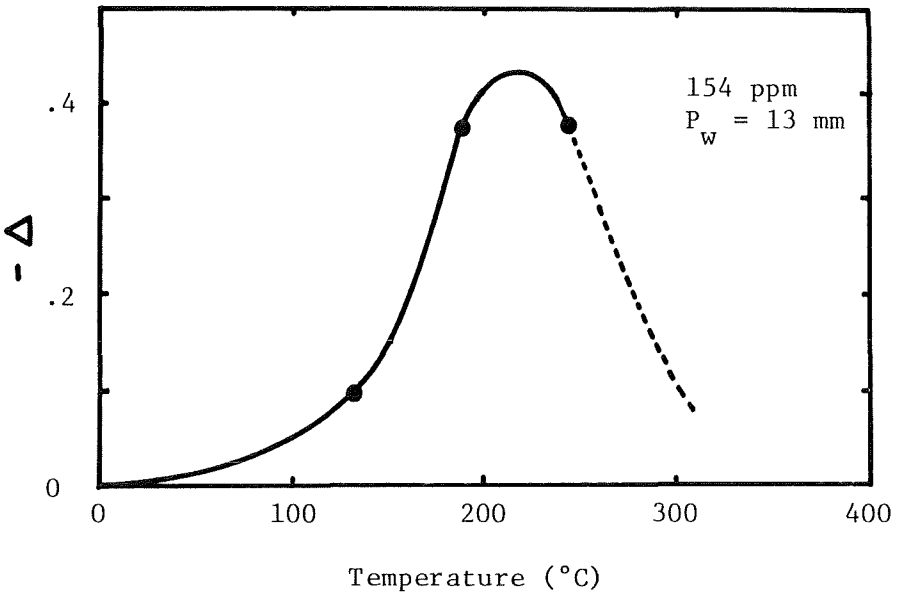

Figure 8. Temperature Response.

According to Rideal (Ref. 20), the coefficients of the Langmuir isotherm are temperature dependent for adsorption of a gas. That is,

$$\theta = \frac{Pb_T}{1 + Pb_T} , \tag{16}$$

where θ is the fractional coverage and b_T is in the form

$$b_T = D\, T^{-5/2}\, e^{-E/RT} . \tag{17}$$

The function b_T has a maximum value at

$$T_{max} = \frac{2}{5}\frac{E}{R} . \qquad (18)$$

The line drawn through the points in Figure 8 was calculated on the basis of these assumptions, but unphysical (negative) constants were required to do so. Unlikely as it seems that the Δ response would be measured at precisely the two temperatures at which it would be equal, the response of an MnO_2 sputtered film also showed a peak in response as a function of temperature. The binding energy corresponding to the peak temperature response is 2.4 kcal/mole, a very reasonable energy for chemisorbed molecules.

The form of Equation 17 shows competing temperature terms, which correspond to the processes of activated chemisorption and evaporation (desorption) of the molecules. The actual exponent of T is determined by the physical processes and may well be different from -5/2. It does not include other temperature-dependent effects which could be expected, such as surface reactions, changes in the intrinsic electron-hole population, etc.

It is important to note that there is a fairly broad temperature range over which Δ is approximately constant, which means that much less stringent temperature regulation would be required to eliminate temperature-induced calibration changes in a CO-detecting instrument.

Figure 9 details the effects of various interfering gases in comparison to the carbon monoxide response. These tests were run on the Teflon-disc labeled Unit 2 in Table 1 under dry conditions and with a water vapor pressure of 12.4 mm.

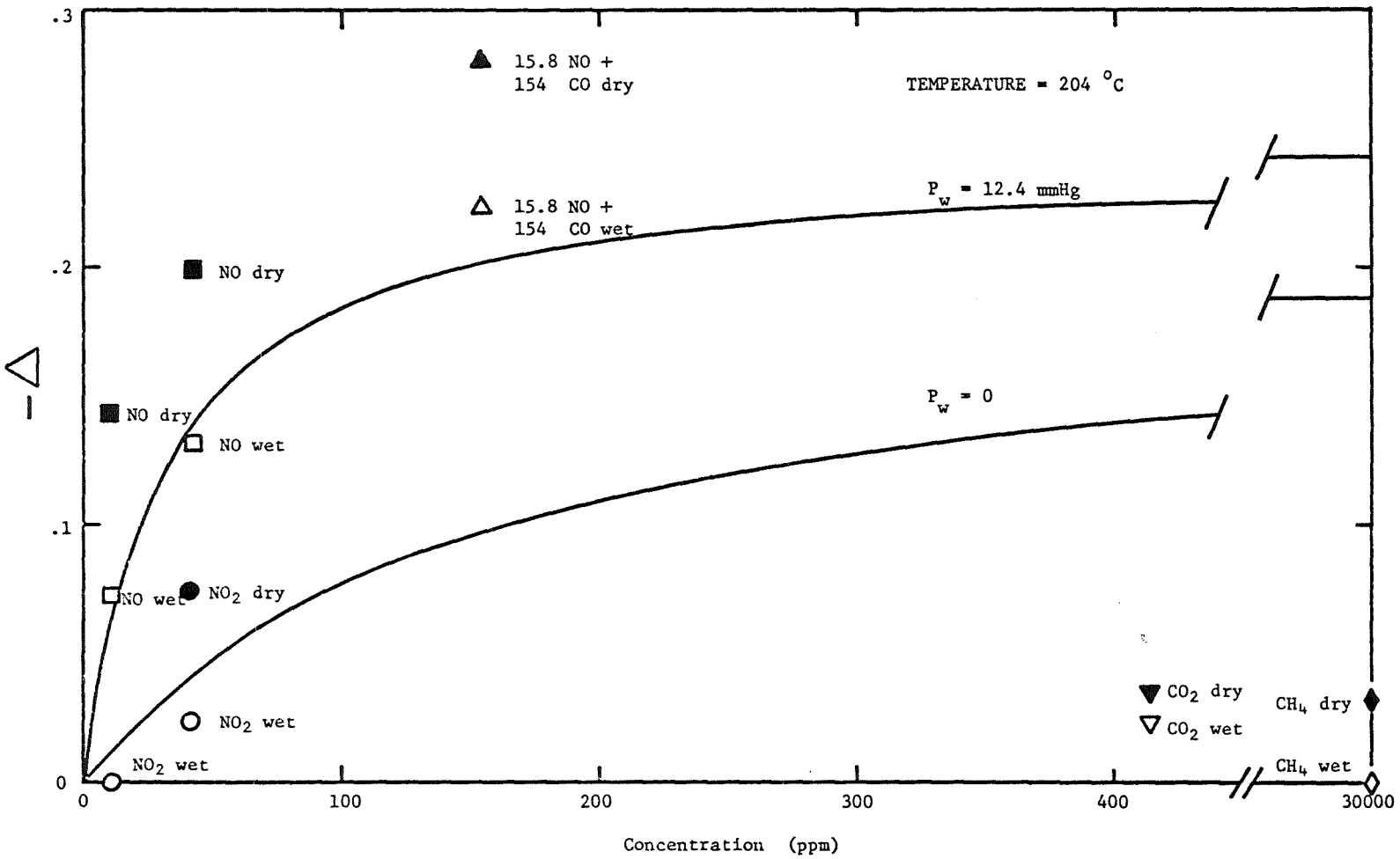

Figure 9. Response of MnO_2 Sensor to Interferants.

The nitric oxide has less effect in a wet atmosphere, approximately on the same order as carbon monoxide. There is not enough data to determine whether the sensitivity shows an initial enhancement for very low water vapor pressures, then a decline at higher vapor pressures, as it does for carbon monoxide. This is probably not the case, because the dry response to NO is so large.

The next most important interferant of those tested was NO_2. Again, the response of the sensor to NO_2 was greater in the absence of water vapor than in the presence of it.

Methane and carbon dioxide also exhibited the same order of the effect, although at much higher concentrations. The response of the sensor to CO_2 and CH_4 is much less than to carbon monoxide, but the response is not insignificant--for instance, the presence of 414 ppm CO_2 in a dry atmosphere would give the same Δ as 34 ppm CO. Since CO_2 and CH_4 can be present in quantities as large as those tested, this response would have to be corrected for. The normal concentration of CO_2 in the atmosphere is 330 ppm. For this test, a nitrogen-oxygen mixture with 744 ppm CO_2 was used, and the response was plotted at 414 ppm. This makes an assumption that the sensor response is linear at these concentrations, but it is the best assumption that can be made.

Because of the non-linear response of the sensor to these gases, it is not possible to predict what the combined effect of two together would be. Two tests were made using a mixture of 154 ppm CO and 15.8 ppm NO, both wet and dry.

For the dry case, it is approximately true to say that the Δ response to the mixture is equal to the sum of the responses to 154 ppm CO alone and 15.8 ppm NO alone. This result is unexpected, according to Equation 2. For the wet case, this no longer holds true. The major implication of the dry case result is that NO and CO not only do not compete for the same active sites but enhance the response of one another. When water vapor is also present, other interactions take place which modify this result. Interpretations of the interference data will be given in the next section.

Another type of pressed powder used was "hopcalite." This is a mixed compound consisting largely of manganese dioxide with small percentages of copper, zinc, or silver oxides. Commercial hopcalites are available, but the compositions are proprietary.

Homemade samples of Zn-Mn and Cu-Mn hopcalites were prepared according to the formula of Pitzer and Frazer (Ref. 24). The powder was pressed into Teflon discs and also packed into a cylindrical glass tube. These units exhibited resistances greater than 10^9 ohms at room temperature. None of these sensors exhibited a response to 248 ppm CO, in either a wet or dry atmosphere. Hopcalites are notoriously sensitive to moisture, which destroys their catalytic activity, so the wet tests were run after the dry tests.

A refill kit for a catalytic oxidizer (Mine Safety Appliances Co, part number 459547) provided a commercial hopcalite for tests. There were two components: the first, labeled #1, was a light brown in appearance; the second, labeled #2, was dark brown.

The #1 hopcalite, packed in the cylindrical glass tube, had an impedance of 5×10^{11} ohms and was too unstable to obtain any indication of its response to CO. The #2 hopcalite, at room temperature, exhibited a Δ of -.05 in response to 248 ppm dry CO at an impedance of 1.5×10^{6} ohm. Exposure to moisture destroyed this response.

It was found that baking the hopcalite in air at about 100°C for 48 hours could rejuvenate the response. The rejuvenated powder had a $\Delta = -.08$ at 248 ppm CO, but with successive cycles of air and CO, the base line resistance decreased. Tests at higher temperatures brought no significant change in Δ, but the resistance exhibited semiconductor behavior, one sample dropping from 5.7×10^{5} ohms at room temperature at 19.8×10^{3} ohms at 93°C and to 3.1×10^{3} ohms at 204°C.

After a series of tests, the response of the #2 hopcalite was very small. This may have been due to atmospheric moisture, or to a slow saturation of the active sites with a more strongly sorbed CO state. Attempts to repeat the rejuvenation, once by heating under vacuum to 100°C, once by heating in air, failed to achieve any increase in sensitivity, and the hopcalite study was discontinued.

One further MnO_2 powder device was tested. It was designed to test a hypothesis that the important sites for chemisorption were at the actual points of contact between crystallites.

Two flat metal plates of stainless steel were prepared and cleaned; a small amount of MnO_2 powder (small crystals) was placed on one plate and spread out to keep the crystals from touching one another. The second plate was placed over the first, creating a "sandwich" supported by the crystals. This unit was then placed in the test chamber.

The unit showed absolutely no response to CO from room temperature to 200°C. It did exhibit a very strong decrease in resistance with temperature, most of which was due to the intrinsic conductivity of the MnO_2. There may also have been a thermal expansion effect, because the unit was held by one of the spring contacts of the test chamber. The unit was very sensitive to the force applied to the upper plate, since more and more crystals would come into contact with both plates as the force increased. A better test might be to use precisely three crystals, or to use a constant force provided by a small weight, rather than a spring. The interpretation of this result will also be in the next section.

A check of the response of the manganese dioxide sensors to different partial pressures of oxygen was made as a last test. No change in resistance was found for partial pressures from 0.1 atm. to 0.5 atm. An earlier unit had been left in a wet flow of pure N_2 over a weekend; when the flow was changed to air, the resistance increased from 210 Ω to 310 Ω linearly over the period of two hours. Of course, in this case the partial pressure of O_2 increased from zero to 0.2 atm. The sensor was at a temperature of 132°C.

5.5 Evaporated Slurries

The last class of sensors that was fabricated was based upon the patent of Bott, et al. Many compounds were tried, and several proved very successful, exhibiting the only significant room temperature response. The results of this series of experiments is summarized in Table 3.

Table 3. Evaporated Slurries

		Composition	R(Ω)	T(°C)	[CO](ppm)	Δ	Comments
Water Slurries		$CaS + CuC\ell$	100	25,132	154 dry, wet	0	
		MoO_3	10^9	188	154 wet	0	
		SnO_2	10^{10}	188	154 wet	0	
"Bott" Slurries	#1	MoO_3	1.9×10^8	25	248 wet	+.20	slow
	#2	MoO_3	5×10^8	25	248 wet	-.09	avg.[1]
	#4	MoO_3	1.8×10^{11}	25	248 dry	-.20	avg.[1]
	#5	$MoO_3 + .011^3Zn$	1.7×10^{11}	25	248 dry	-.46	peak[2]
	#6	$MoO_3 + .011Cu$	3.5×10^{11}	25	248 dry	0	
	#7	$MoO_3 + .009Co$	1.6×10^{11}	25	248 dry	0	
	#8	MoO_3	2.6×10^9	25	248 dry	-.05	4
	#11	$MoO_3 + .052Zn$	1.8×10^{11}	25	248 dry	0	
	#12	$(.5Mo + .5Zn)O_x$	4.2×10^{11}	25	248 dry	-.23	avg.[1,2,5]
	#13	$MoO_3 + .011Zn$	4.1×10^{10}	25	248 dry	-.32	avg.[1]
				25	36.9 dry	-.07	avg.
	#14	$MoO_3 + .005Zn$	5.2×10^{10}	25	See Figure 10 and Text		
	#15	$MoO_3 + .005Zn$	1.3×10^{10}	25	11.07 dry	-.06	avg.[1]
					36.9 dry	-.09	avg.[1]
	#16	$MoO_3 + .005Zn$	1.7×10^{10}	25	36.9 dry	-.05	avg.[1]
	#18	$MoO_3 + .0065Cr$	1.1×10^{12}	25	248 dry	0	
	#19	$MoO_3 + .005V$	4.8×10^{11}	25	248 dry	0	

1. Large Δ on first run, much smaller Δ on subsequent runs.
2. Δ exhibits a peak and decreases to zero with time.
3. Atomic fraction.
4. Exhibited voltage between terminals.
5. Exhibited strong response to oxygen.

Two types of sensors were prepared: water slurries and "Bott" slurries. The "Bott" method uses ammonium salts of the desired oxides and a solution of ammonium nitrate. The specific details of preparation are given in Appendix 5.

The water slurries were prepared by making a paste of the desired powders and evaporating it to dryness with gold-wire electrodes embedded within it. This formed a rather dense, solid mass, and sensors prepared this way did not respond to CO.

The "Bott" method produces sensors that are highly porous and have a large surface area. The sensor material is firm, and the electrode wires are fixed in place. This is advantageous in comparison with the compressed powders.

The compositions of the slurries given in Table 3 are nominal and are based upon stoichiometric chemical decomposition. Many of the starting materials, particularly ammonium molybdate, are hydrated crystals. These were used as supplied, so that any dehydration would not be accounted for in calculating in the present work. The process of decomposing the salts does not guarantee that only the oxide will be left, or that it will be stoichiometric.

Three types of behavior could be found in these sensors, though not all together. These will be called loss of sensitivity, the peaking response, and slow desorption response.

Nearly all of the sensors that showed significant response exhibited a much larger response on the first exposure to CO than on subsequent exposures. This is the loss of sensitivity. In many cases, the sensor

resistance returned close to the baseline value when air replaced the carbon monoxide, indicating that the strongly chemisorbed CO was reversilby sorbed. Over a period of several hours, the response remained low.

The peaking response was observed on a few sensors. With these, there was a fast decrease in resistance as soon as CO was admitted to the test chamber, but then, while CO was still present, the resistance increased back toward the baseline value. Switching back to pure air did not noticeably increase the rate of approach to the baseline resistance. On subsequent exposures to CO, the magnitude of the peak was smaller than in the first exposure (loss of sensitivity).

The slow desorption response describes the behaviour of some slurry sensors after CO is replaced with pure air. After the first exposure to CO, there is an increase in resistance with a time constant of the order of 5-10 minutes; this is longer than for the MnO_2 sensors, but probably because of the lower temperature of operation. There is also an increase in resistance that appears to be a baseline drift with a time constant of several hours; this is the slow desorption.

These phenomena are interrelated and the interpretation of them will be explored in the next section.

We will not describe the response of some of the sensors tested.

Unit #1 in Table 3 was allowed to stabilize in a flow of wet (12.4 mm water) air. When CO was admitted to the chamber, the resistance slowly increased; returning to pure air brought no change in resistance. No other sensor of this type exhibited an increase of resistance.

Unit #2 showed a normal decrease of resistance with CO and had the loss of sensitivity characteristic. When the unit was heated to 63°C, it showed no response to CO.

The initial response of Unit #4 to CO was $\Delta = -.38$; the next two cycles produced $\Delta = -.032$ and $-.014$. The following day the initial response was $\Delta = .-67$; the second and third responses were $-.14$ and $-.11$. There was considerable baseline drift in the direction of increasing resistance after the first run, indicating the slow desorption response.

Unit #5 exhibited the peaking response, with the return to baseline resistance taking about 30 minutes. The subsequent peaks were also of much lower amplitude than the first peak. After exposure to pure air overnight, the sensor failed to respond at all to CO and was abandoned.

Unit #8 was unique. After a day's run giving the response noted in the Table, it was observed that there was a voltage across the terminals of the sensor. Initially, it was 0.925 volt, measured with an electrometer with $<10^4\Omega$ input resistance. The voltage was monitored this way for 4 hours, during which time, it decreased nearly linearly to .825 volt. This would correspond to an exponential time constant of 35 hours.

During the 4 hour period, the sensor was exposed to CO, then air, then pure oxygen. The voltage changed slightly during these exposures but generally maintained its steady decrease.

Then an internal shunt resistor of $10^9\Omega$ was connected across the voltmeter. The voltage reading dropped to .565 volt, indicating an

effective internal resistance of about $4.6 \times 10^8 \Omega$, as compared with $2.6 \times 10^9 \Omega$ measured with the ohmmeter the day before. With this lower resistance across the sensor, the terminal voltage dropped much more rapidly, but in a non-exponential fashion. That is, the calculated time constant changed with time from 2.3 hr to 4.9 hr. During this period the sensor was exposed to CO; the voltage measured increased about 22%. This is consistent with a decrease in the internal resistance of the sensor. The magnitude of the change is, approximately, $\Delta = -.7$. Subsequent exposures to air and then CO produced minor changes in voltage.

Although the phenomenon was very interesting, pressure of time precluded further investigation. No evidence of this effect was seen in any of the remaining sensors fabricated.

Unit #11 had an initial $\Delta = -.075$, but further responses were zero.

Unit #12 was mistakenly conditioned in 248 ppm CO prior to its first run. Therefore, when pure air was introduced to the unit, it was expected that the resistance would rise. Instead, it decreased. The initial decrease was $\Delta = -.40$, and was followed by a long period of slowly increasing resistance. It should be noted that the partial pressure of oxygen was essentially unchanged for this first step.

Switching back to CO produced a small decrease in resistance ($\Delta = -.03$). Changing to a flow of pure oxygen, the response was $\Delta = -.32$, with the resistance slowly increasing above the value it had attained in air. Further changes that day in response to either CO or O_2 were minimal.

After being left on air overnight, the initial response to CO was $\Delta = -.59$, but subsequent responses to CO were small.

This response to the effect of pure oxygen was also noted in the runs on Units 2 and 4; a large drop in resistance, followed by a slow increase. They were not tested for the changes from complete CO saturation to pure air. The strange behaviour associated with this sensor is believed due to its composition of 50% Mo and 50% Zn, leading to a very disordered oxide.

Unit #13 exhibited a useful and fairly constant sensitivity. The runs of CO and then air were done fairly quickly (1/2 hour total), so that equilibrium conditions were not reached. For the 248 ppm CO, the first four Δ's were -.44, -.35, -.23, and -.21. There is a decline in response, but not as drastic as in prior sensors.

The sensitivity was sufficiently high to warrant study with 36.9 ppm CO. Five consecutive runs produced Δ's of -.072, -.073, -.083, -.061, and -.055.

This sensor showed promise in terms of sensitivity and reproducibility, so further sensors of similar composition were made.

Unit #14 was very sensitive to CO, although it had defects in reproducibility. The first series of runs with 248 ppm CO showed an initial $\Delta = -.67$, followed by Δ's of -.28, -.18, -.16, and -.14. There was a considerable change from the first run to the second. After allowing the sensor to remain overnight in a dry air flow, the responses to 36.9 ppm CO were -.65, -.34, -.27, -.26, and fairly constant values thereafter.

The initial response after an overnight purge of dry air was usually much larger than succeeding responses, indicative of a fairly strong loss of sensitivity. The recovery of the resistance to its zero concentration value was also very slow, appearing as a constant increase in resistance between exposures to CO.

Therefore, measurement at different concentrations were taken on successive days, allowing the sensor sufficient time between runs to return to equilibrium. A plot of the first Δ's for four different concentrations is shown in Figure 10.

At each concentration, the second run produced a Δ roughly half the first Δ; succeeding responses were slightly smaller. The solid line drawn through the data points in Figure 10 represents a Langmuir type adsorption. It does not fit the data well, but is somewhat better than an adsorption curve which varies as $P^{1/2}$, Equation 3. A mixed isotherm of the form of Equation 2 might provide a better fit, but the quality of the data does not warrant it.

This sensor is almost fully saturated at a concentration of 36.9 ppm CO. It exhibits a greater sensitivity than any other sensors tested at low concentrations, and its saturated response is about as large as seen for all the sensors tested. The fact that desorption is slow is a serious disadvantage.

When the sensor was switched from dry air to pure O_2 after a series of runs in which the response to CO had fallen very low, the sensor had a $\Delta = -.58$, in the same direction as CO. It was a transient response, with the resistance slowly increasing to somewhat above the initial value.

This O_2 treatment did little to increase the sensitivity to CO; the response was only slightly better after the oxygen than before.

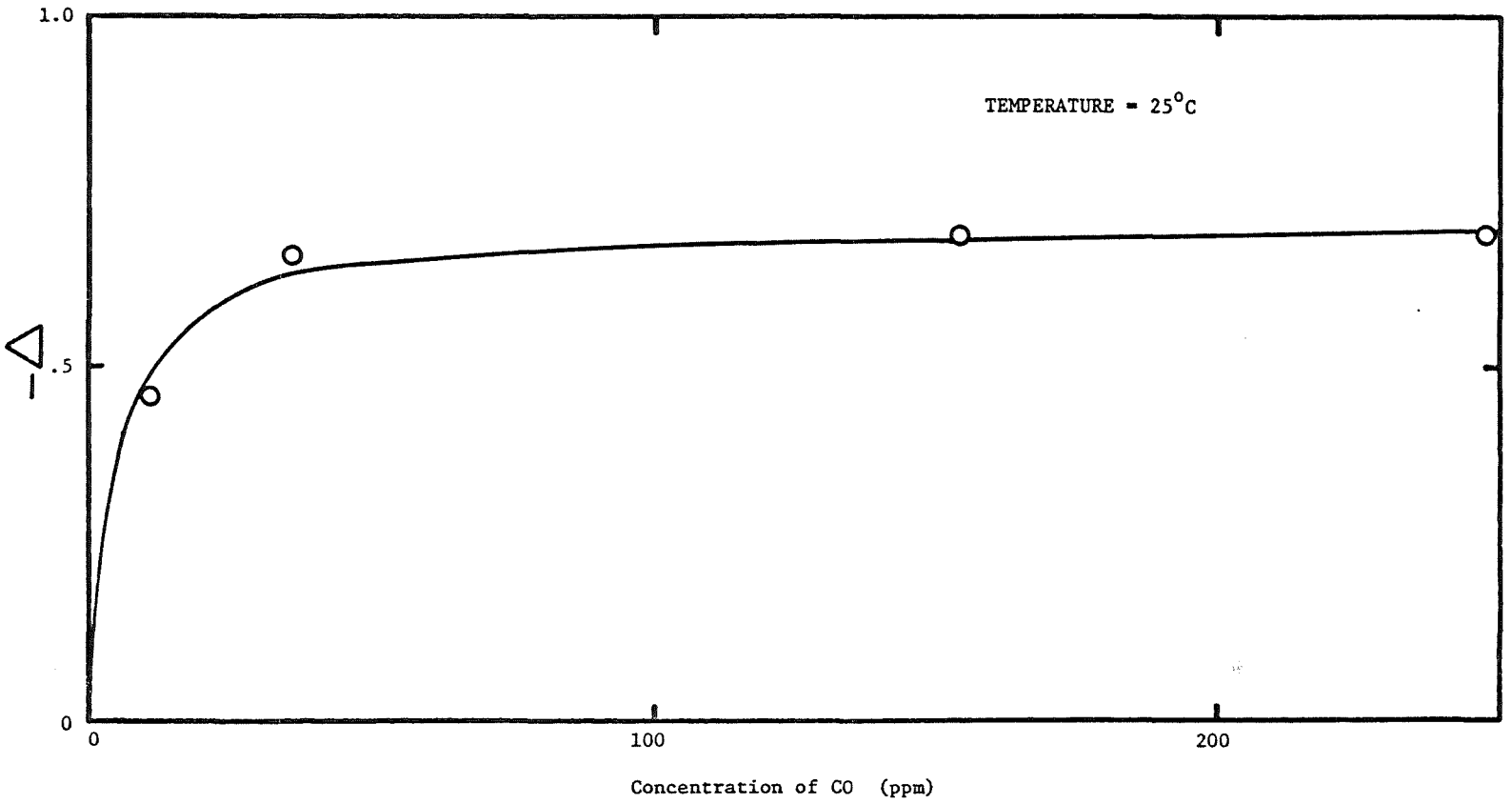

Figure 10. Response of Slurry Sensor #14 to Carbon Monoxide.

Therefore, the amount of oxygen necessary to desorb the CO from the sensor is not critical.

In an attempt to speed the desorption, the sensor was operated at a slightly elevated temperature, 63°C. The initial response to 11.07 ppm CO was roughly what was expected, but successive tests at higher concentrations produced rapidly decreasing responses. The temperature was reduced to 32°C, but the unit still had small responses.

Leaving it overnight, it showed an initial Δ in 154 ppm CO of -.34, but the second response was -.01. The unit was declared inoperative after several more tests.

Because of its failure, no tests were made to determine the effects of water vapor or of interfering gases.

Two more units were constructed with identical formulations to attempt to repeat the success of Unit #14. Both showed a moderate sensitivity, about half of #14, but both quickly saturated and produced very small responses to CO. Tests on this composition were terminated by time limitations.

6.0 INTERPRETATION OF RESULTS

In this Section we offer an interpretation of the experimental evidence and try to present a unified concept of the physical processes involved. From this viewpoint, we will make recommendations for further lines of investigation.

A most important point that must be kept in mind from the beginning is that the processes of adsorption, whether physical or chemical, are dynamic processes. There are continual exchanges of molecules between the surface and the gas. Moreover, no one site can remain occupied indefinitely, so that when we talk about competition for a site, it is an active competition.

Carbon monoxide may be adsorbed on surfaces with either one bond or two. This is referred to by Rideal (Ref. 20) and by Pitzer and Frazer (Ref. 24). This is a result of the two unsaturated orbitals of the carbon atom.

It is because of the unsaturated orbitals that the CO molecule is chemisorbed to metal oxide surfaces, and it is because of the strength of that bond, whether covalent or ionic, that it is nearly always desorbed as CO_2. Once a bond can be established between an adsorbed CO molecule and an oxygen atom, the resulting CO_2 molecule is so weakly bound that it can be thermally desorbed. This was observed by Garner, et al., (Ref. 19) and referred to in Section 4.

Pitzer and Frazer offer a simple illustration for the adsorption in the two configurations reproduced in Figure 11. The surface is represented by a single O Mn O unit, and the CO molecule can coordinated

with either the manganese or the oxygen

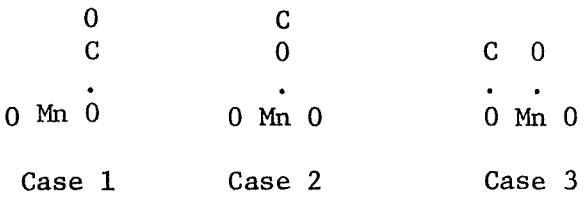

Figure 11. Configurations of Adsorption.

It is clear that Case 2 is incompatible with desorption of CO_2, whereas both Case 1 and Case 3 are compatible. Case 1 represents a single bond between the molecule and the surface; Case 3 represents the double bond.

Case 1 is interpreted as weak chemisorption because there is no energetically favorable way for the carbon atom to transfer an electron to the oxygen atom. In simple terms, it would leave the CO molecule positive and the surface oxygen atom negative, tending to return the electron to its initial position. We can interpret Case 3 as the state of strong chemisorption. Here, the transfer of an electron from the molecule to the surface atom can be at least partially compensated for by a shared electron between the manganese atom and the oxygen atom.

This interpretation also provides an explanation for the activation energy observed in the temperature dependence of Δ. The O-Mn atomic spacing is 1.84 Å, while that of C-O is 1.15 Å. Stretching the molecule to accommodate it to the surface would require an additional energy. Another mechanism that could explain the activation energy

is that strong chemisorption, the transfer of an electron from the carbon atom to the surface, might require the additional electrostatic energy of a nearby hole. The population density of holes would be an exponential function of temperature, everything else being equal.

If the temperature became sufficiently high, either or both of these mechanisms would decrease the amount of strong chemisorption. High thermal energies could convert Case 3 molecules to Case 1 molecules (or desorb them) at a more rapid rate than the molecule could ionize. If the hole mechanism is the important one, the time a hole spends in the neighborhood of any point decreases with temperature because its velocity increases. Therefore, the probability of it's assisting in an electron transfer would diminish.

At any temperature there is a probability that the oxygen atom in the surface will be more coordinated to the carbon than to its manganese neighbors. When this occurs, the molecule (now CO_2) is less tightly bound and can be desorbed. In so doing, an oxygen vacancy is created, which must be filled by atmospheric oxygen, or by mobile oxygen atoms on the surface, if the sensor is to return to its original state. The hole which was in the vicinity of the absorbed molecule may remain attached to the vacancy because of the difference in energy at the micro-defect as compared with the interior of the crystal.

Despite the fact that both a manganese and an oxygen atom are involved in this chemisorption, it is still one-site adsorption, because the CO molecule initially sorbs only on an oxygen atom. There is no competition among CO molecules for the manganese atoms. (Oxygen atoms may sorb on the manganese sites; this will be considered later.)

This occurs for the dry case only, with no water molecules present. The presence of water vapor was observed to increase the response of the sensor to CO substantially. Also, at very low concentrations of CO, the response of the sensor seems to be relatively insensitive to the amount of water vapor present.

The increase in sensitivity can be explained by hydrogen bonds between water molecules and the oxygen atoms of Case 1. This is illustrated in Figure 12.

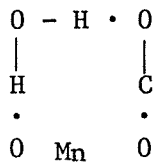

Figure 12. Hydrogen Bonding of CO Molecules.

Since hydrogen bonding occurs only for electronegative atoms such as oxygen, the water molecule will attach to the surface only on oxygen atoms. The bond lengths of the water molecule are too small to allow a simultaneous coordination of the oxygen atom of H-O-H with the manganese atom. On the other hand, the bond lengths for the configuration shown in the figure are in reasonable agreement.

The effect of the hydrogen bond is to make the CO molecule easier to ionize. The hydrogen partially shares its electron with the oxygen atom; this increases the electronic energy of the molecule and tends to displace an electron away from the carbon atom. Thus, in the presence of water vapor, the weak chemisorbed form of Case 1 can become a strongly chemisorbed form.

The temperature dependance of Δ, shown in Figure 8 for a powder sensor, indicated an activation energy of 2.4 kcal/mole. This was in the presence of water vapor. From Table A3 in Appendix 4, a sputtered MnO_2 film also showed a peak in its temperature response, with an energy of activation of approximately 2.9 kcal/mole, in the absence of water vapor. While this evidence is not conclusive, because of the differences between the two types of sensors, it is strongly supportive of the hypothesis that hydrogen bonding lowers the activation energy.

If the amount of water vapor on the surface is constant, then this single-site adsorption is the dominant form of chemisorption, since the probability of two-site adsorption is much lower. Therefore it is not unreasonable to find that the response obeys the Langmuirian form of Equation 1. In actuality, a mixed expression combining one-site and two-site adsorption should be used, but again, the amount of data does not justify the effort.

From Figure 12, it appears that a second water molecule could participate in bonding on the opposite side from the first molecule. It is not clear that this is physically possible, either from the bond lengths or from the orbital angles of all the electrons involved. Multiple hydrogen bonds would make the CO molecule still easier to ionize, but the number of sites that could satisfy all the criteria would be much smaller than for the case illustrated.

Since each water molecule occupies one oxygen site, there is a site-competition for the CO molecules. This explains the decrease in Δ with increasing water vapor pressure at the higher concentrations

of CO, as shown in Figure 7. Still, at low concentrations of CO, there is not a very large difference in Δ for large variations in the water vapor pressure.

The explanation for this effect is that hydrogen bonding is a fairly weak form of interaction, intermediate in strength between the Van der Waals interaction and covalent electron bonding. It will influence the ionization of only the most easily ionized molecules, those for which there is a large hole population to interact with. This corresponds to the first molecules ionized; at low concentrations, essentially all of the Case 1 molecules could be strongly chemisorbed. At higher concentrations, only a part of the population can become strongly chemisorbed, the rest remaining weakly chemisorbed.

The hydrogen bonding interaction is so relatively weak that the water molecules have a very short residence time on the surface. Therefore, the concentration must be very high to saturate the surface sites. From Figure 7, a vapor pressure of 24 mm does not completely saturate the response of the sensor to CO.

The effects of interferant gases are consistent with this point of view. Referring to Figure 9, the principal interferants are NO and NO_2; of much less importance are CO_2 and CH_4, even taking into account their greater abundance in a mine atmosphere. All of the interferants have a smaller effect when water vapor is present than when water vapor is absent.

As discussed before in Section 5, NO is expected to give a larger response than CO because the NO molecule has an anti-bonding electron, one that is much more loosely bound than the electrons of the CO molecule. We therefore assume that the NO molecules are all strongly chemisorbed at low coverages.

This cannot remain true indefinitely, and the data bears this out. Every NO molecule that is ionized (donates an electron) lowers the chemical potential, reduces the hole population, and makes it more difficult for the next molecule to be ionized. The experimental results show that Δ is not linear in concentration even as low as 10 ppm of NO.

The above discussion assumes the NO molecule absorbs on an oxygen atom and loses a valence electron to it, and is based on the fact that NO produces a decrease in resistance, which for an n-type material such as MnO_2, requires a donor type gas. On the other hand, the NO molecule also has strong acceptor properties and could be adsorbed on the manganese atom. This adsorption would decrease the electron population and lead to an increase in resistance.

Such complicated behavior, absorption in two different ways, would be strongly dependent on the chemical potential, and would definitely not obey simple Langmuir adsorption.

The response of the sensor to the presence of NO and CO combined is much greater than can be explained by a combination of isotherms, as in Equation 2. Whereas the response to low concentrations of NO appears to be that of a donor gas, the presence of large amounts of CO may change the adsorbed NO to an acceptor gas. The net effect of this change is that more CO molecules can be strongly chemisorbed than if the NO were not present. Without more data than is available, little more can be said along this line.

The presence of water vapor adsorbed on the surface will also affect the response of the sensor to NO. The mechanism is not clear, but it is probably a combination of site competition for the donor

adsorption on the oxygen sites and enhancement of the acceptor type adsorption on the manganese sites. The enhancement effect that is prominent with CO is non-operative here because the NO molecules are so readily ionized on the donor sites.

The interference of NO_2 is weaker than NO because the molecule is more stable. Nonetheless, for equal quantities of gas, NO_2 produces a stronger response than does CO. Examination of the ionization potentials for CO, NO, and NO_2 reveals that NO_2 lies between NO and CO, being nearly equal to NO in magnitude. The ionization potential is related to the donor ability of a molecule, with lower potentials corresponding to better donors. It is not the sole influence on electron donation, since the presence of other bonds has a very large effect.

The presence of water vapor probably prevents the NO_2 molecule from interacting with the surface by forming an acid complex with the water molecule. The possible reactions are complex and have many possible paths, but the main effect is to reduce interactions which would influence the resistance of the semiconductor.

It is rather difficult to explain why CO_2 has as much effect on the sensor response as it does. The CO_2 molecule is very stable, although its ionization potential is very similar to that of CO. It has no dipole moment and all the valence electrons are saturated. The most likely explanation for its effect is competition with atmospheric oxygen for adsorption sites.

We have not discussed the effect of oxygen on the conductive properties of the surface, but, for an n-type semiconductor, oxygen will be an acceptor gas and will increase the resistance of the material. Any effect which desorbs oxygen will tend to free electrons and decrease the resistance.

The presence of water vapor reduces the effect of CO_2, as might be expected. Instead of interacting at the surface, it forms a bicarbonate complex with the water molecules.

The weakness of the CO_2 interaction is evident in the fact that 414 ppm CO_2 produces the same change in resistance as only 36 ppm CO in the dry condition and as much as only 4 ppm CO in the wet condition.

The effect of methane is probably also due to its interaction with adsorbed oxygen, both by site competition and by hydrogen bonding to oxygen atoms. The coordination that results from the hydrogen bond would tend to reduce the electron affinity of the oxygen atom, thereby freeing an electron for conduction. In a wet atmosphere the methane would have little more effect than the water molecules do, and so, in the presence of a much larger concentration of water vapor, would not be detectable.

The effect of oxygen on the sensor is of a different order, since atmospheric oxygen comes into equilibrium with the oxide, given sufficient time. The state of the manganese dioxide powder is not known, but it is almost certainly a mixed oxide, probably with manganese ions of valence +3 and +4. This is based on its electrical characteristics: Mn^{+3} can be ionized to Mn^{+4} and donate an electron in the process, making the material n-type.

With such a material, an increase of oxygen pressure should result in more oxygen atoms in the crystal, effectively raising the average valence and decreasing the number of free electrons. This would cause an increase in resistance. Such behavior coincides with the observed results on one sensor. It was left in a flow of dry nitrogen gas for an overnight purge ($pO_2 = 0$); when air ($pO_2 = .2$ atm.) was admitted to the sensor, a slow increase in resistance took place.

Even at a temperature of 200°C, the rate of change was very slow. Later measurements on another sensor showed no changes in resistance for oxygen pressures from 0.1 to 0.5 atm. The sensor had equilibrated in air for many days, and it is possible that observation times were not long enough to detect resistance changes.

Some of the MnO_2 sputtered films initially showed a response to CO at NCSU. When they were rechecked at the RTI laboratory several days later, there was no response. Subsequent measurements of resistance showed that the sensors had decreased, and moreover, that their temperature coefficients had also changed. This would indicate that the stoichiometry of the films had changed in the presence of atmospheric oxygen.

The sputtering target was nominally stoichiometric MnO_2 and the films were sputtered in argon. This would tend to produce stoichiometric films of MnO_2. The decrease in resistance would indicate a loss of oxygen to the atmosphere and the creation of a mixed valence state for the manganese ion. Gould (Ref. 26) points out that absolutely stoichiometric MnO_2 has yet to be prepared, the closest actual compound being $MnO_{1.95}$.

All of this evidence, together with the hopcalite work of Pitzer and Frazer (Ref. 24), indicates that the catalytically active form of the manganese oxide is indeed the Mn^{+4} with stoichiometric oxygen. This is the form for which CO is strongly chemisorbed, and from which CO is desorbed. In the powder samples, this form must reside at least in patches on the surface of the crystallites, while the lower valence manganese atoms represent defects within or at the surface of the crystallites.

The overall resistance of the powder sensors is also determined by the surface layer of the crystallites. This was borne out in the "crystal-sandwich" experiment, where no response to CO was found for single crystals between metal plates. This is illustrated in Figure 13.

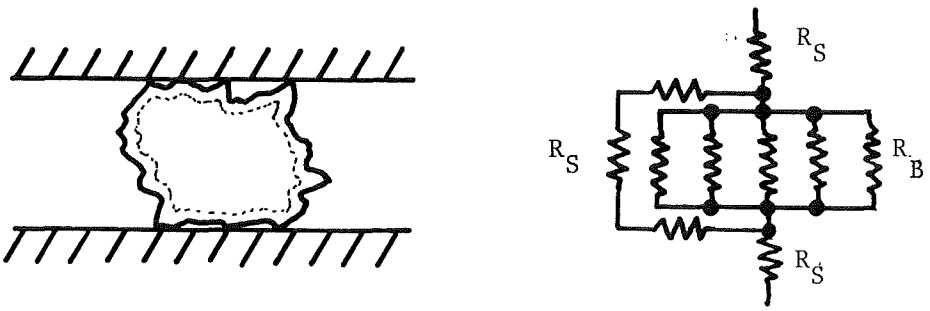

Figure 13. Equivalent Circuit for Crystallite.

In this figure, the resistors R_S represent the resistance of the surface layer of the crystallite. The resistors R_B represent all of the parallel paths through the crystallite afforded by the bulk carriers. If the bulk conductivity is much lower than the induced surface conductivity, then the surface would contribute most of the carriers and determine the total resistance. In that case, this sensor should also respond to CO, since most of the surface is exposed and should be active. If, on the other hand, the bulk conductivity is larger than the surface induced conductivity, then only the surface resistances R_S which are in series with R_B would have much effect on the total resistance of the sensor; and because of the mechanical stress at the point of contact, the number of carriers is probably

determined more by defects than by adsorbed gas molecules, so that there should be little or no response to CO.

The second explanation fits the observed facts. In a regular powder sensor, there are many resistances of the type R_S in series between thousands of crystallites. Therefore, they play a much more important role in the conductivity of the whole sensor.

The corollaries of this observation are that there should be a pronounced dependence of the resistance of a powder sensor on the size of the crystallites used and that excessive bulk conduction may account for at least part of the failure of the thin films to respond to CO.

The manganese dioxide powder sensors, operating at elevated temperatures, had little difficulty in desorbing the CO_2 molecules, once formed. This was evident from the fact that the calculated response time on admitting air to the test chamber was not much different from the time calculated on the basis of the response characteristics, Equations 14 and 15.

This may not be completely true. The response characteristics were determined by averaging a large number of runs. The resistance before and after each sorption-desorption run were allowed to become constant, which took times on the order of an hour. The Δ's for a series of runs exhibited large standard deviations about the mean values. But there is some indication that at least part of the variance in the Δ's was due to a changing baseline resistance. The changing baseline may have been due to a very slow desorption of CO_2 molecules.

The explanation for the slow desorption lies in the fact that the molecules strongly sorbed at the lowest concentrations are also the most strongly bound, and therefore are the last ones desorbed. The probability of desorption is an exponentially decreasing function of the binding energy.

If this slow desorption was taking place, then the first run of the day should produce a larger Δ than subsequent runs. This occurred for some of the pressed sensors, but not for others, and the effect was definitely less than for the slurry sensors.

The powdered MnO_2 sensors might exhibit sufficient stability for use with a daily calibration, provided this slow desorption could be verified and overcome.

The slurry sensors based on MoO_3 exhibited many similar features to the powder sensors, except for the important difference of operating at room temperature. There is less background available for this material, so that detailed examination of the molecular interaction is not possible.

The success of the Bott slurries is in great part due to their highly porous structure, formed by the forced evaporation of NH_3 and NO_2 during the process of constructing them.

The operation at room temperature is desirable from an instrument point of view and also because the formation of the sensor material proceeds at relatively low temperatures. Application of higher temperature may well cause irreversible changes in the sensor.

Unfortunately, low temperature operation slows the desorption process considerably. It is immediately evident in the slow response to pure air

after exposure to CO, and also shows up as the long term baseline drift which we call slow desorption.

The peaking response, in which the sensor responds initially to CO and then decays back to its zero-concentration resistance while still in the presence of CO, is another aspect of the slow desorption of CO_2. In this case, the CO molecule is intially strongly chemisorbed; within a short time, the bonds of the surface oxygen atom shift to form a CO_2 molecule. The CO_2 molecule becomes weakly chemisorbed, because it is not a good electron donor, and therefore the carrier concentration decreases. But, if the molecule is not desorbed from the surface, no further CO molecules can be sorbed on that site, and the resistance increases toward the value it had when no CO molecules were adsorbed.

Furthermore, the competition of the CO_2 molecules persists for a long time, so that it would be expected that a sensor showing the peaking response would have smaller Δ's on subsequent runs. This is indeed the case.

Other slurry sensors did not exhibit the peaking response but reached a steady resistance value upon exposure to CO. When the gas concentration was reduced to zero, these sensors began an immediate, but very slow, change back toward their pure air resistance values.

In the case of these sensors, the physical desorption of the CO_2 molecule did not seem to be the rate-limiting factor so much as the actual formation of the molecule at the surface site--that is, the conversion from the strong to the weak form of chemisorption. This is deduced from the fact that the resistance became constant in the presence of CO, indicating that nearly as soon as a CO_2 molecule was formed at the

surface, it was desorbed and soon replaced by another CO molecule.

This type of sensor exhibited a loss of sensitivity, which would be expected from the fact that the desorption of CO_2 was slow.

Another indication that the controlling factor was the CO_2 desorption was found in the response of the sensors to pure oxygen. In general, switching a sensor which was in the process of recovering from a CO exposure from a flow of air to a flow of pure oxygen produced a transient change in resistance. But upon switching back to the flow of air, the sensor resistance resumed its slow recovery at a value which was a reasonable extrapolation of the characteristic before the oxygen was admitted. The presence of the oxygen seemed to have little or no permanent effect on the change of resistance.

The transient response of these sensors to oxygen was itself very interesting. Introducing pure oxygen in place of air produced a large negative Δ, in the same direction as CO, which then increased back toward the air-value resistance. This behavior is not readily explicable, except in the general terms of a change in stoichiometry. The sensors that exhibited the effect were those doped with zinc ions, so it is possible that the valence state of the ions was changed by the added oxygen atoms.

The fact that the effect decays with time indicates it is primarily a surface effect (because of the rapid onset) which is compensated by the migration of ions from the bulk of the semiconductor. The process involving the oxygen is probably a change in stoichiometry, because the reverse effect on exposure to air is observed to occur very slowly, if at all.

The one sensor, Unit #12 which was 50% Mo and 50% Zn, exhibited the very strange result of a decrease in resistance due to pure air after a long time in 248 ppm CO. Later exposure to CO produced a decrease in resistance as well. An atmosphere of pure oxygen produced a sizeable decrease in resistance. All of these changes decayed with time back to the initial values before the gas was introduced.

This is very difficult behavior to explain, with the principal difficulty being the first observation. The only change here was a decrease of CO from 248 ppm to zero and an increase in the partial pressure of oxygen from 200,000 ppm to 200,050 ppm (assuming the CO displaces the components of air equally). This amount is utterly negligible in the effect it should have.

One possible explanation of the effect can be made with the assumption that the CO_2 molecules formed were not readily desorbed. This is in keeping with the fact that this sensor exhibited the peaking response. Then, since the sensor was in 248 ppm for many hours, we assume that all the active sites were covered with CO_2 molecules in equilibrium with the gas around them. Finally, if the air that replaced the carbon monoxide mixture had a higher carbon dioxide content, the surface would be out of equilibrium with the gas, and in such a direction as to favor the dissociation of some of the surface CO_2 molecules. These would become ionized and cause the conductivity to increase, at least until equilibrium was restored.

With these hypotheses in hand, a check was made of the CO_2 content of the air used (in cylinders) and of the CO mixture in air. The test was the precipitation of $CaCO_3$ from an ammoniacal $CaCl_2$ solution.

Based on the rate of formation of the carbonate as the gas was bubbled through it, the air did indeed have a considerably higher CO_2 concentration than the prepared mixture. This may be due to the method of formulating the mixture, if it were made from elemental gases.

Unfortunately, this difference between the gases used was discovered too late to verify its effect on the sensors. However, consideration of the effect of CO_2 interference on the MnO_2 powder sensor, Figure 9, shows that its effect amounts to only a few parts per million of CO. In the absence of further data to the contrary, we consider that the absence of CO_2 in the CO gas mixture would have a small quantitative, but not qualitative effect, on the response of the sensors tested.

The presence of CO_2 in the air may have had its most important effect on the NO and NO_2 interference tests. The nitrogen oxides, supplied in nitrogen gas, were blended with oxygen to simulate air. No carbon dioxide was added to the mixture, but it was present in the air used to flush the test chamber and, therefore, would produce an unobserved effect on the baseline resistance. This would have been in such a direction as to diminish the observed response of the sensor. The methane interference tests were done by blending 3% methane with 97% of cylinder air; in comparison with the pure air, this represents a 3% change in CO_2 and would be completely negligible.

The electrical characteristics of Unit #8, which showed an e.m.f. across its terminals, are also difficult to explain. Since the terminals were gold wires, it is probable that no electrode reactions could cause the voltage not only because of the non-reactivity of the gold but also

because the same reactions should occur on each wire. The decay of the voltage was roughly exponential with time, which would correspond to a depletion of charge at a rate proportional to the charge. Also, the change of terminal voltage with a change in the external load resistance indicated an internal resistance an order of magnitude lower than that measured by the ohmmeter.

All of these observations can be explained by a separation of ionic charge, a polarization of real charges in the sensor due to the applied potential of the ohmmeter. (The Keithley ohmmeter operates by passing a constant current through the resistance to be measured; the current was always adjusted so that less than one volt appeared across the sensor.) As the charge separation occurred, the observed resistance increased. When the electrometer was connected, the polarization charge acted as a voltage source.

The ions involved may have been nitrate and/or ammonium ions which had not been completely removed during the preparation of the sensor. It is not inconceivable that some similar effects could have been taking place in other slurry sensors, but none of them exhibited large increases of resistance or such non-ohmic behaviour: a voltage source connected to this type of ohmmeter tends to give the same reading no matter what the resistance scale is.

The difference in Δ for alternating current and direct current measurements described in Appendix 4 for sputtered MnO_2 films may also be evidence of a migration of ions. The steady field of a D.C. measurement could result in an ion current that is large compared with the electronic current; this would result in a smaller Δ, since the ion

current is not affected by the semiconductor properties of the film. The AC measurement tends to suppress any current due to movement of ions because of the lower mobility of the ions as compared to the electrons and holes.

The implication of this for the sensors is that an alternating current measuring technique may be very advantageous in detecting the response of the materials to carbon monoxide. It could reduce the effect of the parallel conductance of ions, and might reduce some of the instabilities that cause drifting resistances.

Operation of Unit #14 at an elevated temperature, in an attempt to speed its desorption time, resulted in a rapid, permanent decrease of its sensitivity to zero. The first exposure to 11 ppm CO gave a reasonable response, but successive ones gave smaller and smaller responses. There was a partial recovery of sensitivity after returning to room temperature and purging with dry air overnight, but the response to CO quickly became small on repeated exposures.

The response to pure oxygen was still the same as before the heating. It gave a large negative Δ and had the same peaking response. This response suggests that the porous structure of the sensor was not radically altered by the high temperature operation, but rather that the active sites for CO adsorption were reduced in number.

The mechanism by which this could occur is not clear, but it is possible that a more stable surface state of CO could have been formed at the elevated temperature. After the initial exposure to CO, the sensor resistance remained nearly constant, showing no indication of

returning to its pre-exposure value. The sensor was cooled to a lower temperature almost immediately after the last exposure to CO, which was at a concentration of 154 ppm.

If the loss of response were due to a more strongly bound state (which could only be activated at an elevated operating temperature), then we would expect a fairly long desorption time at the same or higher temperature, based on the room temperature results. The fact that only a short time was allowed suggests that the sensor might have been returned to operation by a prolonged period at elevated temperature. There was, in fact, a partial recovery after an overnight period at 32°C.

7.0 RECOMMENDATIONS

In light of the original aims of the contract, this research must be termed a failure, because the investigation failed to discover and develop a semiconducting sensor material that could be incorporated in a portable instrument.

Of the four qualities necessary for such an instrument--sensitivity, stability, fast response time, and freedom from interference--the most lacking was that of stability. Response time and susceptibility to interference were serious secondary defects. The sensitivity demonstrated was more than satisfactory, with both the manganese dioxide sensors and the slurries.

Stability in the MnO_2 powder sensors would be difficult to attain because the success of their operation depends on the surface layer resistances of the many crystallites. Attempts to fuse, sinter, or bind the crystallites will probably also destroy their sensitivity to carbon monoxide.

On the other hand, investigation of alternating current methods of measuring the sensor resistance could possibly eliminate the contribution of ionic currents in the total conduction, and thereby improve the stability and sensitivity.

Stability problems in the slurry sensors may be, at least to a large extent, the result of very long desorption times. Investigation of this effect would determine whether the sensor could be used in a practical instrument. The influence of elevated temperature operation has not been adequately explored, and offers some hope, still, of decreasing the lengthy desorption time.

Even if all other problems are solved, the susceptibility to interferents, particularly the nitrogen oxides, will be a difficult problem to overcome. The semiconductor is not specific enough to distinguish between gases, and the nonlinear response makes separation of the effects with different sensors difficult. No data was obtained for the interferents on slurry sensors; the amount that was obtained for the powder sensor was insufficient to make other than qualitative statements.

The sensitivity problem appears to have found a solution in the MnO_2 powder sensors and the Bott slurries. Further work characterizing their response should be done, particularly with respect to variation with temperature and humidity. The concentrations of carbon monoxide to be used should also be extended to lower values (10, 20 ppm) and intermediate values (50, 100, 200 ppm) as well as the ones used in this investigation. It is of some importance to learn the comparative roles of one- and two-site adsorption in the response of the sensors, and this can only be done if more concentration data is available.

Moreover, since the operating temperature has a very strong effect on the response, adequate characterization of a sensor requires measurements over a wide enough temperature range to be able to determine its optimum operating temperature. Such measurements also give valuable information about the activation energy of the processes involved in the response and aid in understanding the effect of the ambient conditions.

At this point, the limiting factor to building a portable carbon monoxide measuring instrument is an adequate sensor. Until such a sensor can be demonstrated, it will not be fruitful to pursue development of such an instrument. Further basic research will be required to develop such a sensor, and this work has investigated at least two promising materials, along with their limitations. The directions that the research should follow have also been indicated, but it is not clear that a sensor which embodies all the characteristics desired can in the end be developed.

REFERENCES

1. T. M. Royal, J. J. Wortman, and L. K. Monteith, NASA CR-1182 (1968).

2. F. Ansbacher and A. C. Jason, Nature 171, 177 (1963).

3. F. J. Brousaides, AFCRL Instrumentation Papers, No. 151, AFCRL-68-0547 (1968).

4. J. R. Lai and G. M. Hidy, Rev. Sci. Inst., 39, 1197 (1968).

5. C. M. Stover, Rev. Sci. Inst., 34, 632 (1963).

6. J. J. Wortman and K. S. Canady, Appl. Phys. Lett. 9, 75 (1966).

7. T. H. Ansbacher, Surface Science 14, 461 (1969).

8. T. Sugita, S. Ebisawa, and K. Kawasaki, Surface Science, 13, 159 (1968).

9. O. Levy and M. Steinberg, Surface Science 5, 385 (1966).

10. V. M. Chong, J. V. Connoy, and P. Mark, Phys. Status Solidi A 1972, 9(2), K133.

11. C. M. Parker and R. B. Strong, Final Report NIOSH Contract No. HSM-99-73-1 (Task Order No. 1).

12. F. F. Vol'kenshtein. The Electronic Theory of Catalysis on Semiconductors, New York, MacMillan Company, 1963 Trans. by N. G. Anderson.

13. P. B. Weisz, J. Chem. Phys. 21, 1531 (1953).

14. J. C. Yen, "An Investigation of the Electrical Properties of Zinc Oxide Thin Films Influenced by Oxygen Adsorption" Ph.D. Dissertation, North Carolina State University, Raleigh, N. C. (1973).

15. PerKofstad, "Nonstoichiometry, Diffusion and Electrical Conductivity in Binary Metal Oxides" (John Wiley and Sons, Inc., New York, 1972)

16. I. Langmuir, J. Am. Chem. Soc. 40, 1361 (1918).

17. E. C. Pitzer and J. C. W. Frazer, J. Phys. Chem. 45, 761 (1941).

18. A. Terenin and Yu Solonitzin, Discussions Farad. Soc. 29, 28 (1959).

19. W. E. Garner, T. J. Gray, and F. S. Stone, Proc. Roy. Soc. A 197, 294 (1949).

20. E. K. Rideal, "Concepts in Catalysis" Academic Press, Inc., (New York, 1968), p. 90.

21. B. Bott, J. G. Firth, A. Jones, and T. A. Jones. Offenlegungschrift 2142796. Assigned to National Research Development Corp. London, 2 March 1972.

22. Figuro Engineering Inc., 3-7-3, Higashitoyonaka, Toyonaka City, Osaka 560, Japan.

23. G. E. Fredericks and R. S. Scott, Rev. Sci. Instrum. 46, 749 (1975).

24. E. C. Pitzer and J. C. W. Frazer, J. Phys. Chem. 45, 761 (1941).

25. T. J. Gray, "Experimental Methods in Catalytic Research," R. B. Anderson, ed., Academic Press, N. Y. 1968.

26. E. S. Gould, "Inorganic Reactions and Structure," (Holt, Rinehart and Winston, New York, 1962).

27. S. J. Gregg and K. S. W. Sing, " Adsorption, Surface Area, and Porosity." Academic Press, London (1967).

APPENDIX 1

Chemisorption may be of two types, normal and activated. In normal chemisorption, a molecule may attach to the surface rapidly, without hindrance. Activated chemisorption requires that the molecule possess sufficient energy to cross an energy barrier--that is, an "activation energy." The principal observable difference between the two types is the rate at which the system approaches equilibrium.

Normal chemisorption equilibrates with the gas phase very rapidly with only a weak temperature dependence. Activated adsorption exhibits a slow reaction rate that is strongly dependent on temperature, approximately exponential, with the activation energy in the exponential factor. In some cases, adsorption may occur in both types sequentially; for instance, a molecule may be quickly bound in one state to an adsorption center and then change to another state with an appreciable activation energy at a finite rate.

Once the molecule is bound to the surface, whether or not it had to cross an energy barrier, the molecule and its adsorption center may remain electrically neutral, or it may attract and trap a free electron or a free hole and become electrically charged, with the charged particle taking part in the bond. The first case (neutral) is called "weak" chemisorption by Vol'kenshtein and the second is called "strong" chemisorption.

In strong chemisorption, the adsorbed molecule may behave as either an electron acceptor or donor, depending on the characteristics of the surface. Furthermore, it is not necessary for an acceptor molecule to be bound to a donor or "n"-type surface or vice versa; it is entirely

feasible that a donor molecule be bound to a donor surface, or even an insulating surface. The presence of the strongly bound molecule may lead to a decrease or an increase of the free carriers in the surface.

One theory of chemisorption, the boundary-layer theory (Ref. 13), concerns itself with strong chemisorption only. It makes no allowance for the neutral sorption of molecules on the surface. One of the consequences of this theory is that the surface coverage can proceed only to a certain critical value, a value reached when the accumulated charge at the surface is so large as to repel any further carriers of the same sign from reaching the surface from the bulk. In practice, this critical coverage of the surface is on the order of 1% of the experimentally measured adsorption.

To understand the nature of this critical coverage as well as the influence of the adsorbed molecules on the substrate conductance, we will consider some of the physics of semiconductors.

Due to the Pauli exclusion principle, no two electrons can occupy the same state, where the state is defined by the energy, momentum, and spin of the electron. In electronic conduction in solids, the application of an electric field to the solid tends to accelerate the electrons, thereby changing their energies and momenta. If the new state is already occupied by another electron, a given electron cannot be shifted into it; only if the new state is vacant can the electron move into it, and so take part in the flow of current. This is illustrated in Figure A1.

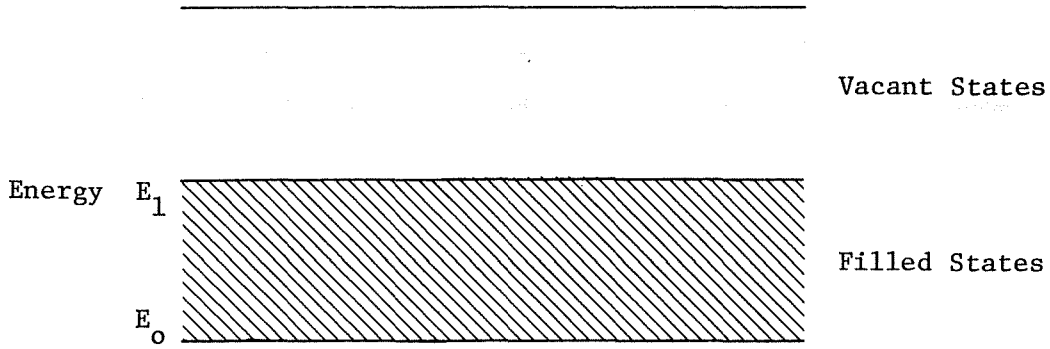

Figure A1. Electron States.

Suppose the diagram represents all the electrons in a metal. First, by the exclusion principle, only two electrons, of opposite spin, can have precisely the lowest energy, E_o. All others must have successively higher energies up to energies near E_1. At absolute zero in temperature, the highest energies are precisely E_1, but at finite temperatures the thermal energy of the solid lattice can add an energy of about k_BT, where k_B is Boltzmann's constant and T is absolute temperature, to the kinetic energy of the electrons. For comparison, E_1 might be about 2 electron volts for a metal, while k_BT is about .025 electron volt at room temperature.

If an electric field is applied to this metal, the electrons with energies near E_1 can easily accelerate into vacant states. In so doing, they leave their original states vacant, and electrons of lower energy can

accelerate into them, and the process can be repeated all the way down to the lowest states. Thus under the application of even very weak electric fields, the electrons in the metal can be accelerated and contribute to the flow of current.

The mathematical function which describes the distribution of electrons among the states available to them is called the Fermi-Dirac function, $n(\varepsilon)$:

$$n(\varepsilon) = [\exp\ (\varepsilon-\mu)/k_B T + 1]^{-1}, \qquad \text{(A1)}$$

where ε is the energy of the electron and μ is the chemical potential of the electron. The chemical potential is also called the "Fermi level" of the system. It is a function of the density of electrons and, to some extent, the temperature and is defined by the relation:

$$N = \int_0^\infty n(\varepsilon)d\varepsilon\ , \qquad \text{(A2)}$$

where N is the total number of electron energy states (equal to 1/2 the number of electrons.)

According to this distribution function, those states with ε well below $\mu-k_B T$ are completely filled ($n(\varepsilon) = 1$), and those with ε well above $\mu + k_B T$ are essentially empty ($n(\varepsilon) = 0$). For states of energy $(\varepsilon-\mu) >> k_B T$, the population of states varies as $\exp[-(\varepsilon-\mu)/k_B T]$.

In regular crystals, metals, semiconductors, and insulators, the available states occur in broad bands separated by energy regions in which there are no available states, called the band-gaps. These

gaps are caused by the periodic electric potential in which the electrons move. The presence of the band gaps has a large influence on the availability of electron conduction states. This is illustrated in Figure A2.

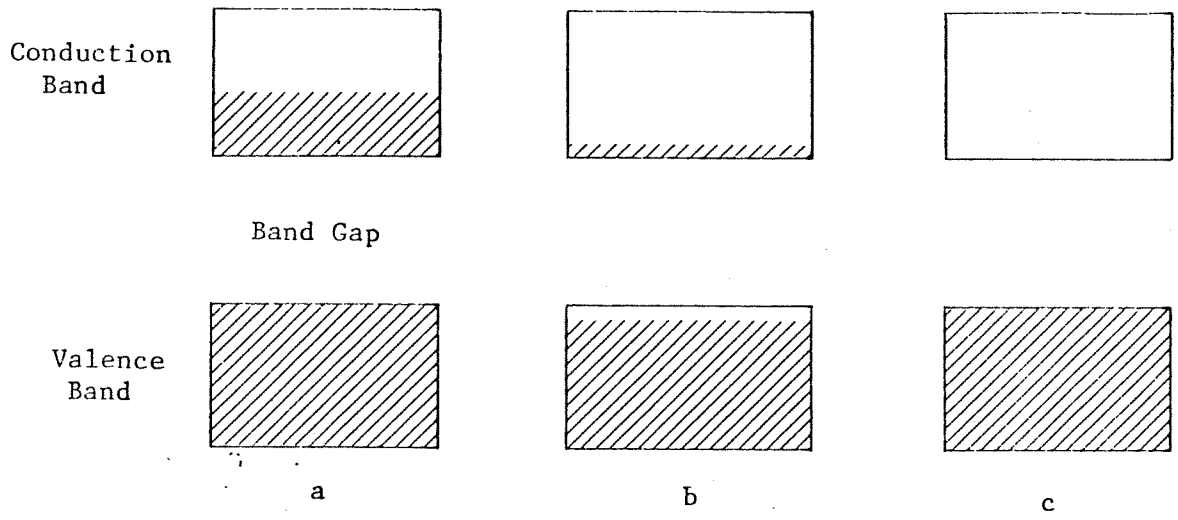

Figure A2. Illustration of Band Gaps.

In Figure A2a, the lower band, also called the valence band filled and the upper band is partially filled. The electrons in the upper band have many vacant states available for conduction, and so this diagram is characteristic of a metal. The energy E_o of Figure A1 would correspond to the energy at the bottom of the conduction band. The electrons in the valence band would not take part in conduction because the applied electric field cannot accelerate the valence-band electrons to energies greater than the band gap.

In Figure A2b, the valence band is only slightly filled. This may be due to thermal excitation of electrons out of the valence band. The conduction band electrons have many vacant states available, but the number of electrons, due to the thermal excitation, is so small that the current carrying ability of the material is small. This is a semiconducting material.

Figure A2c shows the case for an insulator. The valence band is filled, the conduction band empty. There are no vacant states for the electrons to move into and therefore there is no conduction. Insulators in general have wider band gaps than semiconductors, so that thermal excitation cannot populate the conduction band. Conversely, even with the narrower band gap of the semiconductors, at absolute zero the semiconductor becomes an insulator.

An expression for the concentration of electron and hole states (the states left open by thermal excitation of electrons across the band gap) can be derived assuming $n(\varepsilon) = \exp[-(\varepsilon-\mu)/k_BT]$:

$$n \cdot p = A(k_BT)^3 \exp[-Eg/k_BT], \qquad (A3)$$

where A is a constant, Eg is the band-gap energy, n is the electron concentration and p is the hole concentration. This is an expression of the law of mass action, which finds widespread use in physical chemistry. It says that forcing the concentration of electrons in one direction causes a compensating change in the concentration of holes. In this way, introduction of donor atoms into the crystal not only increases n directly but also decreases p.

An intrinsic semiconductor is one in which the number of electron carriers equals the number of holes; that is, the carriers are generated thermally in pairs. For this condition, $n = p$, and from the definition of the chemical potential in Equation A2, it can be shown that

$$\mu = Eg/2 \qquad (A4)$$

It is important to realize that μ varies with the electron concentration according to Equation A2, and that changes in electron concentration are strongly reflected in the thermal population of the conduction band.

It is in this fact that we see the reason for a critical value of the number of strongly chemisorbed molecules. Suppose the molecules are acceptors, for definiteness; they therefore hold electrons in the substance near the surface and the chemical potential becomes larger and larger until eventually the number of thermally excited electrons in the conduction band becomes negligible. With no more free electrons to partake in the "strong" bond, no further chemisorption of the molecules can take place.

As mentioned before, this occurs at a surface coverage that is only a fraction of what is observed. It therefore seems that the boundary-layer theory lacks the ability to account for all the sorbed molecules. Vol'kenshtein's hypothesis of weak chemisorption, in which the free electron concentration is not directly affected, offers an explanation for the large surface absorption measured. The evidence also indicates that most of the sorbed molecules are bound by the weak chemisorption rather than by the strong form.

At this point we must note a very important result. Even though the strong chemisorption saturates when the number of free electrons diminishes (for acceptor gas molecules), the number of current carriers increases greatly because of the law of mass action. As n decreases, p must increase, but in such a way that the sum of n + p becomes larger. Mathematically, the law of mass action causes the sum of the carriers, n + p, to be a minimum when n = p. This is illustrated in Figure A3.

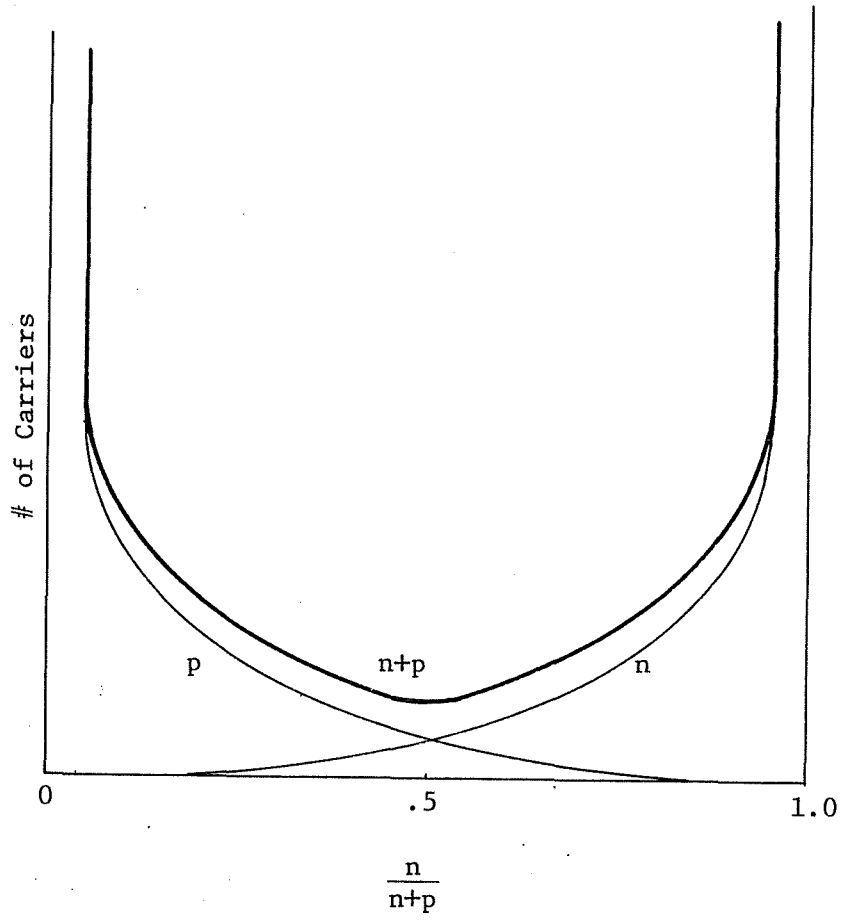

Figure A3. Number of Carriers as a Function of the Fraction n/n+p.

Thus far we have considered intrinsic semiconductors. In the real world, most semiconductors at room temperature are not intrinsic, but have their carrier concentrations determined by impurities or defects. Impurity doping in semiconductors determines carrier concentration by placing atoms in the crystal lattice with either more or fewer valence electrons than the crystal itself. If the impurity has an extra valence electron, it is relatively loosely bound to the donor atom and can be thermally removed from it. If the impurity has one fewer electrons than the lattice atoms, it is an acceptor impurity because any electron in its vicinity can be bound to it more stably than to the lattice atoms; it tends to create a hole in the valence electrons of the lattice atoms.

Defect doping is a result of non-stoichiometry in the crystal; that is, chemical composition which differs from the formula composition. A typical case is a metal oxide. If the metal atoms are in the correct proportion to the oxygen atoms, the substance will be an insulator because the band gap for the oxide is very large compared to intrinsic semiconductors. An excess of metal atoms will lead to donor characteristics because the metal atoms have outer valence electrons which are easily removed. An excess of oxygen atoms will lead to acceptor characteristics because the oxygen valence shell is unfilled and offers a stable site for electron residence.

Without going into great detail about the properties of extrinsic semiconductors, we observe that addition of a dopant to an intrinsic semiconductor will change the chemical potential of the substance in the neighborhood of the dopant atom. In effect, the impurity places a

local energy level within the band gap. It is therefore more accessible to thermal population than the conduction band itself is. This local level is associated with the impurity itself, whether within the substances or on the surface. Thus, if the impurity is an adsorbed molecule, the weak form of chemisorption occurs when the local level is unpopulated and strong chemisorption occurs when it is populated. The relative positions of these local levels is shown in Figure A4.

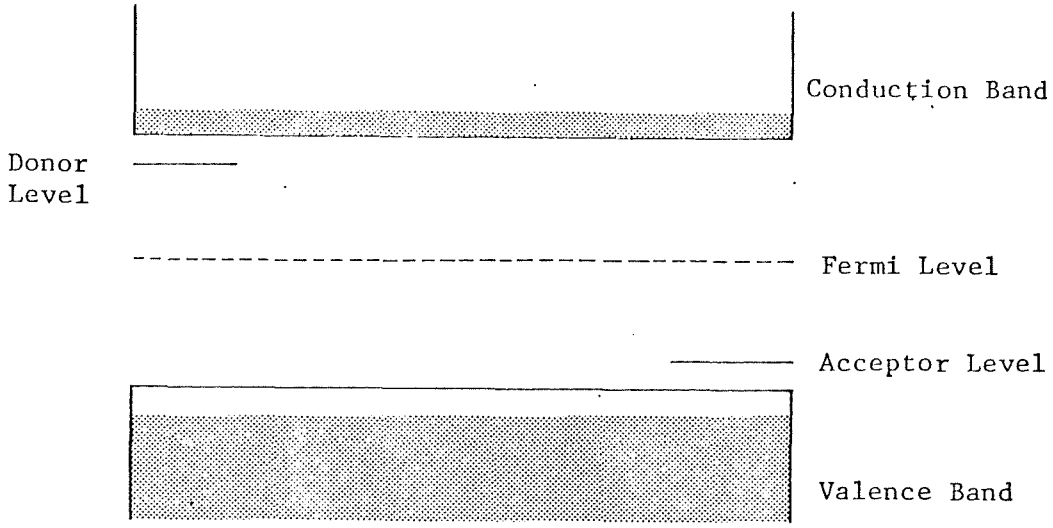

Figure A4. Band Gap with Local Levels.

The levels represent the energy difference between the impurity atoms and the lattice. If a lattice has donor-type impurities in it, and they become ionized, then the number of free electrons increases. and the chemical potential of acceptor levels raises the chemical

potential. In point of fact, both types of levels can be populated at the same time, and the position of the chemical potential is determined uniquely by their relative proportion and the intrinsic carrier concentrations of the solid.

When we dealt with the properties of a gas strongly chemisorbed on the surface of an intrinsic semiconductor, we observed that the number of free current carriers increased for either acceptor or donor type behavior because of the law of mass action. When we deal with extrinsic semiconductors, the number of current carriers may either increase or decrease, depending on the type of material and adsorbed gas.

Consider a metal oxide--ZnO, for example; suppose that there is an excess of Zn, which is a donor dopant. Then, the number of electrons will exceed the number of holes by an amount depending on the population of the donor levels. If a donor-type gas is then adsorbed on the surface, it will further increase the electron population and the number of carriers will increase. If, on the other hand, an acceptor-type gas is adsorbed on the surface, it will reduce the free electron population, moving the total number of carriers toward the minimum where $n = p$. It is even conceivable that, with sufficient adsorption, the majority of carriers could be switched over from electrons to holes, the number of carriers increasing with further strong adsorption. This is called inversion.

Let us further note that, all else being equal, the amount of donor-type gas that can be adsorped on donor-doped (or n-type) materials is much less than the amount of acceptor-type gas that can be adsorbed. This is a consequence of the number of free carriers available to take

part in strong chemisorption. Therefore, we state that donor-type gases tend to be adsorbed best on p-type materials, and acceptor gases on n-type materials. Further, the gases have the greatest influence on the number of free carriers with those materials on which they are best adsorbed.

APPENDIX 2

In looking for the effect of adsorbed gases on the bulk electrical conductivity of the solid, immediate attention must be given to the strongly chemisorbed gases because of their direct influence on the carrier density. Since each gas molcule that is strongly bound holds a free charge in its immediate neighborhood, the surface of the semiconductor acquires a potential that is different from the bulk of the material. This potential produces a bending of the valence and conduction bands near the surface. This is illustrated in Figure A5.

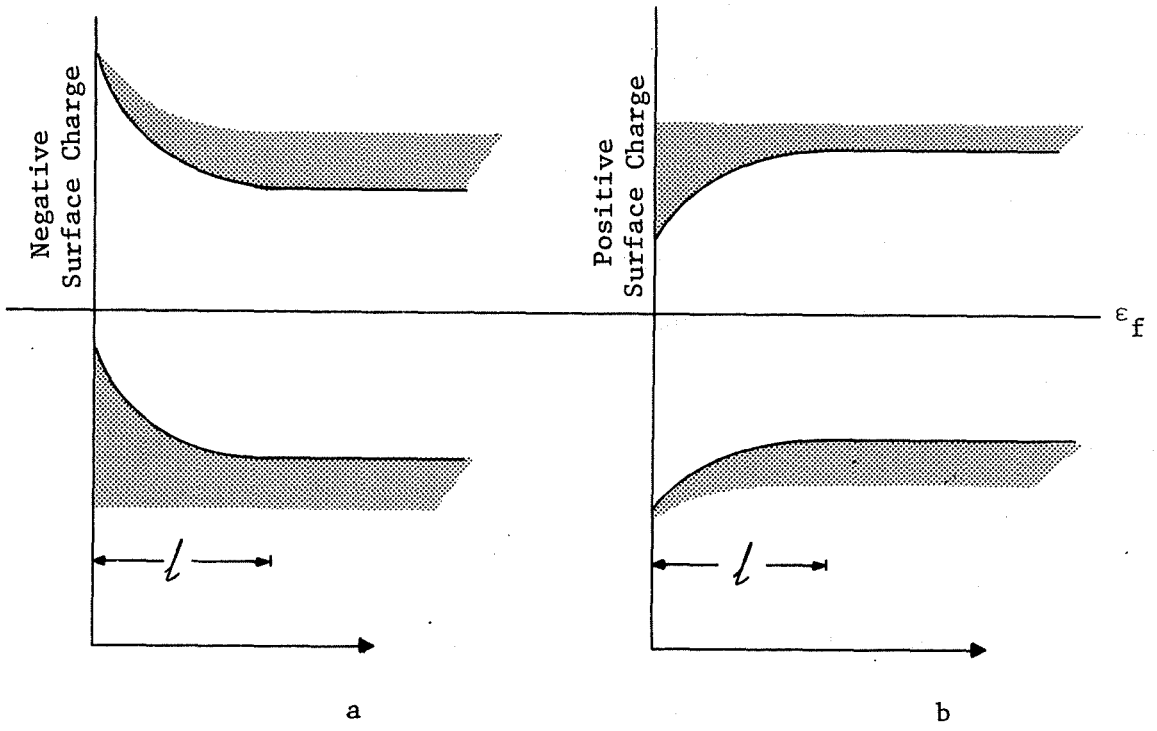

Figure A5. Bending of Bands Due to Surface Potential.

The explanation for the bending of the bands can be interpreted simply. The conduction and valence bands in the crystal represent the energy eigenstates of the electrons moving in the periodic potential of the lattice ions. If an electric potential which varies slowly in space (compared to the lattice dimensions) is applied, the energy eigenstates must also change to follow the potential. The basic structure of the bands remains unaffected, because on the scale of the lattice ion spacing, the electrons see the applied potential as constant. The result is the bending of the bands.

The bending occurs whether the surface charge is a real charge or is induced by an external electric field, which is effectively the case for adsorbed molecules. The bending effect does not mean that electrons or holes change energy as they approach the surface, but that certain energies are allowed for free carriers near the surface which are not allowed in the bulk of the crystal.

If the number of charges at the surface is in equilibrium with the bulk semiconductor, then the chemical potential is everywhere the same. (This is the condition for equilibrium.) As a result the occupation in the conduction band will be radically different near the surface compared with the bulk. This too is in agreement with the intuitive expectation that a negative surface charge will repel electrons from the region near the surface and a positive surface charge will attract them to the surface.

The effect of the surface charge does not penetrate indefinitely far into the bulk crystal because the carriers which are in the lattice are easily polarized or displaced from their equilibrium positions.

This results in a screening of the surface charge and a gradual reduction in its effectiveness as the crystal is penetrated. The distance ℓ in the figure indicates the penetration depth at which the effects of the surface charge are of the same order of magnitude as the thermal effects. This screening effect is most significant when there are a large number of carriers of sign opposite to the surface charge in the region adjacent to the surface--i.e., for an acceptor gas on a p-type semiconductor.

In Reference 14, J. C. Yen calculates the characteristic screening length from Poisson's equation:

$$\frac{\partial^2 V}{\partial x^2} = -\frac{\rho}{\varepsilon} , \tag{A5}$$

where V is the lowest energy level of the conduction band, x is the distance into the semiconductor, ρ is the surface charge density, and ε is the dielectric constant. His result is:

$$L_D = \left(\frac{\varepsilon k_B T}{q^2 N}\right)^{1/2} , \tag{A6}$$

where q is the unit charge of the electron and N is the majority carrier density in the bulk material. L_D is the distance over which the perturbed bands return to their bulk level. This length is also known as the Debye length. A result of the same order is calculated when the sign of the surface charge is the same as that of the bulk majority carriers (a condition resulting in the depletion of carriers in the region adjacent to the surface.) This will be discussed later in this section.

The magnitude of L_D is on the order of a few hundred Angstroms, depending on the carrier density. Thus, an adsorbed gas could affect

the carrier density to roughly that depth. This is the prime reason for attempting to use films for the substrates of a thickness up to a few thousand Angstroms only.

This is not to say that the conductivity of the specimen as a whole cannot be strongly influenced. Consider the case of an intrinsic semiconductor with total carrier concentration n+p. The presence of a strongly sorbed donor gas on the surface will result in a large increase of n within a Debye length of the surface. This increase may be so large that, for currents parallel to the surface, almost all the carriers involved are those induced by the presence of the gas.

To formalize the concept of electrical conductivity, it is necessary to introduce the mobility of the carriers. The presence of an electric field within the crystal causes the carriers to be accelerated, electrons in one direction, holes in the opposite direction. The carriers do not accelerate indefinitely but are scattered from other carriers, by defects in the crystal, and especially by the lattice atoms. As a consequence of the scattering, the average velocity of a carrier is much less than its peak instantaneous velocity. The mobility of the carrier is defined as:

$$\mu_i = |v_i|/E \ , \qquad \text{(A7)}$$

where the subscript on the mobility μ can stand for electrons or holes, $|v_i|$ is the value of the drift (or average) velocity of the carrier under an applied field E. The mobilities of holes and electrons depend upon their individual rates of scattering and effective masses in the crystal. In general, electrons tend to be more mobile than holes, but for the purposes of this analysis it is sufficient to treat them as equal.

The electrical conductivity in the presence of both carriers is given by:

$$\sigma = (ne\mu_e + \rho e\mu h), \tag{A8}$$

where e is the electronic charge. The conductivity exhibits a strong temperature dependence in intrinsic semiconductors, primarily because of the exponential dependence of carrier concentration on temperature. The temperature dependences of μ_i are usually power-law functions of T.

The macroscopic resistance R is related to the conductivity by the equation

$$\frac{1}{R} = \frac{1}{L}\int \sigma dA \ , \tag{A9}$$

where σ is taken as a function of the cross-sectional area, but not of the length L; this corresponds most closely to the concepts under consideration.

In Figure A6, we present a model for the resistance of a thin film with an adsorbed layer of gas which influences the conductivity.

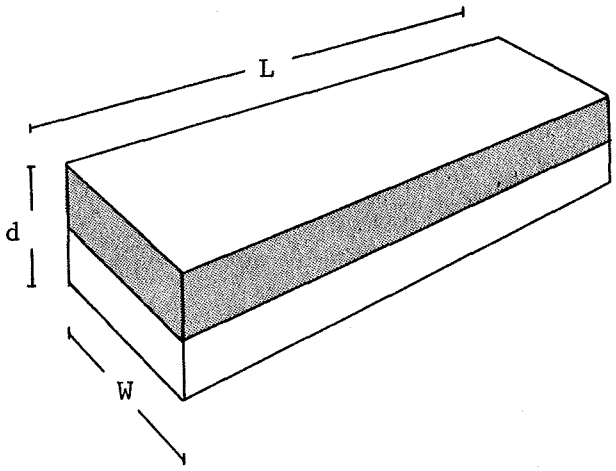

Figure A6. Conductivity Model of a Thin Film.

The shaded region represents a layer within a Debye length of the surface, for which the adsorbed gas changes the conductivity. The unshaded region is the remainder of the semiconductor. If we denote the conductivity within the surface influenced region as σ_D and that in the bulk as σ_B, the total resistance of the film along the length L is:

$$R = L\ (\sigma_D \cdot L_D \cdot W + \sigma_B \cdot (d-L_D) \cdot W)^{-1}, \qquad \text{(A10)}$$

which can be reduced to

$$R = \frac{L}{W} \frac{1}{(\sigma_D L_D + \sigma_B (d-L_D)}\ , \qquad \text{(A11)}$$

where L_D is the Debye length.

This simple model serves to illustrate the relative influence of the induced and bulk conductivities. It has the limitation of showing no response to changes in the adsorbed gas except as implied in σ_D. (Recall that L_D depends only on the bulk density of charge carriers.)

In Reference 14, Yen expands this model to include variations with surface charge. Detailed calculations of the conductivities are not given, because the properties of the particular semiconductor have a great influence. Instead, the relative change in resistance with adsorbed gas concentration is calculated. Two types of influence are considered.

In the depletion model, the number of free carriers is reduced below the normal bulk value, as for a donor-type gas on a donor substrate. Assuming there is a large difference in carrier concentration between the depleted and the normal regions, Poisson's equation can be solved for the potential distribution. Two important features emerge in the solution.

First, a depletion depth is defined, corresponding to the Debye length, which depends on the surface concentration of adsorbed atoms:

$$\text{(number of atoms/unit area)} = D \cdot \text{(number of donors/unit volume)}, \tag{A12}$$

for the case of n-type semiconductors. Thus, the more surface atoms adsorbed, the greater the depletion depth. Since it is assumed that the number of carriers in the depleted region is small compared with the bulk region, the resistance would vary, in fashion similar to Equation 11 as

$$R = \frac{L}{W} \frac{1}{\sigma_B (d-D)} \cdot \tag{A13}$$

This is a slowly varying function of D until $\underline{D}$ is comparable to $\underline{d}$, implying that a sensor of this type should have a physical thickness not much larger than the depletion depth for maximum sensitivity.

The second feature of the solution is an evaluation of the amount of bending of the conduction bands. The additional potential at the surface is:

$$E_S = \frac{e^2 \text{ (number of atoms/unit area)}^2}{2\varepsilon \text{ (number of donors/unit volume)}}, \tag{A14}$$

where E_S is the additional energy, e is the electronic charge and ε the dielectric constant. This potential presents a barrier for the communication of charge carriers with the adsorbed atoms, and is a cause of the appearance of activated adsorption properties.

In the accumulation model, the number of carriers in the influenced region is greatly increased over the bulk value, as for intrinsic semiconductors or acceptor atoms adsorbed on an n-type substrate. The accumulation layer has an increased conductivity over the bulk value for small numbers of adsorbed atoms.

Again a depth D is defined, less than the Debye length, for the influenced region. Assuming the number of carriers is much greater than in the bulk, the resistance has the following behaviour:

$$R = \frac{L}{W} \frac{1}{\sigma_D \cdot D} \tag{A15}$$

Therefore, the resistance is independent of sample thickness since essentially all of the current is carried within a layer very close to the surface.

The energy bands are bent down at the surface by an amount:

$$E_S = -k_B T \, \ell n[\sec^2 \frac{-D}{\sqrt{2}\, L_D}]. \tag{A16}$$

The depth $\underline{D}$ is again a function of surface coverage, but not in any simple manner. This downward bending of the bands results in a lowering of the energy of activation for strong chemisorption with increasing numbers of adsorbed molecules.

It is possible to adsorb so many molecules that an inversion layer is formed in which the majority of carriers are of the opposite type from the bulk semiconductor. In such a case, the energy bands are then bent upward, the more so with increasing adsorption.

It is important to note that the same semiconductor can exhibit both kinds of behavior, depletion or accumulation, depending on the amount of gas adsorbed on the surface.

To summarize the results of Yen's work, we make the following statements.

1) In the depletion mode of influencing resistance, sample thickness is of prime importance, since the bulk carriers determine the sample resistance.
2) In the accumulation mode, sample thickness is unimportant, since the sample resistance is determined by the surface layer.
3) The depletion or accumulation depth is a function of the surface coverage, increasing with increasing coverage.
4) The bending of bands increases the surface potential in the depletion modes, leading to an increase of activation energy with surface coverage.
5) The bending of bands decreases the activation energy with coverage because the bands are bent downward. With further coverage the energy of the bands at the surface will again increase.

APPENDIX 3

An array of granular particles of random shapes and size can be modeled simply, as far as its electrical parameters are concerned, by a simple resistor capacitor circuit:

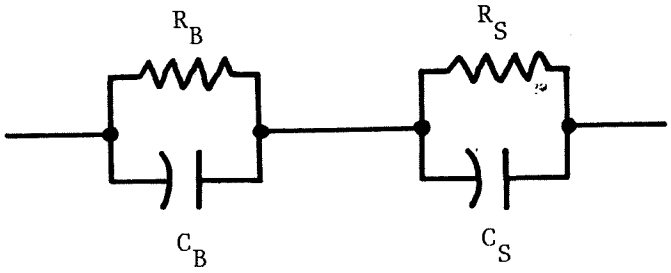

The subscripts B refer to the bulk properties of the material and S to the surface properties of the grains. For the DC and low frequency AC measurements used in this investigation, the parallel capacitors can be neglected and the resistance of the whole array is simply $R_S + R_B$.

At high frequencies, the magnitude of the complex resistance is $R_S R_B (C_S + C_B)^2 / R_S C_S^2 + R_B C_B$. By combining measurements at very low and very high frequencies, the components that make up the total resistance can be deduced, and the contributions of bulk and surface conductances assessed.

APPENDIX 4

Sputtered MnO_2 films as CO sensor are reported on here. The change in film resistance from exposure to CO is used as a basis to detect the presence of CO.

Sample Preparation

The MnO_2 films were prepared by radio-frequency sputtering on 3/8" square Corning glass substrates. The substrates were ultrasonically cleaned in an acetone bath, degreased and stored in methanol. Prior to their use, they were blown dry in a N_2 jet.

MnO_2 was sputtered at 50W total target power. The substrates were heated in vacuum for 75 min. at approximately 125°C prior to sputtering. The substrate holder was water cooled during film deposition. The samples were deposited in a mixture of O_2 and Ar plasma of varying composition. Chamber pressure prior to sputtering was typically lower than 5×10^{-6} Torr. The pressure during sputtering was kept such that the Pirani gauge reading was constant in all the runs. This corresponds to a pressure of 6 mTorr for the Ar plasma and to a somewhat lower value for plasma containing oxygen along with Ar.

Some Physical Properties of Sputtered Films

Table A1 shows the thicknesses of sputtered films obtained by optical interference measurement. For the same sputtering time, the thickest films were obtained in a 100% Ar plasma. Addition of O_2 to the plasma seems to decrease the deposition rate initially. However, a plasma composition of 40% O_2 and above does not seem to have any further significant effect on the deposition rate.

Table A1. MnO_2 Film Thickness by Interference Measurements

Sample No.	Plasma Composition % O_2	% Ar	Sputtering time (min.)	Thickness Å
MnO_2-6-3	100	-	100	1400
MnO_2-3-3	60	40	100	1550
MnO_2-4-3	50	50	100	1300
MnO_2-8-3	50	50	50	650
MnO_2-2-3	40	60	100	1450
MnO_2-1-3	20	80	100	1950
MnO_2-7-3	0	100	100	2500

Table A2 shows the results of thermal probe measurements carried out on these films in ambient room atmosphere. A Keithley model 602 electrometer was used to measure the voltage generated by the temperature difference between the two probes on the film. From this table, it is seen that the sample sputtered in 20% to 100% O_2 plasma were all n-type with increasing magnitude of thermal probe voltage for increasing O_2 content in the plasma. The sample sputtered in 100% Ar plasma showed initially a positive deflection corresponding to a p-type substrate which then decayed towards zero or a small negative value. Similar nature in thermal voltage was also observed at the substrate temperature of approximately 250°C.

Experimental Set-Up

The electrical measurement set-up is shown in figure A7. A 2 Hz, 400 mV r.m.s. signal was fed to the sample in series with a lock-in amplifier. The input impedance of the lock-in amplifier was $10^7\Omega$.

Table A2. Thermal Probe Measurements on Sputtered MnO_2 Films

Sample No.	Plasma Composition		Film at Room Temp. Hot Probe at 75°C		Film at Approx. 250°C Hot Probe at 140°C	
	% O_2	% Ar	Measured Voltage	Conductivity Type	Measured Voltage	Conductivity Type
MnO_2-6-7	100	-	-49 mV	n	-65 mV	n
MnO_2-5-7	80	20	-42 mV	n	-55 mV	n
MnO_2-3-7	60	40	-32 mV	n	-50 mV	n
MnO_2-4-7	50	50	-33 mV	n	-46 mV	n
MnO_2-2-7	40	60	-32 mV	n	-46 mV	n
MnO_2-1-7	20	80	-26 mV	n	-40 mV	n
MnO_2-7-7	-	100	See	Text	See	Text

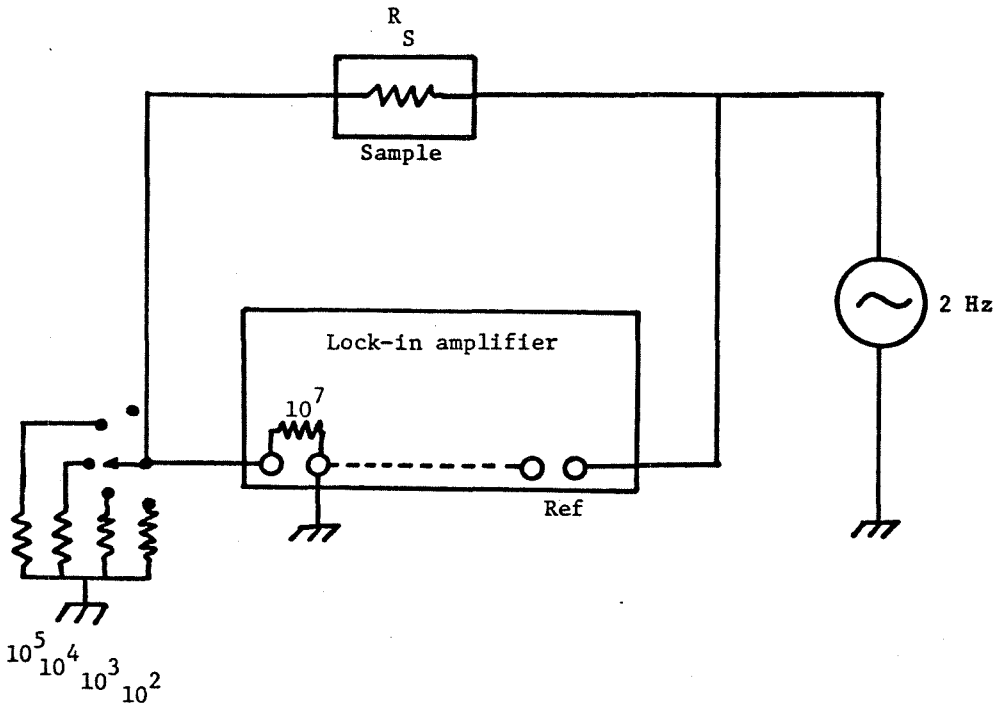

Figure A7. The AC Measurement Set-Up.

This was shunted by a parallel resistance, when necessary, such that the value of the combination was at least two orders of magnitude lower than the sample resistance R_S. This way the voltage read by the lock-in amplifier was essentially proportional to the current through the sample.

Results

Measurements were carried out on films sputtered in two different plasma compositions of 50% O_2-50% Ar and 100% Ar. A 1300 Å thick film deposited in 50% O_2-50% Ar plasma showed no response to exposure to 110 parts per million (ppm) CO in air mixture at temperatures up to 350°C. At 350°C, the sample resistance decreased in time rather rapidly to a value several orders of magnitude lower.

Next measurements were carried out on a 2500 Å MnO_2 film sputtered in 100% Ar plasma. The results of exposure of this sample to 110 ppm CO in air mixture are shown in Table A3. From this table, the maximum change in the value of R_S is obtained at 315°C. The value of R decreases on exposure to 110 ppm CO in air.

Table A3. Response of Film to Exposure of 110 ppm CO

Sample Temp. °C	Sample Resistance R_S (Ω)	Δ
Room	6.95×10^8	0
115°C	8.5×10^7	0
260°C	9.27×10^6	-.022
315°C	6.84×10^6	-.156
385°C	2×10^6	-.058

The value of the film resistance appeared to be steady during short term measurements but was found to increase at the rate of about 1.15%/hour at 260°C. This may be attributed to gain of O_2 or loss of any water vapor

present in the film, the presence of which is known to decrease the sample resistance.

The above sample was taken out and stored in ambient air for 9 days. Subsequent d.c. measurements on this sample at RTI failed to show any response to $\sim$248 ppm CO in air mixture. When put back in the a.c. measurement set-up, the resistance of the film was found to be slightly greater at room temperature. However, the activation energy was now found to be different. Figure A8 shows the activation energy for this sample on the first and the second set of runs. The value has changed from 0.24 eV/particle to 0.46 eV/particle. During the second set of runs, on the first exposure to 110 ppm CO in air mixture at 315°C, a steplike Δ of approximately -.047 was obtained, followed by a gradual decrease in R for 80 more minutes to give a total Δ of about -.15. The film was noisy and appeared to drift in time. On shutting off the CO flow, the film resistance remained unchanged, indicating an absence of desorption. The subsequent exposures to 110 ppm CO in air mixture at 315°C showed a very small decrease in film resistance without any observable desorption. So it appears that CO does initially absorb to the surface but does not desorb in any reasonable time. Between the two sets of runs, the film properties have changed; and in the second case, the film is no longer usable as a CO sensor.

Observations were then made on a MnO_2 film sputtered in 100% Ar atmosphere but with half the thickness of the previous case. On the first measurement run, the film resistance was found to be extremely high. The film showed no response to CO exposure up to 400°C. The capacitance

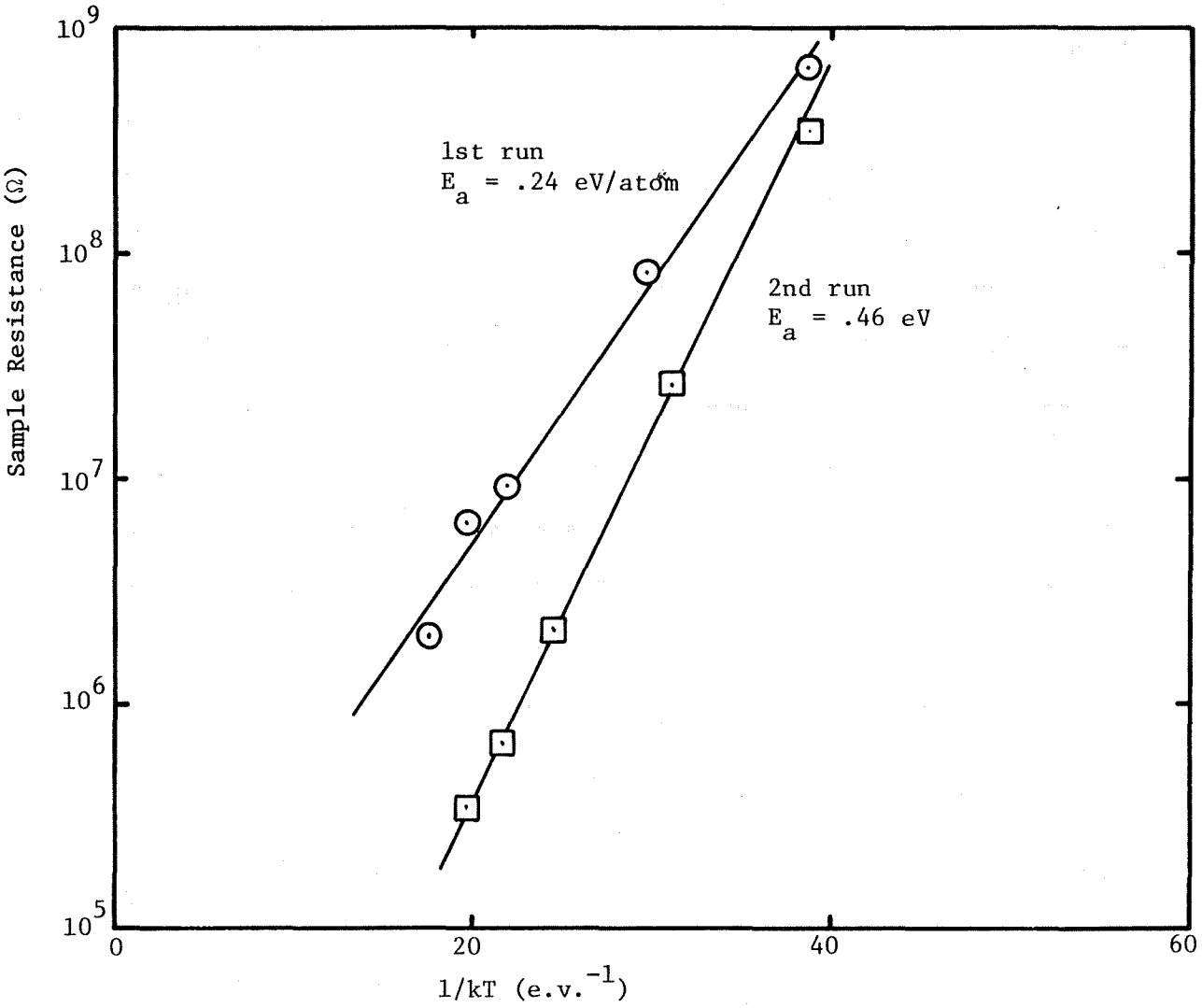

Figure A8. Temperature Response of MnO_2 Film at Two Times.

current due to stray capacitance partly made it difficult to observe changes in the film resistance. The film resistance at room temperature was found to be extremely sensitive to the air flow rate--the resistance being lower for lower flow rates. Also, on heating the sample from room temperature, under a constant flow rate, the film resistance was found to first increase and then decrease. For the first heat cycle, the film resistance at 400°C was slightly greater than the film resistance at room temperature under the same flow ratio. A possible reason again may be due to loss of water vapor from the film on heating, loss of which increases the film resistance.

The above film was stored in ambient air for 10 days. The device resistance was found to be about the same at room temperature but had decreased at higher temperatures. The film was now responsive to CO. However, both an increase in R and a decrease in R were obtained on the thicker film on CO exposures. The reason for this is not known. For the thinner films, whenever a decrease in R_S was obtained, the otherwise steady value of film resistance became unsteady and drifted upon CO exposure. In one case both an increase and a decrease in film R_S were increasingly obtained on the same exposure to CO (observation time 195 hours) with a step like decrease in R during desorption indicating a net increase in R during absorption. Whenever ΔR_S was positive, the film behaved normally with a step-like increase in R_S during adsorption cycle and a slow decrease in R_S during the desorption cycle. After 220 hours of observation time, the film gradually became insensitive to further CO exposure.

The film resistance was also measured by DC technique at 315°C between the observation time of 55 and 80 hours. A slight decrease in

R_S ($\Delta = -.05$) was seen on exposure to 110 ppm CO in air mixture with adsorption time being less than 10 min. The AC method showed a $\Delta \approx -.3$ at the same time.

The film, on application of approximately $\pm$30V from the curve tracer at 315°C, became extremely conductive. Greater than 3 orders of magnitude decrease in film resistance was observed at 315°C. The film remained insensitive to CO exposure after this change. The activation energy was found to be 0.36 eV/particle and is plotted in figure A8.

Appendix 5

Method of Preparation of "Bott" Slurries

The starting materials for a slurry sensor was as follows:

1.0 g	NH_4NO_3
50 mℓ	distilled water
2.0 g	$(NH_4)_6\ Mo_7O_{24} \cdot 4\ H_2O$
X	

The X represents a salt of the added metal ion; its weight was adjusted to give the desired fraction in the final composition. The salts used were: $Zn(NO_3)_2 \cdot 3H_2O$; $Cu(NO_3)_2 \cdot 6H_2O$; $(NH_4)_2CrO_7$; and $(NH_4)VO_3$. In the case of Unit #12, 0.2 g of ammonium molybdate was used with 3.0 g of zinc nitrate.

The above materials were stirred in a 50 mℓ beaker and heated on a hot plate for 2 hours (250°C surface temperature). The liquid was evaporated to the point of dryness, but care was taken not to bake the material. A few drops of distilled water were added to make a paste of the material, a small amount of which was bridged across the gold wire electrodes, mounted on a glass slide.

The water was evaporated from the sensor by holding it near the hot plate. The slide was then placed directly on the hot plate to decompose the ammonium nitrate. The length of this heating period was 15 minutes, and it was during this time that the material acquired a frothy appearance. For some sensors a small amount of material at the surface of the slide (the hottest part) became colored gray.

The slide was removed from the hot plate and allowed to cool to room temperature before being mounted in the test chamber.

Catalogue of Sensors

	Material	Form	Best Δ @ [CO] ppm		Remarks
1.	CdS	600 Å Sp. film	0	100	See p. 34
2.	CdS	1200 Å Sp. film	0		
3.	CdS	1200 Å Sp. film	0		
4.	CdS	800 Å Sp. film	0		
5.	CdS	1600 Å Sp. film	0		
6.	CdS	1800 Å Sp. film	0		
7.	CdS	1800 Å Sp. film	0		
8.	CdS	1800 Å Sp. film	0		
9.	CdS	1800 Å Sp. film	0		
10.	CdS	880 Å Sp. film	0		
11.	CdS	1800 Å Sp. film	0		
12.	CdS	1200 Å Sp. film	0		
13.	CdS	2400 Å Sp. film	0		
14.	SnO	1500 Å Sp. film	0	36.9 wet	p. 34
15.	ZnO	1800 Å Sp. film	0	100	p. 32
16.		1800 Å Sp. film			
17.		1800 Å Sp. film			
18.		1800 Å Sp. film			
19.		1800 Å Sp. film			
20.		1800 Å Sp. film			
21.		1800 Å Sp. film			
22.		1800 Å Sp. film			
23.	Cu_2O	2000 Å Sp. film	0	248 wet&dry	
24.	Cu_2O	2000 Å Sp. film	0	248 wet&dry	

	Material	Form	Best Δ @ [CO] ppm		Remarks
25.	$Cu_{1+x}O$	2000 Å evap. film	+.21	154 wet	p. 35
26.	$Cu_{1+x}O$	2000 Å evap. film	0	248	
27.	MnO_2	pressed disc with polyisoprene sulfone binder	0	150	p. 39
28.	TiO_2	pressed disc with polyisoprene sulfone binder	0	150	p. 39
29.	5.7Ω YSI thermistor	bead	0	154	p. 36
30.	35kΩ YSI thermistor	bead	0	154	p. 36
31.	MnO_2	powder pressed into Teflon	-.21	154	p. 40
32.	MnO_2	10,000 Å evaporated, oxidized	>-.05	248	p. 34
33.	MnO_2	10,000 Å evaporated, oxidized	0	248	p. 34
34.	MnO_2	10,000 Å evaporated, oxidized	0	248	p. 34
35.	MnO_2	10,000 Å evaporated, oxidized	0	248	p. 34
36.	MnO_2	10,000 Å evaporated oxidized	0	248	p. 34
37.	MnO_2	10,000 Å evaporated oxidized	0	248	p. 34
38.	MnO_2	2000 Å evaporated, oxidized	0	248	p. 34
39.	MnO_2	2000 Å evaporated, oxidized	0	248	p. 34
40.	MnO_2	300 Å sputtered	0	100	p. 34

	Material	Form	Best Δ @ [CO] ppm		Remarks
41.	MnO_2	300 Å sputtered	0	100	p. 34
42.	MnO_2	1200 Å sputtered	-.04	100	p. 34
43.	MnO_2	2000 Å sputtered	-.10	100	p. 34
44.	MnO_2	3000 Å sputtered	-.05	100	p. 34
45.	MnO_2	170 Å sputtered	0	100	p. 34
46.	MnO_2	powder pressed into Teflon	-.20	154	p. 40
47.	MnO_2	powder-epoxy A	0	154	p. 42
48.	MnO_2	powder-epoxy B	0	154	p. 42
49.	MnO_2	powder-RTV rubber	0	154	p. 42
50.	MnO_2	powder-epoxy on quartz	0	154	p. 42
51.	MnO_2	powder-epoxy on Pyrex	0	154	p. 42
52.	MnO_2	powder-epoxy on ceramic	-.25	154	p. 42
53.	MnO_2	powder pressed into heated Teflon	0	248 wet	Figure 7
54.	$Cu_{1+x}O$	evaporated film on germanium substrate	0	248	p. 37
55.	$Cu_{1+x}O$	evaporated film on germanium substrate	0	248	p. 37
56.	$Cu_{1+x}O$	evaporated film on germanium substrate	0	248	p. 37
57.	MnO_2	evaporated film on germanium substrate	0	248	p. 54

	Material	Form	Best Δ @ [CO] ppm		Remarks
58.	MnO_2	evaporated film on germanium substrate	0		
59.	MnO_2	evaporated film on germanium substrate	0		
60.	Hopcalite	powder, homemade	0	248	p. 54
61.	Hopcalite	powder, homemade	0		
62.	Hopcalite	powder, homemade	0	248 wet,dry	
63.	Hopcalite	commercial, #1	0	248	p. 54
64.	Hopcalite	commercial, #2	-.08	248 dry	p. 54
65.	NiO	2000 Å film, evaporated	0	248	p. 35
66.	NiO	2000 Å film, evaporated	0	248	p. 35
67.	NiO	2000 Å film, evaporated	0	248	p. 35
68.	MnO_2	powder, pressed into Teflon disk	-.39	248 wet	
69.	MnO_2	powder, pressed into Porex	0	154	
70.	MnO_2	powder, pressed into Porex	-.007	154	
71.	MnO_2	powder, pressed into Porex	-.058	154	
72.	MnO_2	powder, pressed into Porex	0	154	
73.	MnO_2	powder, pressed into Porex	-.087	154	
74.	MnO_2	powder, pressed into Teflon cup	-.38	154 wet	p. 43

	Material	Form	Best Δ @ [100] ppm		Remarks
75.	MnO_2	powder, pressed into Teflon cup	-.45	154 wet	p. 50
76.	MnO_2	powder, pressed into Teflon cup	-.21	154 wet	
77-94.	Slurry sensors - see Table 3, p. 59				
95.	MnO_2	powder, packed in resonant inductor	0	154	p. 38
96.	MnO_2	powder, packed in resonant inductor	0	154	p. 38
97.	CuS	powder, packed in resonant inductor	0	154	p. 38
98.	$(NH_4)_6 Mo_7O_{24}$	powder, packed into Teflon	0	154	p. 38
99.	MnO_2	powder, pressed into Teflon cup	-.22	248 wet	p. 52
100.	MnO_2	2500 Å film, sputtered	-.16	110	Appendix 4
101.	MnO_2	1400 Å film, sputtered	0	248	Appendix 4
102.	MnO_2	1550 Å film, sputtered	0	248	Appendix 4
103.	MnO_2	1300 Å film, sputtered	0	248	Appendix 4
104.	MnO_2	650 Å film, sputtered	0	248	Appendix 4
105.	MnO_2	1450 Å film, sputtered	0	248	Appendix 4
106.	MnO_2	1950 Å film, sputtered	0	248	Appendix 4
107.	MnO_2	powder, sandwiched between plates	0	154	p. 55

BIBLIOGRAPHY

Adams,D.L. and L.H. Germer, Surface Science 32, 205 (1972)

Adsorption of CO on tungsten (210)

Anderson, J and P.J. Estrup, J. Chem. Phys. 46, 563 (1967).

Andreev, A., C. R. Acad. Bulg. Sci. 20, 1309 (1967).

Nature of the bond between CO and a transition metal surface; effect of orbitals.

Ansbacher, T., Surface Science 11, 159 (1968)

Change in conductivity of Molybdenum films due to adsorbed CO

Altschuler, O. V., O. M. Vinogradova, V. A. Selznev, I. L. Tsitovskaya, and M. Ya. Kushnerev, Problemy Kinetiki Katalcse 15, 56 (1973).

Arafa, A.A., M.E. Kenaway and El-Daoushy, Acta Phys. Pol. A 40, 413 (1971).

Arizumi, T., and S. Kotani, J. Phys. Soc. Japan 7, 152 (1952).

Adsorption of CO by barium getter at low temperatures.

Armstrong, R. A., Canad. J. Phys. 46, 949 (1968).

Atkinson, S.J., C.R. Burndle, and M.W. Roberts, Chem. Phys. Lett 24, 175 (1974).

Baker, M. McD. and E.K. Rideal, Trans. Far. Soc., 1597 (1955).

Adsorption of CO on nickel.

Bastl, Surface Science 22, 439 (1970).

Baumback, H.H. v., H. Dunwald, and C. Wagner, Zeits. F. Phys. Chem. 22, 226 (1933).

Electrical conductivity of copper oxide.

Baumback, H.H. v., and C. Wagner, Zeits. F. Phys. Chem. 22, 199 (1933)

Electrical conductivity of zinc oxide and cadmium oxide

Baumback, H.H. v. and C. Wagner, Zeits. F. Phys. Chem. 24, 59 (1934)

Electrical conductivity of nickel oxide.

Beebe, R.A. and D.A. Dowden, Am. Chem. Soc. J. 60, 2912 (1938).

Low temperature adsorption of various gases, incl. CO, on chromic oxide. Van der Waals adsorption and activated chemisorption are distinguished.

Berkstresser, G.W., R.J. Brook, and J.M. Whelan, J. Mater. Sci. (GB) 9, 491 (1974)

Effects of mixed electronic and ionic conduction in ZrO_2 and ThO_2 as a function of CO oxidation rate

Biberacher, G. and G. Zirker, Ger. Offen. 2,023,813

Boonstra, A.H. and J. vanRuler, Surface Science 4, 141 (1966)

Adsorption of various gases on cleau and oxidized germanium surfaces.

Bykova, T.T. and N.S. Tsypkina, Fiz. Tech. Polnprov. 5, 262 (1971)

Changes in surface conductivity of single crystal Germanium for CO pressures of 10^{-8} to 10^{-5} torr.

Burch, D.E., D.A. Gryvnak, and J.D. Pembrook. U.S. Patent 3,793,525 (19 Feb. 1974)

Dual cell gas analyser

Chebotin, V.N., V.N. Konev, N.V. Mironova. Sov. Electrochem (USA) 9, 800 (June 1973)

Detection of SO_2 by solid electrolytes ZrO_2 + CaO, CeO_2 + Nd_2O_3, CeO_2 + SnO.

Chong, V.M., Dissertation, Princeton Univ., Princeton, N.J. 1971

Chong, V.M., J.V. Connoy and P. Mark. Phys. Status. Solidi A 9, K133 (1972).

Electronic effects of chemisorption on a powdered zinc oxide catalyst. CO, O_2 at one atm. and 10^{-8} torr.

Christman, K. and G. Ertt, Surface Science 33, 254 (1972)

Adsorption of CO on silver-palladium alloys

Clark, Alfred, "The Theory of Adsorption and Catalysis," Academic Press, New York 1970

Colburn, J.W., Surface Sci. 11, 61 (1968)

Dissociative electron desorption of CO from a tungsten surface

Cotton, J.D. and P.J. Fensham, Trans. Far. Soc. 59, 1444 (1963)

Experimental work on adsorptoin of H_2 and CO on NiO. The adsorption depends on the oxygenation of the surface. CO seems to adsorb as carbonate. Some conductivity measurements are provided.

Crowell, A.D., J. Chem. Phys. (USA) 36, 1171 (1962)

Measured CO chemisorption on nickel using a radioactive tracer

Charachorin and Elowitz, Acta Physicochimica SSSR 5, 323 (1936).

Datsiev, M.I. and N.I. Ionov, Soviet Physics-Technical Physics (USA) 62, (Dec 1967).

DeBoer, J.H. and P.G. Menon, Proc. K. Ned. Akad. Wetensch B (Netherlands) 65, 17 (1962)

Adsorption of N_2 and CO on abinuma at high and low pressures

Dell, R.M. and F.S. Stone, Trans. Far. Soc. 50, 501 (1954).

Deschauvres, A., Bull. Soc. Chim. France, No. 4, 732 (1956).

DeWitt, J.H.W., J. Solid State Chem (USA) 8, 142 (1973).

Dowden, D.A. and W.E. Garner, Chem. Soc., J, 893 (1939).

Heat of adsorption of CO, CO_2, H_2 and O_2 on Cr_2O_3 at 18°C. The interactions of the gases on the surface is explored.

Ehrlich, G., T.W. Hickmott, and F.G. Hudda, J. Chem. Phys. 28, 506 (1958).

Chemisorption of CO and N_2 at low temperatures.

Eisinger, J., J. Chem. Phys. 27, 1206 (1957).

Effect of CO on work function of tungsten.

Elovich and Kharakhoren, Problemy Kinetiki i Kataliza 3, M. (1937).

Elovich, S.I. and L.I. Margolis, IzV. Akad. Nauk SSSR, Physics Series 21, 206 (1957).

Electrical conductivity of MnO_2 as influenced by gases: O_2, CO_2, CO, H_2O, C_2H_6, and C_6H_6.

Engel, T. and R. Gomer, J. Chem. Phys. (USA) 50, 2428 (March 1969).

Enikeev, A. Kh., L. Ya. Margolis, and S.Z. Roginskii, Kokl. Akad. Nauk. SSSR 124, 606 (1959).

Effect of adsorbing gases on surface charge of oxide semiconductors.

Fontijn, A. and S.E. Johnson, J. Chem. Phys. 54, 6193 (1973).

Fritsch, O., Ann. d. Physik 22, 375 (1935).

Electrical conductivity and other measurements on zinc oxide

Ganhi, H.S. and M. Shefel, J. Catal 24, 241 (1972).

Adsorption of NO and CO on nickel oxide

Garner, W.E., Disc. Farad. Soc. 8, 211 (1950).

Review of oxide catalysts; H_2, CO, and hydrocarbons are considered

Garner, W.E. et al, Proc. Roy. Soc. (London) A 211, 472 (1952).

Reaction between CO and O_2 at room temperature on Cu_2O

Garner, W.E. and J. Maggs, Trans. Far. Soc. 32, 1744 (1936).

Adsorption of CO on zinc oxide

Garner, W.E. and F.J. Veal, Chem. Soc., J., 1488 (1935).

Adsorption of CO, H_2, O_2 and hydrocarbons on zinc oxide and mixed $ZnO-Cr_2O_3$

Garner, W.E. and T. Ward, J. Chem. Soc. 6, 323 (1936).

Measurements of heat of adsorption of gases on MnO_2, at room temperature.

Gasser, R.P.H., P.M. Gowan, and D.G. Newman, Surface Science 11, 317 (1968).

Chemisorption of CO on TaC

Gato, G., L. Fay and B. Jover, Chem. Ztg. 95, 907 (1971).

German: CO oxidation over chromium oxide-molybdenum oxide

Ghosh, J.C., M.V.C. Sastri, and S. Vedaraman, Curr. Sci. 19, 342 (1950).

Adsorptoin of CO and H_2 on $ZnO-Cr_2O_3$ mixture

Gossner, K., and H. Poelzi, Z. Phys. Chem. 86, 199 (1973).

Gravelle, P.C., G. Marty, G. ElShobaky, and S.J. Teichner, Bull. Soc. Chim. Fr. 1969, 1517 (1969).

Adsorption of CO on nickel oxide effects of Ga and Li dopants. Evidence shows sorption on both cationic and avionic sites.

Gray, T.J., and S.O. Savage, Disc. Farad. Soc. 8, 250 (1950).

Semiconductivity measurements on copper oxide

Harris, J.J. and A.J. Crocker, Surface Science 30, 692 (1972)

Haskell, D. and B.L. Munro, German Offenlegungsschrift 2,142,470

Preparation of a cuprous-cupric oxide for the oxidation of ppm CO in ethylene.

Hopkins, B.J., S. Usami, B. Williams, Vide (Fr.) 24, 26 (1969)

Hurd, J.J. and R.O. Adams, J. Vacuum Sci. Technol. (USA) 6, 229 (1969)

Intemann, K. and F. Stöckmann, Z. Phys. 131, (1951)

Hall-effect measurements in zinc oxide.

Jackson, A.G. and M.P. Hooker, Surface Science (Netherlands) 6, 297 (1967)

Study of CO and CO_2 adsorbed on M_o (110) by low energy electron diffraction.

Jones, H.A. and H.S. Taylor, J. Phys. Chem. 27, 623 (1923)

Reduction of copper oxide by CO catalytically in the presence of mixed copper and copper oxide. The main catalysis occurs at the copper-copper oxide interface.

Joyner, R.W., C.S. McKey, and M.W. Roberts, Surface Science 26, 303 (1971)

LEED study of CO on copper (001)

Kachanova, Zh. P., V.V. Voevodskii and A.P. Purman', Dokl. Akad. Nauk. SSSR 135. 648 (1960)

Russian-English Translation in Soviet Physics-Doklady (USA)

Electrical conductivity of MnO_2 during oxidation of CO. Striking increase in conductivity was observed.

Kamienski, B., Electrochim. Acta 1, 278 (1959)

Kawasaki, K., T. Sugita, and S. Ebisawa, Surface Science 7, 502 (1966)

Interactive effects of O_2, CO, and CO_2 on titanium films.

Kawasaki, K. et al., Surface Science 6, 395 (1967)

Change in conductance of palladium films due to adsorbed CO.

Klein, R., J. Chem. Phys. 31, 1306 (1959)

Klein, R. and J.W. Little, Surface Science 2, 167 (1964)

Kohrt, C and R. Gomer, J. Chem. Phys. 48, 3337 (April, 1968)

Kozlov, S.N, Yu. F. Novototskii-Vlasov, and V.F. Kiselev, Fiz. Tekh. Polnprov. 4, 353 (1970)

On freshly etched surfaces (111) of p- and n-type germanium, CO, NO, and CO_2 all act as acceptors.

Kroger, F.A. and H.J. Vink, Solid State Physics 3, 307 (1956)

Krusemeyer, H.J., Phys. Rev. 114, 655 (1959)

Surface potential, field-effect mobility and surface conductivity of zinc oxide.

Kubokawa, Y., Bull. Chem. Soc. Japan 33, 743 (1960)

Oxygen pretreatment on ZnO has virtually no effect on chemisorption of H_2 or CO.

LaConti, A.B. and H.J.R. Maget, J. Electrochem. Soc. 118, 506 (1971)

Lamb, Bray, and Frazer, Ind. Eng. Chem. 12, 213 (1920)

O. Levy and M. Steinberg, Surf. Sci. 5, 385 (1966).

Adsorption of CO on zinc oxide, measurements of enthalpy of adsorption.

Liashenko, V.I., Trudy (Transactions) Physical Inst., Ukranian SSR Acad. of Sci. 6, 323 (1936)

Liashenko, V.I. and V.G. Litovchenko, J. Tech. Phys. (USSR) 28, 429 (1958)

Effect of alcohol, acetone, benzene, and CO_2 on work function and conductivity of n- and p-type germanium.

Low, M.J.F. and H.A. Taylor, J. Phys. Chem. 63, 1317 (1959)

Adsorption rates for H_2O and CO on zinc oxide.

May, J.W., L.H. Germer, and C.C. Chang, J. Chem. Phys. 45, 2383 (Oct. 1969)

Morozov, N.M., Acta Physicochimica, U.R.S.S. 6, 6 (1937)

Sorption of CO on alumina; measured by pressure.

Morrison, S.R. and J.P. Bonnelle, J. Catal. 25, 416 (1972)

Addition of Nm, Cr to ZnO increase oxidative activity for CO.

Nagarjunan, T.S., et al., Proc. Nat. Inst. Sci. India A27, 496 (1961)

Chemisorption of Hydrogen and CO on zinc oxide

Neville, R.C., Dissertation, Cal. Inst. Tech., Pasadena, Ca., 1971

Electronic properties of zinc oxide and strontium titanium trioxide.

Pakhoniov, V.P., D.M. Shub, and V.I. Yeselovskii, Dvoinor Sloi Adsorptsiyii Tverd. Electrodakh 2, 289 (1970)

Russian

Park, R.L. and H.H. Madden, Jr., Surface Science 11, 188 (1968)

Effect of annealing on CO adsorption on palladium.

Parry, A.A. and J.A. Pryde, Br. J. Appl. Phys. 18, 329 (1967)

Perruca, E., Nuovo Cimento 15, 365 (1938)

Pope, P., D.S. Walker, L. Whalley and R.L. Moss, J. Catalysis 31, 335 (1973)

Rideal, E.K., Disc. Farad. Soc. 8, 96 (1950)

Introductory paper on catalysis on metals. Van der Waals adsorption and chemisorption are discussed.

Rideal, E.K. and B.M.W. Trapnell, Proc. Roy. Soc. A 205, 409 (1951)

CO and O_2 chemisorption on envaporated tungsten films; determination of film surface area.

Roginskii, S.Z., Dokl. Akad. Nauk SSSR, 130, 122 (1960)

Russian: Theoretical considerations of adsorption of CO on oxide semiconductors and effect on catalysis rates and conductivity.

Roginskii and Tselinskayor, J. Phys. Chem. Russ. 21, 919 (1947)

Roginsky, S. and J. Zeldowitsh, Acta Physicochimica U.R.S.S. 1, 554 (1934)

German: catalytic oxidation of CO on MnO_2.

Saltsburg, A. and D.P. Snowden, Surface Science 2 288 (1964)

Transient species of oxygen on NiO.

Schottky, W. and F. Waibel, Phys. Zeits. 34, 858 (1933)

Electrical conductivity of Cu_2O.

G.M. Schwab and G.Z. Drikos, Z. Phys. Chem. B 52, 234 (1942)

Reaction kinetics of CO on cupric oxide.

Schwab, G.M., H. Neller, F. Steinbach, and M. Venugopalan, Nature 193, 774 (1962)

Oxidation of CO on zinc oxide, influenced by ultraviolet light.

Seiyama, T. and S. Kagawa, Anal. Chem. 38, 1069 (1966)

A detector for gases using semiconductive films.

Shalnikov, A., J. Exp. and Theor. Physics, USSR 93, 255 (1939)

Shiskov, D., D. Ivanov, and G. Radveva, Zh. Prikl. Khim. (Leningrad) 44, 1947 (1971)

Smart. R. St.C., L.H. Little, T.L. Slager, and R.G. Greenler, J. Phys. Chem. (USA) 77, 1019 (April 1973)

CO adsorption on MgO

Sinyak, G.S., R.V. Lisovskii, G.I. Chizhikova, M.A. Vitashkina, E.I. Karpova, B.G. Gusarov, and L.L. Zablotskii, Kosm. Biol. MEd. 5, 77 (1971)

Comparison of hopcalite, Cu-Cr, Cu-CO, Pt, and Pd as oxidation catalysts. Pd best.

Sokolskii, D.V., G.K. Alekseeva, V.A. Druz, and G.N. Kotova, Doklad. Akad. Nauk SSSR 203, 398 (1972)

Activities of CuO, Fe_2O_3, Mn_2O_3, CeO_2, and Cr_2O_3 dispersed on alumina for oxidation of CO.

Sparnaay, M.J., A.H. Boonstra, and J. vanRuler, Surface Science 2, 56 (1964)

Effect of chemisorption on electrical properties of germanium surfaces.

Sparnaay, M.J., Surface Science 13, 99 (1969)

Effect of CO adsorption on acceptor and donor surface states in germanium.

Sugita, T. et al., Surface Sicence 14, 461 (1969)

Changes in conductivity of a platinum film due to adsorbed CO.

Suhrmann, R. and G. Wedler, Z. Elektrochem. (Ger.) 63, 748 (1959)

Sultanov, M. Yu. and Kh. A. Sadykova, Azerb. Khim. Zh. 1, 110 (1971)

Russian: catalytic oxidation of CO much slower on rare earth oxides than for CuO.

Takaishi, T., Z. Naturforschung 11a, 286 (1956)

Theory: ionic adsorption of gases on semiconductors and catalytic activity.

Taylor, H.S. and G. Ogden, Farad. Soc. Trans. 30, 1178 (1934)

Adsorption of H_2 and CO on a $ZnO-MoO_3$ mixed oxide. Heats of adsorption and activation energy have been determined.

Trapnell, B.M.W., Chemisorption, Butterworth's Scientific Publications, London, 1955.

Vand, V., Proc. Phys. Soc. Lond. 55, 222 (1943)

Theory: irreversible resistance changes of films evaporated in vacuum.

Viswanath, Y. and L.D. Schmidt, Chem. Phys. 59, 4184 (1973)

Vogt, W., Ann. d. Physik 7, 183 (1930)

Electrical properties of cuprous oxide.

Wright, R.W. and J.P. Andrews, Proc. Roy. Soc. London A 62, 446 (1949)

Temperature dependence of the conductance of nickel oxide.

Yates, J.T., Jr. and T.E. Madery, J. Chem. Phys. (USA) 51, 334 (July, 1969)

Zhuze and Kurchakov, Sov. Phys. 2, 454 (1932)

Zwietering, P., H.L.T. Koks, and C. vanHeerden, J. Phys. Chem. Solids 11, 18 (1959)

Changes in electrical conductivity of metals due to chemisorption